16 JAN 1999

ATNF / File A1 / 39.3/082 MANAGEMENT		
	Action	cc
R.D.EKERS		
J.W.BROOKS		
P.F.HAYNES		
P.P.NORRIS		
R.M.PRICE		X
J.V.SINCLAIR		
J.J.O'CONNELL		X
D.WHITEOAK		
W.E.WILSON		
J.HOWSON		

Technical Report: 39.3/084

CSIRO Australia Telescope National Facility

The Baseline Ripple Problem: The Measurement Program at Parkes in June 1998

J. Reynolds → A. Barends

B. MacA. Thomas, G.R. Graves, L. Staveley-Smith, M.J. Kesteven, R.M. Price

Please email author to see who would like to borrow it.

CONTENTS

1. Background and Methodology.

2. Summary of Measurements.

3. Conclusions and Recommendations.

Attachment A: "Reflectometry measurements on the Parkes radio telescope; February and June 1998" (G.R. Graves and B. MacA. Thomas)

Attachment B: "Daytime baseline-ripple frequency-intensity scan displays" (L. Staveley-Smith, M.J. Kesteven).

Attachment C: "Spectral-ripple at Parkes", draft paper (M.J. Kesteven, R.M. Price, L. Staveley-Smith, B.M. Thomas, W.E. Wilson)

Attachment D: "Another look at multiple reflections on the Parkes 64m radio telescope: a discussion paper", draft report, B. MacA. Thomas

Attachment E: The baseline ripple problem: summaries of earlier work:

- "The Parkes spectral line baseline problem - will it be exacerbated by the upgrade", M.J. Kesteven
- "Some general thoughts from Padman's work (1978) at 5GHz". (1 page summary overhead).

CSIRO Australia Telescope National Facility

The Baseline Ripple Problem: The Measurement Program at Parkes in June 1998

B. MacA. Thomas, G.R. Graves, L. Staveley-Smith, M.J. Kesteven, R.M. Price

1. Background Methodology

Following reports of extensive baseline-ripple problems during day-time observations using the new 13-beam H-line receiver, it was decided to undertake an experimental program to hopefully clarify the major sources of baseline ripple, and as a result, to recommend either further tests or theoretical studies which should be undertaken next.

The measurement program used two approaches:

- Reflectometry measurements, which use a transmitting signal from the feed, and measures the intensity and distance from reflection points on the antenna, including multiple reflections, (see Attachment A).
- Standard displays from the multibeam receiver showing, in effect, intensity variations caused by multiple reflections with the sun as a source. The antenna drive system was modified to enable scans to be made relative to the antenna strut lobes (generally across a strut lobe), or in the region of sky remote from strut lobes, (see Attachment B).

There was not sufficient time to undertake a study of on-source ripple, so as to make a comparison of results from the three methods of measurement. However, there are useful comparative results between the reflectometry measurements and the standard frequency-intensity scan displays, although there was not sufficient time to study the latter for all antenna configurations.

The antenna configurations studied (and their designations for reference purposes) were:

- Ref A: antenna as for normal operation.
- Ref B: absorber mounted on focal-plane (underneath of focus-cabin floor)
- Ref C: as for Ref B, but with the experimental metal cone (see Attachment C) mounted at the vertex. As there were 50mm gaps between the inside radius and the theodolite cover, and between the outer radius and the antenna surface, reflectometry measurements were also undertaken with absorber around the inner edge, and metal plates bridging the outer gaps. Other more drastic modifications included covering the central theodolite cover and cone with absorber (C2), and repeated with absorber around the outer discontinuity (C3).

The attached photographs illustrate the various configurations which formed part of this study.

The vertical dimensions of the absorber used and the frame are as follows:

- absorber depths:
  - inner area, 200mm
  - outer area, 300mm
- effective frame depth: 150mm

Hence the total depth closest to the feeds, and which will have greatest impact on the system temperature, is 350mm.

2. Summary of Measurements

2.1 Reflectometry Measurements:

The methodology and detailed results are given in Attachment A, and the results for the major reflection (feed/focal-plane - vertex cavity) are summarised in Table 1. (Note that using this type of measurement, this cavity reflection process was the only major contributor to indicated reflections).

In Table 1, it should be noted that the "intensity of the first hop" is independent of the surface of the focal-plane (metal or absorber), since the return signal into the feed is dependent only on the reflected components in the vicinity of the vertex (for reflection distances of around 26.2m). However, additional hops will be critically dependent on the surface forming the focal-plane, i.e. whether the energy is absorbed or reflected. (If the energy is reflected, a quasi plane-wave forms, giving a closely-coupled cavity). See Fig. 2.1 which illustrates the spherical-plane wave conversion in the vertex region assuming a perfect paraboloidal surface there, i.e. no cone. If absorber is used on the focal-plane, this configuration should give minimum extraneous scattered energy, which could be critical for minimising sun-induced baseline ripple. (However, it may not be the optimum configuration for minimising on-source baseline ripple!)

Returning to Table 1, let us consider the intensity of the first hop received by the feed. As expected, the intensity is independent of the nature of the focal-plane. The surprise result is where the cone is added - the reflection is increased by 8dB, independent of whether the cone is metal or absorber! One explanation is that there is considerable re-radiation from the discontinuity at a radius corresponding to the edge of the cone (whether the discontinuity be caused by an abrupt slope in the metal surface or by the change introduced by the absorber). Filling the inner gap by absorber and the outer gap by metal has negligible effect on the intensity of the return first hop. It would also appear that the theodolite cover in the centre of the main reflector has negligible effect.

Also shown in Table 1 is the intensity decrease per hop beyond the first. For the existing vertex cone, the absorber on the focal-plane gives an additional 11dB attenuation per hop compared to the metal ground-plane. When the experimental metal cone is added, or if absorber is used in this area, an additional 8dB attenuation per hop is obtained. In the case of the metal cone, energy is diffracted away from the

focal-plane area as shown in Fig. 2.2. Note, however, that concentrating the scattered energy from the metal cone into a conical volume has two effects:

(a) it illuminates the 3 struts along a relatively short length, so that reflected energy will not be insignificant, and,

(b) strong sources (such as the sun) when passing through the conical volume shown in Fig. 2.2, will produce a relatively high level of signal at the feed compared to Fig. 2.1, where the vertex region remains unshaped.

Consequently there would appear to be a delicate balance between not using a vertex cone (so as to minimise the effect of wide-angle strong sources), and an "optimally" shaped vertex cone (to minimise the intensity of successive hops for on-axis sources).

A comparison of the reflected on-axis radiation for the configurations C1 and C2 shows that the metal cone is just as effective as using absorber. However the absorber:

(a) will increase the system temperature, (a disadvantage), and,

(b) will not scatter the energy so that the effect of strong off-axis sources is minimised (an advantage).

The case C3, where absorber surrounds the edge of the metal cone, shows that the design of any vertex cone must not introduce any discontinuity between the main reflector and the vertex cone.

Finally, the effect of struts on the scattering process has not been considered in the measurement program or for this analysis. However, the results would indicate that the focal-plane/vertex areas need to be urgently addressed first prior to addressing the effect of the struts.

Note: Fig. 2.1 and 2.2 are simple ray diagrams which are intended to support the text in this section.

2.2 *Frequency-Intensity Baseline Ripple Measurements*

Standard measurements were used to show baseline ripple displays for scans of the sun, crossing near-in (6° or 12° from main-beam direction) strut lobes, far-out strut lobes of considerably lower intensity, and in areas away from the strut lobes. The technique and the results obtained for the three antenna configurations (Ref A, B and C1), and used for comparative studies in each case, are described in Attachment B. In particular, Table A in this attachment gives a summary of the tracks made and performance comparisons for the above antenna configurations.

In general, close-in scans ($\theta \leq 15°$) across strut-lobes show significant baseline ripple. However, for regions either side of the strut-lobes, the baseline ripple is considerably reduced where absorber is used on the focal-plane. For far-out strut-lobes, the effect

of the lobes is considerably reduced. In regions free of strut-lobes, the use of absorber gives cleaner results. However, when the experimental metal cone is used, the resultant narrow conical volume intercepted by the sun (see Fig. 2.2), gives rise to significant baseline ripple. For the feeds used with the multibeam receiver, and the absorber-frame design employed for the tests, the system temperature was increased by approximately 3.5K.

Note: Fig. 3.1 and 3.2 ray diagrams are intended to support the text in this section.

3. Conclusions and Recommendations

It would appear that for the Parkes geometry, the requirements necessary to minimise baseline ripple caused by strong sources (e.g. sun) arriving at any angle relative to the mainbeam, may not necessarily be compatible with the requirement to minimise on-source baseline ripple.

To achieve the former, it is essential to minimise all scattered energy; ideally it should be absorbed. Therefore the design of a vertex cone and strut "deflectors" is most critical, so as not to diffract significant energy (lobes) throughout space.

To minimise on-source baseline ripple, the vertex cone must also be carefully designed so as not to reflect energy back into the feed (s). One important aspect is that the cone should blend smoothly into the existing paraboloidal surface. The use of absorber on the underneath of the focus-cabin should assist this type of observation also.

Consequently, the following recommendations are made:

1. that consideration of the effect of scattering from the struts be delayed until all aspects relating to the focus-cabin floor/vertex cavity be investigated.

2. that the design of a vertex cone which minimises back-reflection over the feed-area occupied by the multibeam receiver, and which minimises scattered energy in all other directions, be investigated theoretically. The alternative of restoring the vertex area to the original paraboloidal shape should also be considered. These aspects could be undertaken by placing a contract on CTIP. (A starting point for a shaped-design may be the general shape given in Fig. 4).

3. that the possibility and desirability of placing low-profile water-proof and bird-proof absorber across the focal-plane be considered.

4. that any subsequent program involving on-source baseline ripple measurements should include a test where one of the circumferential gaps between reflector panels be bridged with conducting tape. The existing design of the bridging plates across the gap between the high-precision solid surface and the perforated aluminium panels should also be considered, particularly for higher-frequency operation.

Acknowledgments:

The assistance of Brian Wilcockson, staff of the Parkes Observatory and Radiophysics Laboratory Workshop, is gratefully acknowledged for their extensive support prior to and during this measurement program.

Ref:BMT/gam:376-98

Table 1
Reflectometry Tests - A Summary
(Linear Polarisation)

Antenna Configuration	Ref	Intensity first hop (dB)	Intensity decrease per hop (dB)	Fig. No.
Normal operation	A	-50 [1]	5	A1 A2 A5
Absorber on focal-plane	B	-50	16	B1
Add experimental metal cone at vertex	C1	-42 [2]	24	{C1(a) {C1(b) {C1(c)(i)
Add absorber over cone	C2	-42	(24)	C2
Absorber over theodolite and discontinuity between cone and antenna surface	C3	-44	(30)	C3

Notes:
(1)Use of CP typically reduced first hop by
[1]: - 13dB; Fig. A3/A4,
[2]: - 18dB; Fig. C1 (c) (ii), -15dB/hop

(2) Difference between hops: 26.1m, (focal length = 26.24m)

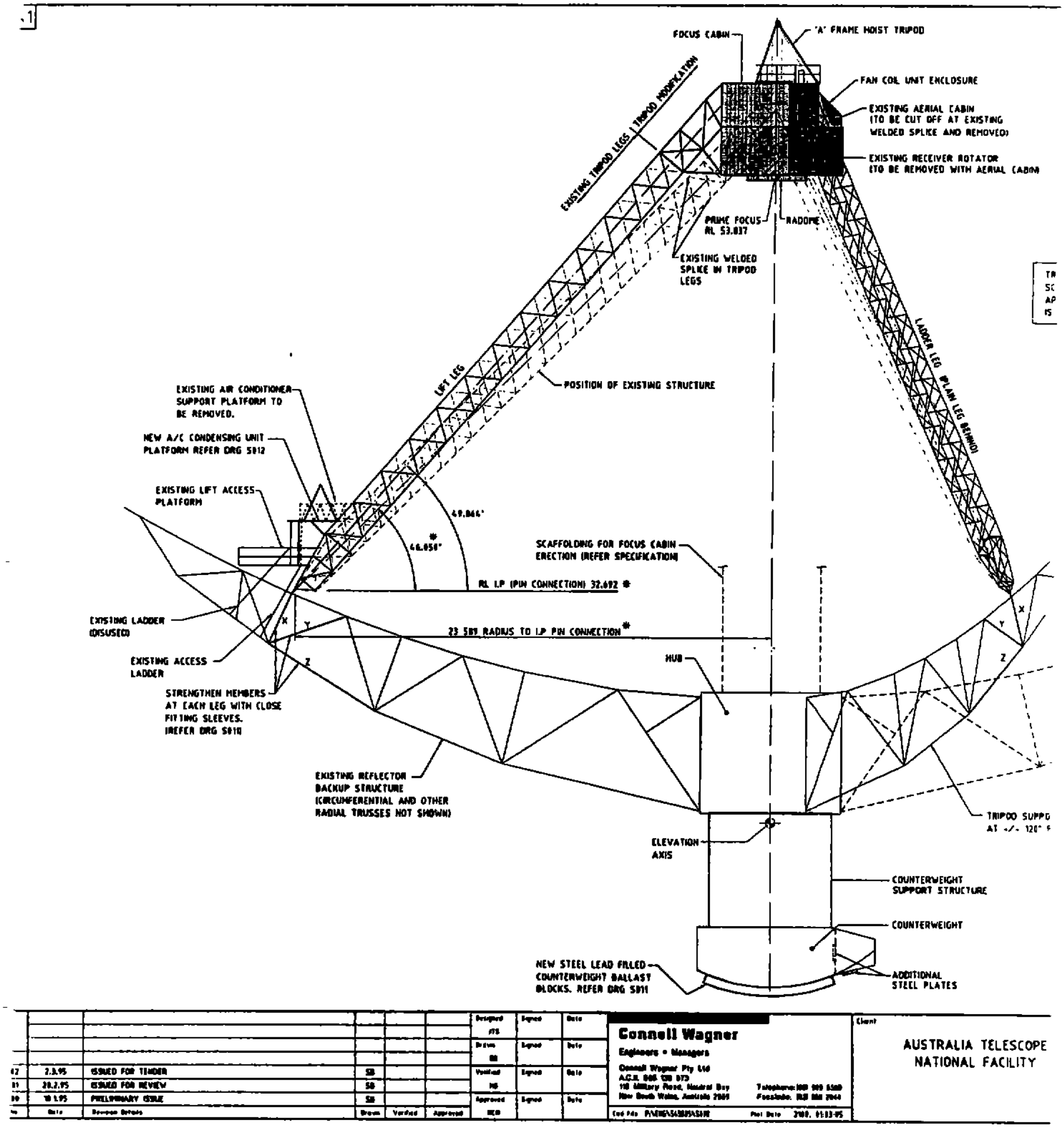

FOCUS CABIN
'A' FRAME HOIST TRIPOD
FAN COIL UNIT ENCLOSURE
EXISTING AERIAL CABIN (TO BE CUT OFF AT EXISTING WELDED SPLICE AND REMOVED)
EXISTING RECEIVER ROTATOR (TO BE REMOVED WITH AERIAL CABIN)
EXISTING TRIPOD LEGS (TRIPOD MODIFICATION
PRIME FOCUS RL 53.837
RADOME
EXISTING WELDED SPLICE IN TRIPOD LEGS
LADDER LEG (PLAIN LEG BEHIND)
LIFT LEG
POSITION OF EXISTING STRUCTURE
EXISTING AIR CONDITIONER SUPPORT PLATFORM TO BE REMOVED.
NEW A/C CONDENSING UNIT PLATFORM REFER DRG S012
EXISTING LIFT ACCESS PLATFORM
49.846°
46.856°
SCAFFOLDING FOR FOCUS CABIN ERECTION (REFER SPECIFICATION)
RL I.P (PIN CONNECTION) 32.692
EXISTING LADDER (DISUSED)
23.589 RADIUS TO I.P PIN CONNECTION
EXISTING ACCESS LADDER
HUB
STRENGTHEN MEMBERS AT EACH LEG WITH CLOSE FITTING SLEEVES. (REFER DRG S010
EXISTING REFLECTOR BACKUP STRUCTURE (CIRCUMFERENTIAL AND OTHER RADIAL TRUSSES NOT SHOWN)
TRIPOD SUPPO AT +/- 120°
ELEVATION AXIS
COUNTERWEIGHT SUPPORT STRUCTURE
COUNTERWEIGHT
NEW STEEL LEAD FILLED COUNTERWEIGHT BALLAST BLOCKS. REFER DRG S011
ADDITIONAL STEEL PLATES
2.3.95 ISSUED FOR TENDER SB
20.2.95 ISSUED FOR REVIEW SB
10.1.95 PRELIMINARY ISSUE SB
Connell Wagner
Engineers • Managers
AUSTRALIA TELESCOPE NATIONAL FACILITY

FIG. 1.

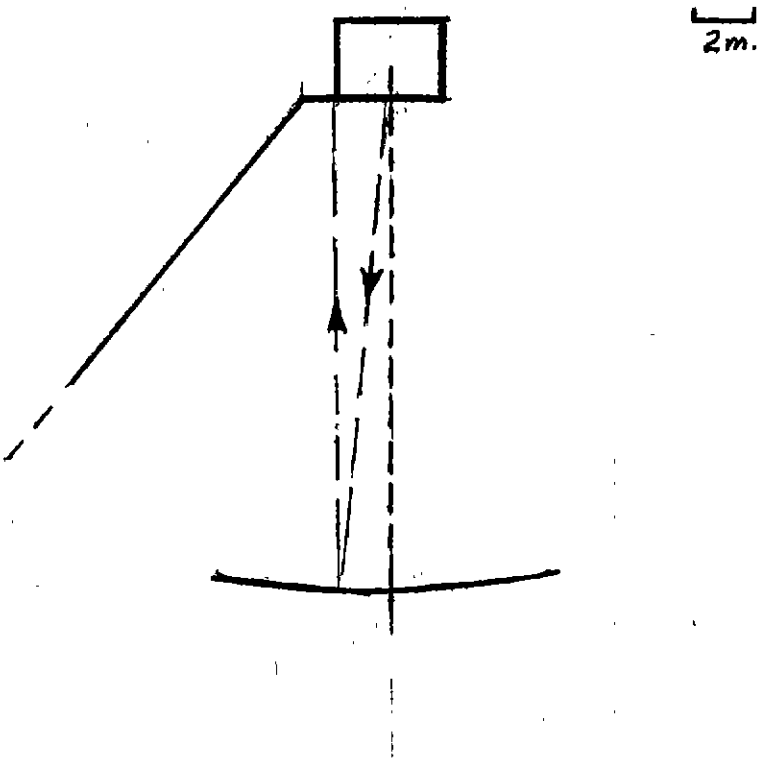

FIG. 2.1: Reflectometer measurement system — first pass. Assuming a paraboloidal surface at the vertex, the transmitted spherical wave radiating from the feed is reflected as a plane wave. At the focal-plane, energy can be absorbed, or if metal, re-reflected as a quasi-plane wave (see Attachment D).

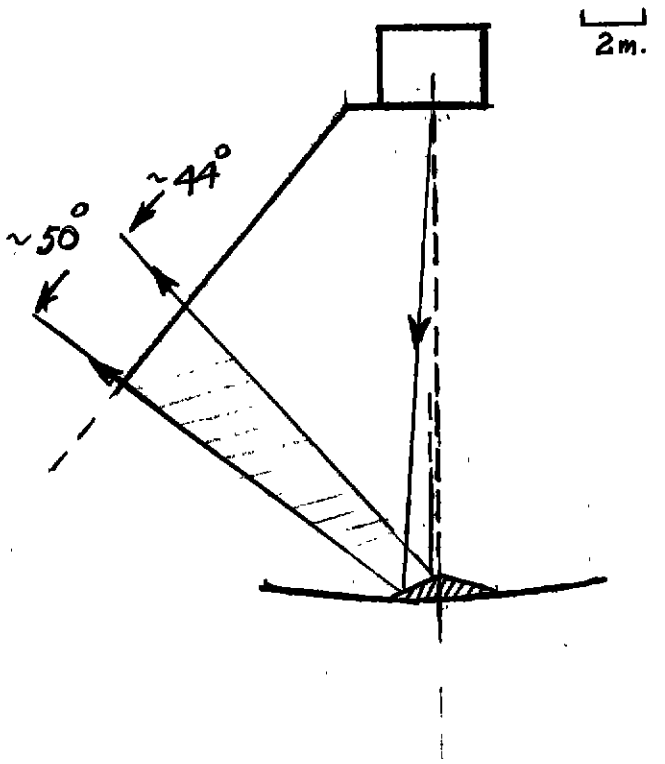

FIG. 2.2: Reflectometer measurement system — first pass with experimental metal cone. Alternatively, on reception, the directions are reversed.

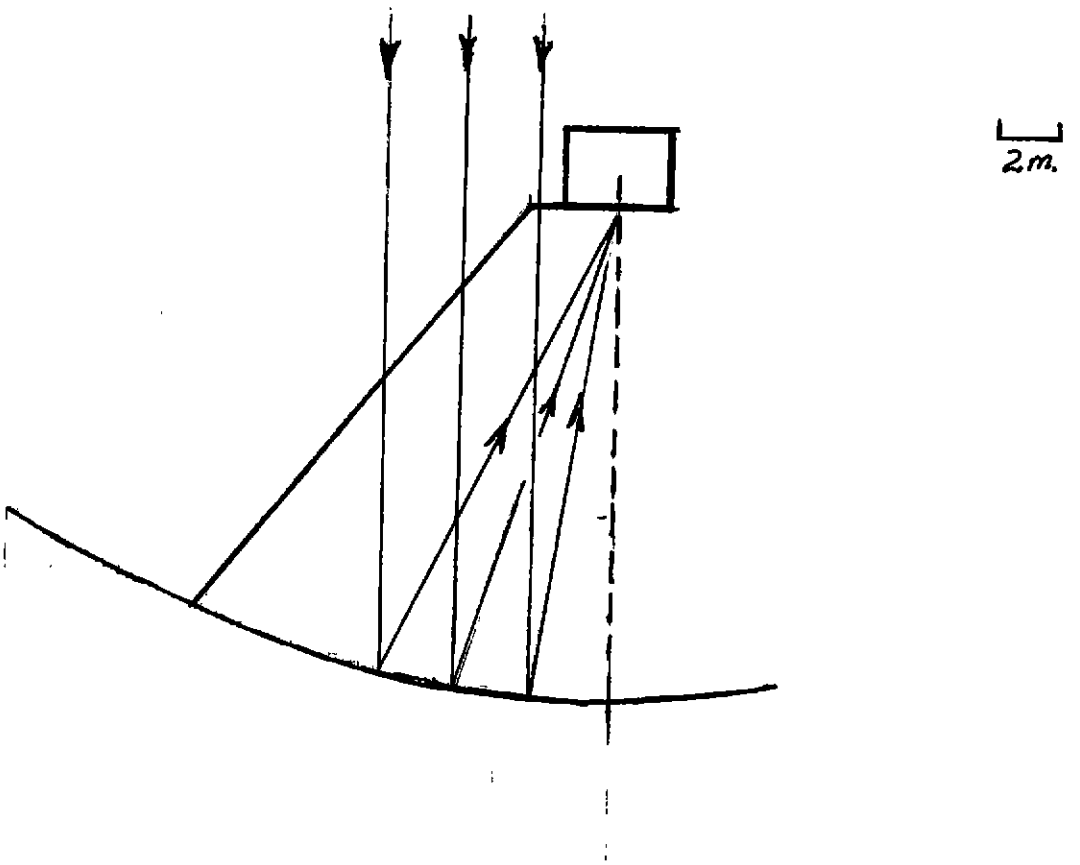

FIG. 3.1: On-axis plane wave incident on reflector. Some of the energy directed to the focus will be incident on the focal-plane, and either absorbed, or if metal, reflected toward the vertex area.

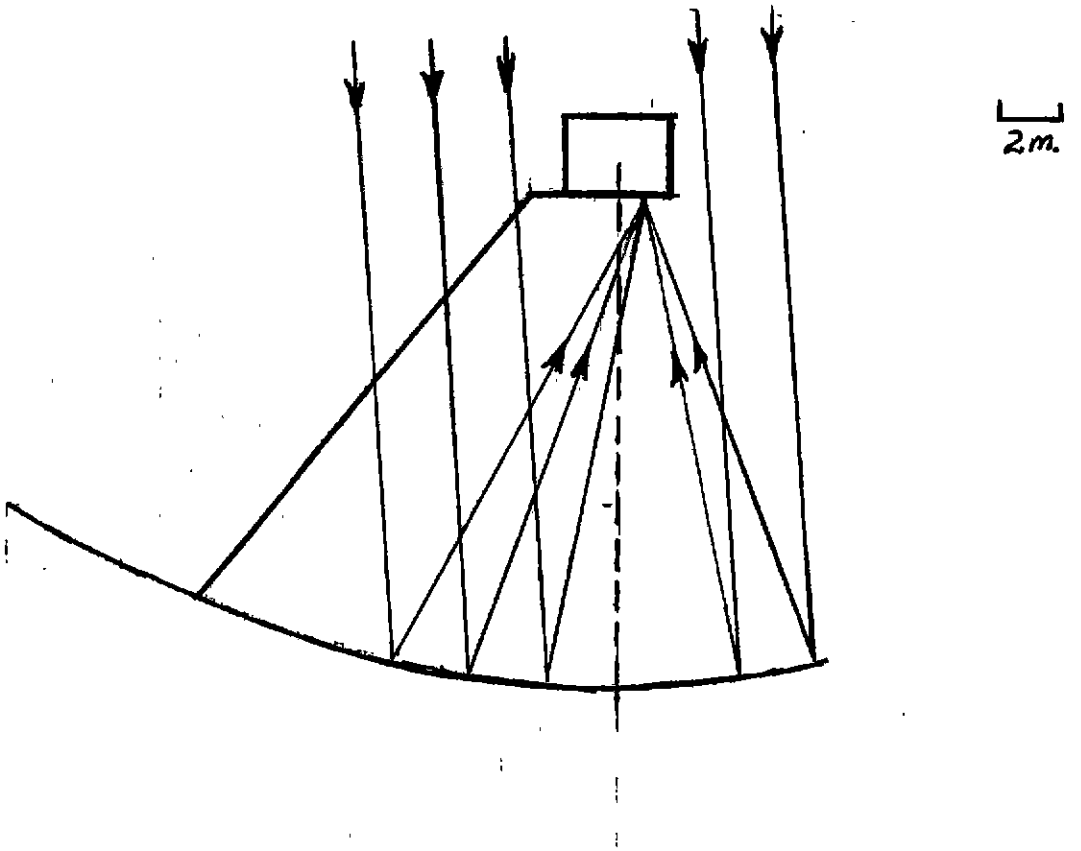

FIG. 3.2: Plane wave incident at a small angle from boresite. The energy incident on the focal-plane can be absorbed, as if metal, totally reflected towards the vertex region.

For larger incident angles, some of the energy will still be incident on the focal-plane (through the "diluted" Airy pattern applicable to the quasi-focussed energy).

BMT/25.7.97

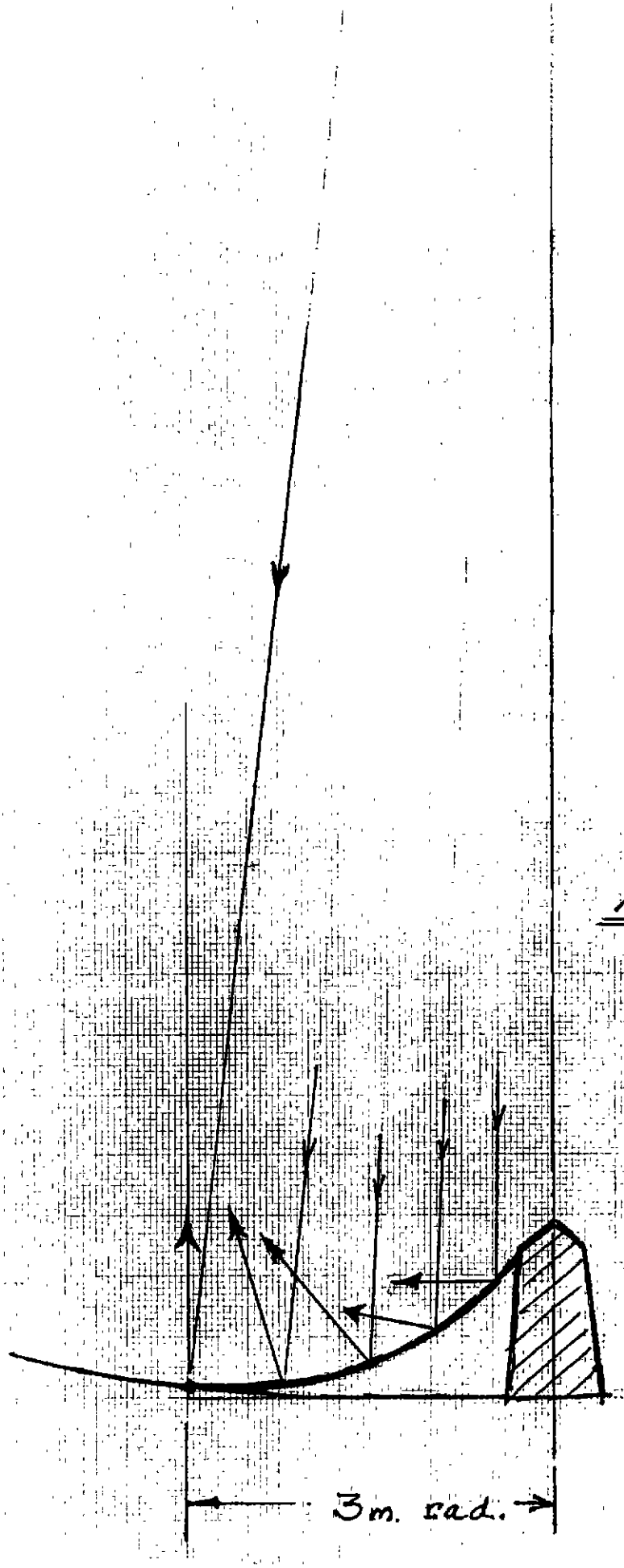

FIG. 4 : Proposed indicative shape of vertex cone for analysis, and optimisation.

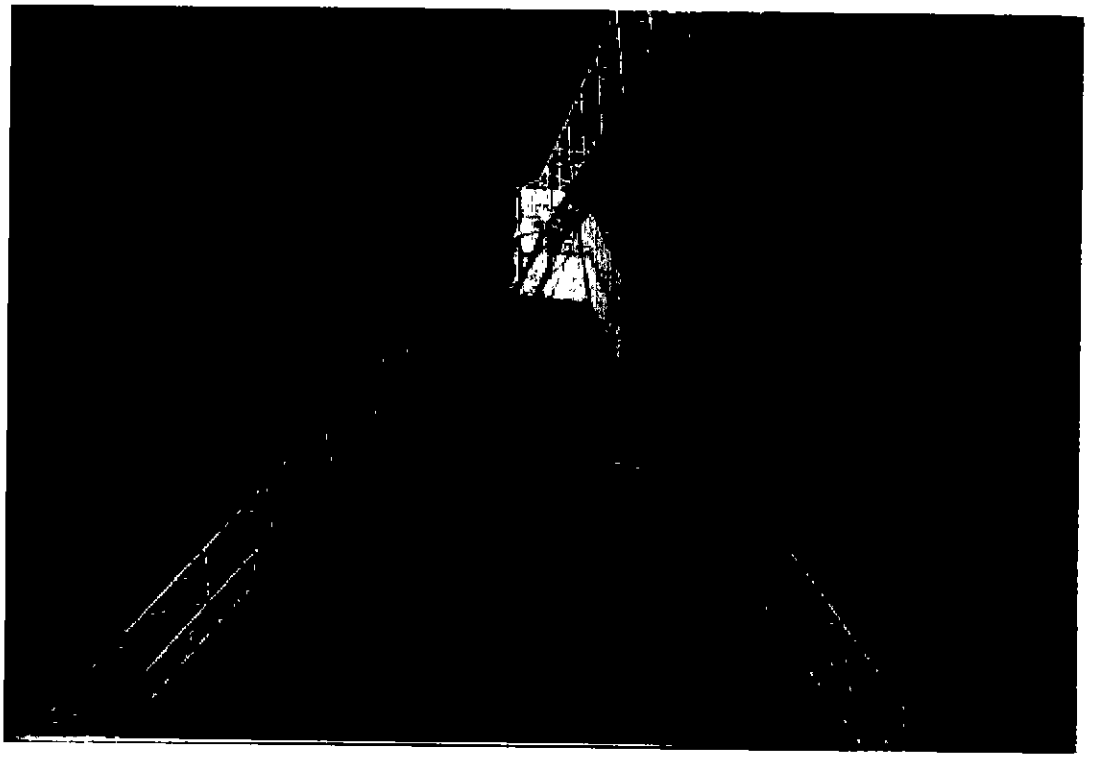

1. Focus Cabin in normal operation configuration

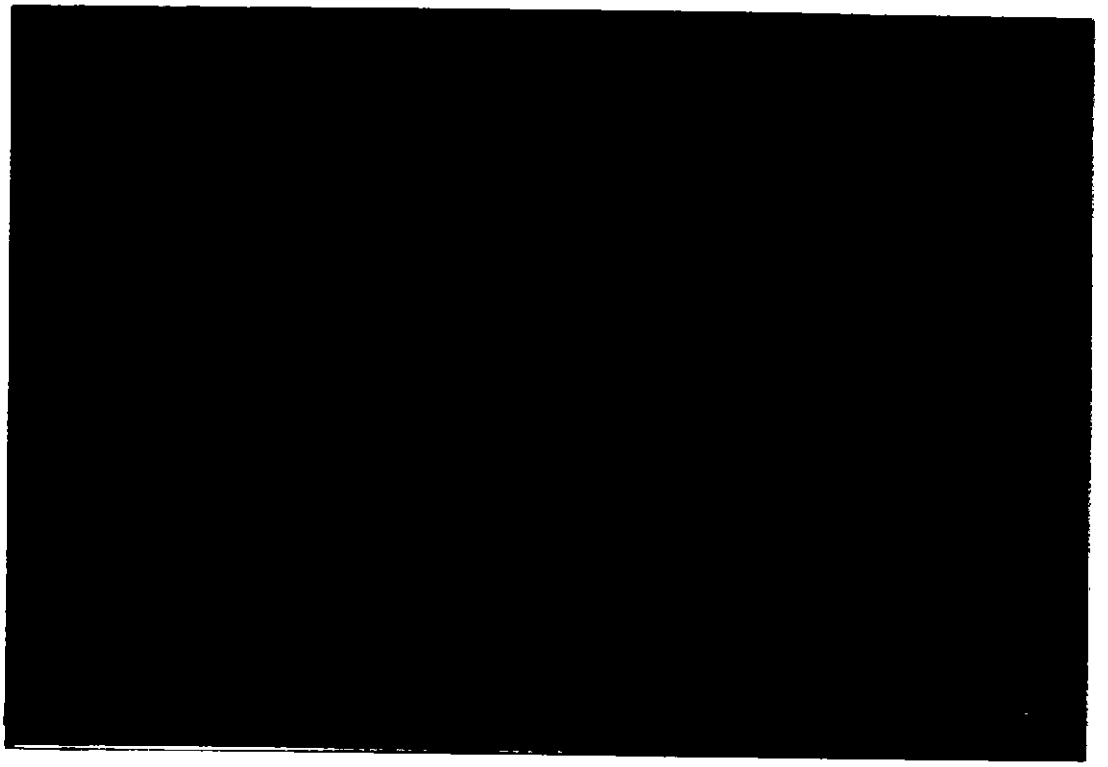

2. *Raising the absorber platform. Note the original precision "correction cone" surrounding the theodolite cover.*

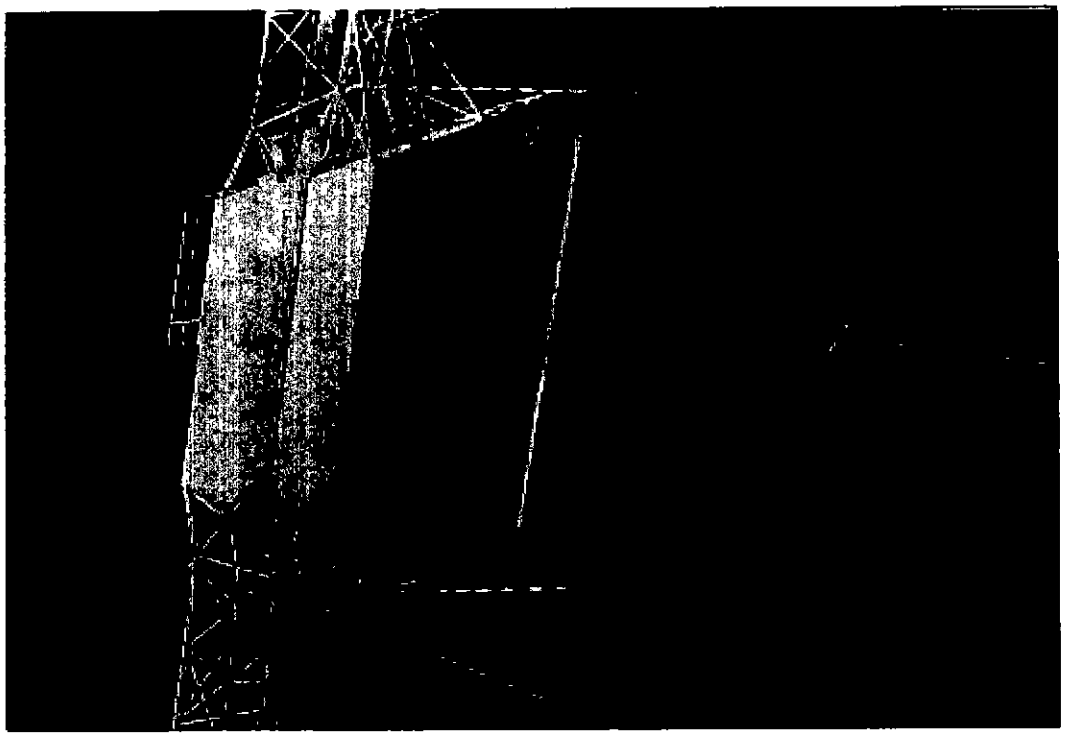

3. The absorber platform being raised

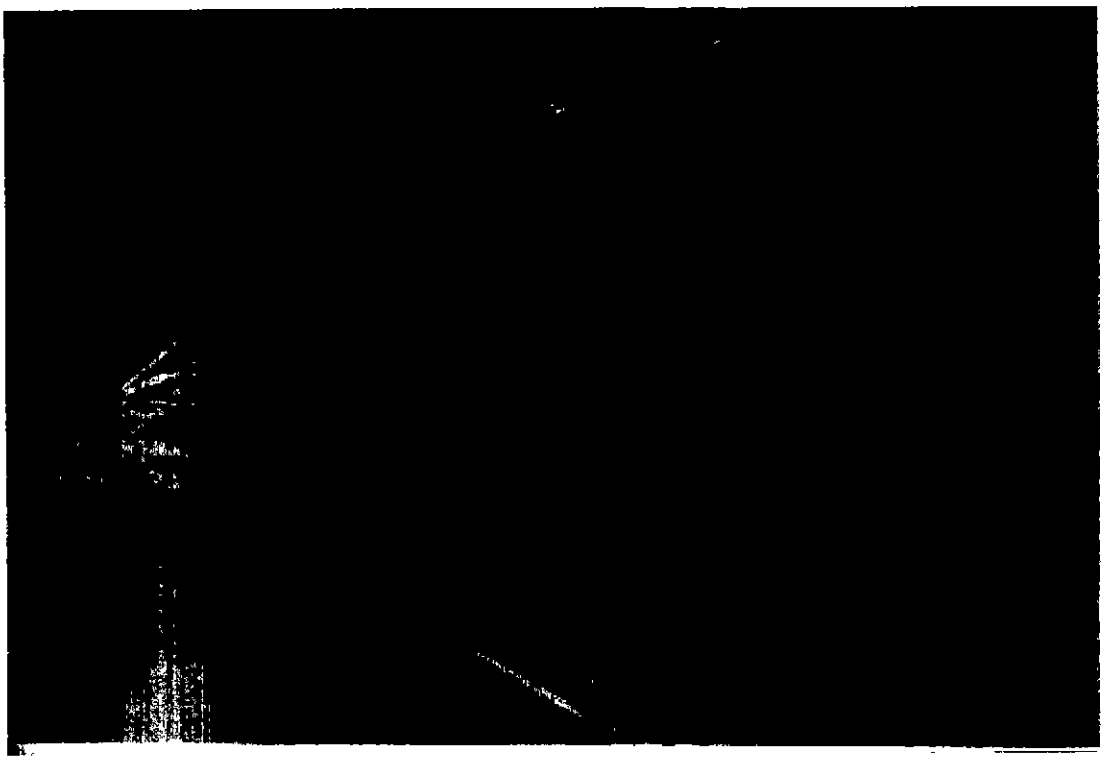

4. The absorber platform attached to the underneath of the focus-cabin in the focal-plane

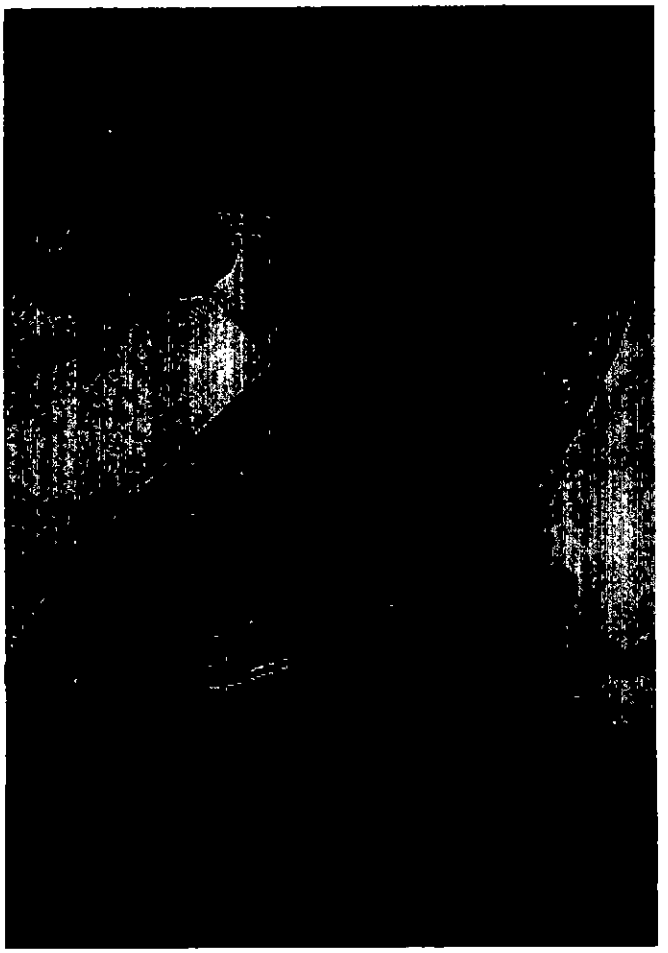

5. The Parkes antenna with absorber platform attached to focus-cabin

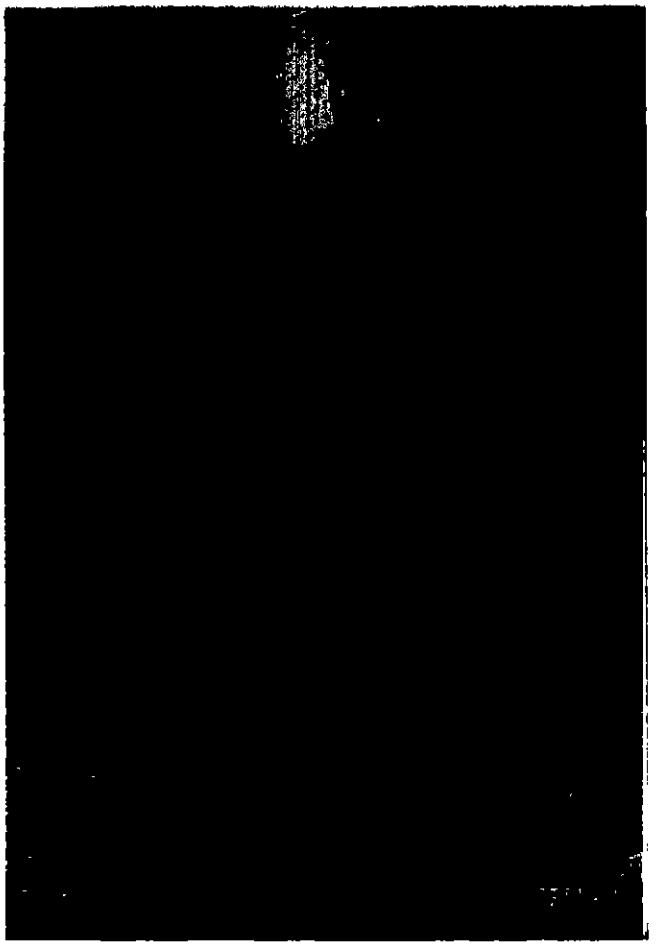

6. The experimental vertex-cone attached to the antenna

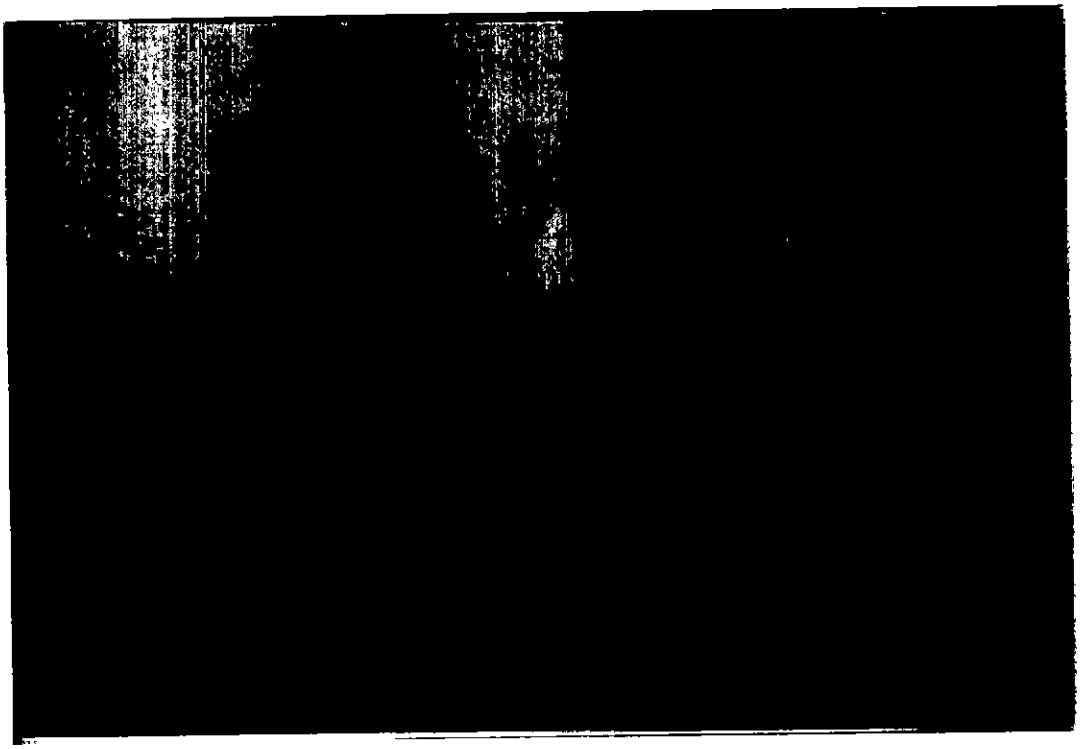

7. Bridging the 50 mm gap between the experimental vertex cone and the antenna surface. Note the absorber bridging the gap between the cone and the theodolite cover

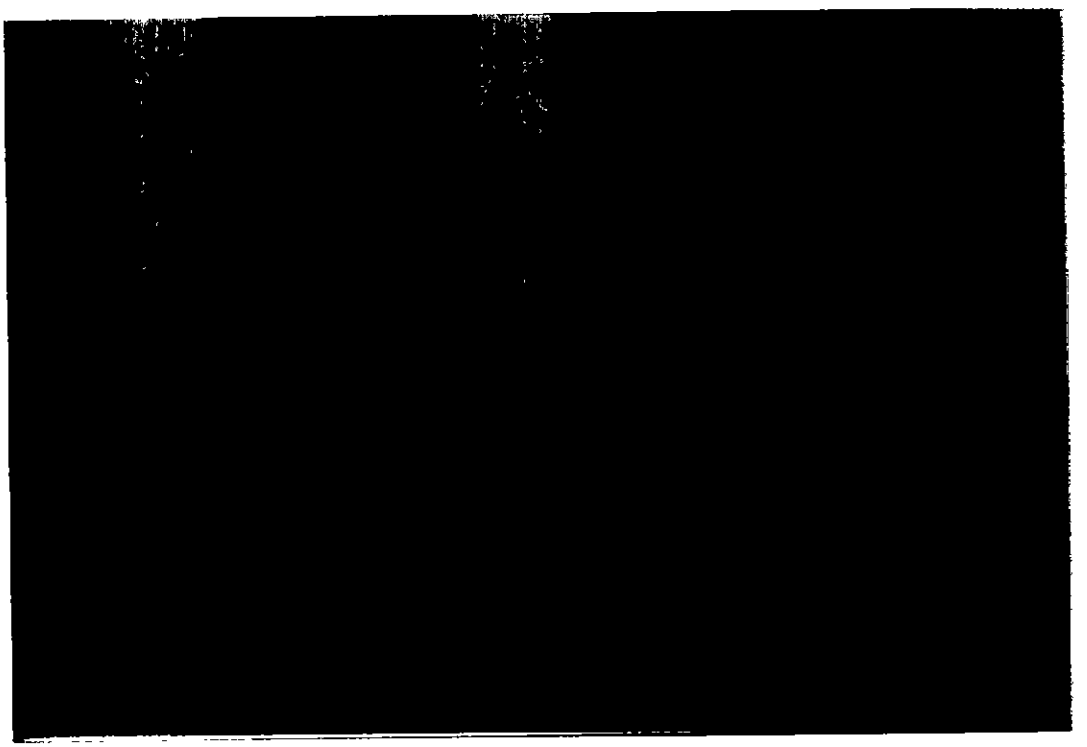

8. Covering the vertex area (experimental vertex cone and theodolite cover) with absorber

Attachment A to Technical Report: 39.3/084

CSIRO Australia Telescope National Facility

Reflectometry Measurements on the Parkes Radio Telescope; February and June 1998

George R. Graves and Bruce MacA. Thomas
24 August 1998

LIST OF CONTENTS

1. Introduction

2. Why reflectometry measurements?

3. The measurement program
   - 3.1 The reflectometry technique
   - 3.2 Equipment and parameters used
   - 3.3 Antenna configurations tested
   - 3.4 General comments on the accuracy and results
     - 3.4.1 Checking the "zero" reference distance
     - 3.4.2 Dynamic range
     - 3.4.3 Resolution
     - 3.4.4 Results near zero range length
     - 3.4.5 Use of circular polarisation
     - 3.4.6 Use of reference plate

4. Interpretation of results
   - 4.1 Primary reflections
   - 4.2 Secondary reflections

5. Conclusions

Acknowledgements

Annex 1: Distance from focus to given positions on reflector surface.

1. Introduction

Antennas, other than those of offset feed or offset subreflector design, tend to suffer from what is known as "baseline ripple problems" due to multipath reflections of the signal within the feed, or subreflector, support structure. If the position of the feed (horn etc) changes, due to say mechanical deformation of the antenna structure for a change in elevation, the phasing between the main path and the extra (unwanted) multipath reflections change, resulting in a change in amplitude in the signal. The signal received is the vector sum of the main path and all the multipath signals.

For the Parkes antenna, the distance from the phase centre of the feed, to the vertex of the parabola is approximately 26.3m, giving a baseline ripple of about 5.5 MHz.

The primary source of baseline ripple appears to be reflections of the signal between the feed/underside of the focus cabin area and some inner section of the surface of the antenna. (This has of course been known for years).

Distances from the feed to discontinuities on the dish surface are given in the Table in Annex 1.

In this report, we will consider what is a "reflectometry measurement", and the reasons for doing it. Then the method of measurement, the parameters, and the interpretation of the results will be given. The measurements were made in February and June 1998.

2. Why Reflectometry Measurements?

Particularly for spectral line observations, it is important that the signal amplitude versus frequency characteristic remain constant when the telescope is moved, otherwise it may be difficult to distinguish between signal spectral changes and 'baseline' changes. Now, the baseline does change, for a change in elevation of the telescope. How can these baseline changes be minimised? What are the signal paths that produce the baseline ripple?

There are various things that may be tried to minimise the baseline ripple; scatter cones at the vertex, absorber under the focus cabin, scatter surfaces or absorber on parts of the focus cabin support legs, conductive tape over the (circular) gaps between the reflector panels, to name a few.

If we can measure the path distance to these multi-path reflections, we may be able to determine what these experimental procedures (scatter cones etc) actually do to the reflections. A reflectometry measurement allows the effectiveness of different mechanical changes to the reflection paths of the telescope to be evaluated.

3. The Measurement Program

3.1 The Reflectometry Technique:

Reflectometry of radio telescopes is not new. Fisher, for example, measured the Greenbank telescopes using this technique in 1978 (Ref. 1). For the preliminary measurement of the Parkes antenna, reflection (S11) data was collected by an Advantest R3762A network analyser over a range of frequencies (e.g. 1350 - 1950 MHz); the data stored in a file, a window function (Hanning or Blackman) applied, and then a FFT (fast fourier transform) applied to give a time, and hence distance, versus reflection intensity graph.

The computer program to control and collect the data from the network analyser was written in QBASIC, with the analyser controlled by a GPIB card. The data analysis programs (FORTRAN) were mainly written by Mike Kesteven with some additional subroutines and alterations performed by GRG.

3.2 Equipment and Parameters used:

The equipment and parameters finally adopted for the June 1998 program were:

Feed:

- H-OH feed with quad-ridged OMT for wide-band operation (1350 - 1950 MHz).
- linear-polarisation (parallel to lift-leg as reference; some measurements were also made in the orthogonal mode).
- circular polarisation (for investigation of two-hop reflections).

Network Analyser:

- Adventest R3762A network analyser
- 10MHz external observatory reference
- Resolution bandwidth, 10Hz
- Sweep time: 240 sec

Transform Parameters:

- Frequency range (1350 - 1861.5MHz, 1024 of 1201 points)
- Window function: Blackman

3.3 Antenna configurations tested:

The first measurement program in February 1998 was a preliminary run with the antenna in its normal operating configuration. These measurements were successful and provided useful information. One set of measurements was repeated in June 1998 and found to

give excellent repeatability. The usual antenna configuration is designated "Configuration A", and the results are given by Fig Ax.

The second measurement program in June 1998 extended over four days and included:

- Configuration B: absorber on focal-plane (attached to focus-cabin floor),
- Configuration C: experimental cone (slope, 22°, diameter, 5.88m and 8 segments) at vertex, with absorber on focal-plane. Measurements were made with various modifications to the experimental cone; e.g. adding absorber across the inner 50mm gap between the cone and the theodolite cover (Fig. C1(b)), and covering the outer 50mm gap between the cone and the antenna surface with a metal strip (Fig. C1(c)). Other major modifications included:

    - Placing absorber over the cone (Fig. C2), and

    - Placing absorber over the theodolite cover and the discontinuity between the cone and the surface (Fig. C3).

  Unfortunately time did not permit measurements to be carried out with the cone alone (without the absorber on the focal plane).

The results are shown in Fig. A, B and C corresponding to the various major antenna configurations described above.

3.4 General comments on the accuracy and results:

3.4.1 Checking the "zero" reference distance:

A check of the distance between the major return reflection peaks from the vertex would tend to indicate that the "zero" should be offset to the right by approximately 0.6m. The distance between peaks is consistently approximately 26.3m, which is the same as the focal length. For the subsequent analysis, 0.6m is subtracted from the scale shown on the attached figures.

The reason for the above discrepancy is not clear. However, there are at least two areas of uncertainty in the absolute distance measurements:

(i) Feed position: the feed was set at the standard position for the H.OH feed. This may be assumed to be close to the optimal position, with the phase centre of the horn close to the focus of the parabola.

(ii) An estimate was made for the path length from the calibration point (at the input of the quadridge orthomode transducer) to the phase centre of the horn. This value was 0.5m and will be slightly incorrect, but is likely to be within ±0.1m. Unfortunately, we did not measure, with a tape, the distance from the horn to the

vertex of the antenna to obtain a better indication of the absolute accuracy of the reflectometry measurements.

3.4.2 Dynamic Range:

For linear polarisation, the magnitude of the reflection for distances between 5 and 25m is about -82dBm (i.e. 82dB below the level of the power applied to the input of the OMT). Except for reflections off the tripod legs, this should be the same as that obtained for a termination (about -100dB). Any noise, or interference, entering the feed will tend to increase the level of the noise floor, in the time/distance domain. The level being, better than -80dB, is quite good. The Blackman window function gave a slightly lower noise floor than the Hanning window (about 2dB better). The results without any window function are shown in Fig. A7.

For al plots, a Blackman window was applied to the data before transformation to the time domain. The highest side lobe for this window is -58dB, with a sidelobe decrease of -18dB/octave. The window is similar to the more familiar Hanning window. However, its highest sidelobe is -32dB. Of course, the time/distance resolution is slightly worse using the Blackman window.

3.4.3 Resolution:

The plots indicate that the resolution, as defined by the 3dB points, is approximately 0.6m. From this we can probably determine actual positions to within ±0.1m provided we know the zero range position accurately.

3.4.4 Results near zero range length:

Referring to the results in the range 0-8m, we can draw the following conclusions:

(a) The reflection from the feed at a distance of 0m is obvious. The magnitude appears to be correct. (The program takes into account the number of data points, the zero padding factor and the window function gain to obtain the correct magnitude).

(b) All plots show reflections between the range 2 to 3m, peaking to about -55dB. It is interesting that the data for the Suhner SMA termination shows a similar characteristic, but at a much lower level (-70dB); see Fig. A6. These latter reflections could be interpreted as being due to the continuous low-level reflections along the cable connecting the network analyser to the feed assembly. The calibration obtains the correct phase, and hence time/distance after the FFT. However, there is no correction for the internal reflection off thin cable. A different instrumental setup was tried, and these reflections, up to 5m, were reduced in level. There may also be reflections from the nearest edge of the wooden frame supporting the absorbers (distance about 2m), and the upper section of the tripod structure (distance 5m). More research is required to resolve these issues.

3.4.5 Use of circular polarisation:

By transmitting in one hand of polarisation (say RHC) and receiving the same polarisation, one may look for double bounce reflections. (A single bounce returns the other hand of polarisation). However, the polarisation generated is never absolutely pure: there will always be some of the other hand present. As we used a hybrid (single section one) to generate the circular polarisation, we probably only had 15dB difference between the two hands of polarisation, and so even a single bounce reflection will be reduced in level, compared to a linear polarisation, by about 15dB.

Because of the relatively poor polarisation purity, the results using circular polarisation are no longer considered, but the results are shown in the attached figures.

3.4.6 Use of reference plate:

Although specific reference plates were not used in the two measurement periods, it was later realised that a small helix antenna on a small ground plane (about 20cm diameter), was mounted on a pole at the vertex for the February 1998 measurement program. This reflector was 1.7m above the vertex of the antenna.

The reflectometry results for linear polarisation (Fig. A1 and A2), show a distinct reflection approximately 1.8m before the first primary reflection. This result is consistent with the measured height.

4. Interpretation of Results

4.1 Primary reflections:

The first primary reflection at 26.3m is obvious. Additional multiple reflections, between the antenna surface and feed/focus cabin floor may also be seen. For the antenna in its normal configuration (see Fig. A1 and A5, corresponding to the same antenna conditions, but at different periods, Feb and June 1998), the reduction in magnitude is only about 5dB per hop. However, a comparison of the measurements undertaken with linear polarisations at 90° shows that there are some significant differences between the peak values of the primary reflections (see Figs A1 and A2). This indicates that the struts are having a minor effect on the peak value of the primary reflections.

With absorber under the focus cabin floor, the first primary reflection at 26.3m remains at -50dB, as expected. However subsequent reflections were reduced in level by an additional 11dB, i.e. 16dB/hop.

The cone at the vertex increases the main response by about 8dB, but reduces the magnitude of subsequent reflections to about -24dB/hop as may be seen in Fig. C1(a). The reason for the increase of 8dB in the first return could be due to the increased diffraction at the discontinuity between the cone and surface, which is consistent with the measurement when the cone is covered with absorber.

The results are summarised in Table 1.

Table 1
Reflectometry Tests - A Summary
(Linear Polarisation)

Antenna Configuration	Ref	Intensity first hop (dB)	Intensity decrease per hop (dB)	Fig. No.
Normal operation	A	-50 [1]	5	A1 A2 A5
Absorber on focal-plane	B	-50	16	B1
Add experimental metal cone at vertex	C1	-42 [2]	24	{C1(a) {C1(b) {C1(c)(i)
Add absorber over cone	C2	-42	(24)	C2
Absorber over theodolite and discontinuity between cone and antenna surface	C3	-44	(30)	C3

Notes:
(1)Use of CP typically reduced first hop by
[1]: - 13dB; Fig. A3/A4,
[2]: - 18dB; Fig. C1 (c) (ii), -15dB/hop

(2) Difference between hops: 26.1m, (focal length = 26.24m)

4.2 Secondary reflections:

The primary reflections are seen to be always considerably stronger than the secondary reflections. Consequently it is difficult to glean a lot from the detail of the plots showing the secondary reflections. This process is made more difficult by the poor resolution corresponding to distances close to the vertex. This is clearly shown by referring to the table in the Annex. For example, the radial distance from the antenna axis to the edge of the solid surface is 8.35m, but in terms of the corresponding distance from the focus, the difference, relative to the vertex, is only 0.66m!

However, an initial study of the secondary reflections corresponding to radial distances of 26.2m (vertex) to 36m (the edge of the antenna), shows the following (using the designators (a) to (i) for each of the peaks in Fig. A5 as a reference);

- "(b)" is consistently present for all measurement conditions. It is at a distance corresponding to the edge of the solid reflector surface.
- "(c)" is consistently relatively high but its distance (29.6m) could indicate that there is some reflection from the gap between perforated-aluminium panels, rings 6 and 7.
- "(f)" corresponding to a distance of 32m (the base of the tripod legs) is consistently observed when linear polarisation in the same direction as one of the legs, is used.
- "(i)" at a distance from the focus of about 35.5m corresponds to the edge of the antenna is consistently present for all measurement configurations.
- Rotation of linear polarisation: a comparison of Fig. A1 and A2 shows considerable differences in the relative levels of many of the secondary reflections when the polarisation is rotated through 90°.
- Circular polarisation: There are differences in the levels, but they are not as marked as with the two linear polarisations.

5. Conclusions

The reflectrometry measurements highlighted the following results:

(a) The primary responses always appear at intervals of about 26.2m which corresponds approximately to the focal length (26.24m).

(b) Absorber under the focus cabin floor attenuates the multiple reflections of the signal, as expected. However, the initial primary response is not changed at all (also as expected).

(c) The cone at the vertex attenuated the primary reflections beyond the first. However, the initial primary response is increased by a factor of about 6 in (power) magnitude (8dB), indicating that for this cone design it is, at least, far from optimum.

(d) For the reflectrometry results, associated reflections off the tripod legs, although generally not significant except for the upper sections close to the feed, do play some role in modifying the peak values of the primary reflections when the (linear) polarisation is rotated through 90°.

(e) The shape of the raised portion in the centre of the surface needs to be addressed and its optimisation considered. One option may be to return the central section of the dish to be paraboloidal, it being impossible to reduce reflections for all observing frequencies with a fixed cone at the vertex.

Acknowledgements

The senior author (G.R. Graves) wishes to thank Mal Sinclair for his support and discussions over the past several years. Both authors thank Mike Kesteven for preparing the software, and the Parkes staff for their extensive support during the two measurement programs.

Reference

(1) J.R. Fisher, "Reflection measurements on the 140-foot and 300-foot radio telescopes", National Radio Astronomy Observatory, Green Bank, Wva, USA, Jan. 1978, (Private Communication).

Ref:19-98

ANNEX 1

Distance from Focus to Given Positions on Reflector Surface

The Reflector Surface:

The reflector surface consists of an inner region of high-precision solid metal panels (dia, 16.7m) 8 rings of perforated aluminium panels (dia, 44m), the remaining surface consisting of the original wire-mesh panels.

The (radial) length of the perforated aluminium panels are 1900mm (Nos. 1-4), and 1870mm (Nos. 6-8), whereas panel No. 5 is approximately one-half the size of the other panels.

There are some significant gaps between some of the panels (see table). The gap between the solid-metal panels and perforated aluminium panels was bridged some years ago with a metal strap. However, approximately 10mm gaps still exist between panels 2 and 3, 4 and 5, and, 6 and 7.

TABLE

Location of critical points on reflector surface

Critical Point	Radial Distance Normal to Antenna Axis (m)	Distance from Focus to Critical Point (m)
Focal length	0	26.24
Edge of expl. Cone	2.94	26.32
Edge of solid surface	8.35	26.90
Gaps between perforated* al. Panels		
• #2 and 3	12.10	27.63
• #4 and 5	15.75	28.60
• #6 and 7	18.50	29.50
Edge of perf. Surface (panel #8)	22.00	30.85
Base of tripod	23.61	31.55
Edge of antenna	32.00	36.00

* Note: At this radius, there was once a gap between the high-precision solid-surface panels and the perforated-aluminium panels. Many years ago it was found that this discontinuity produced a reflection, and contributed to the baseline ripple. To reduce the problem, pieces of aluminium were rivetted over the gap. While the height of this covering metal is not very thick (approx. 3mm), it has a large area (approx. $5m^2$) and it is all in phase for a feed at the focus of the antenna. Holography, at 12.75GHz, clearly shows this ring.

pks06.dat

Parkes Baseline Ripple Tests (Reflection Data)

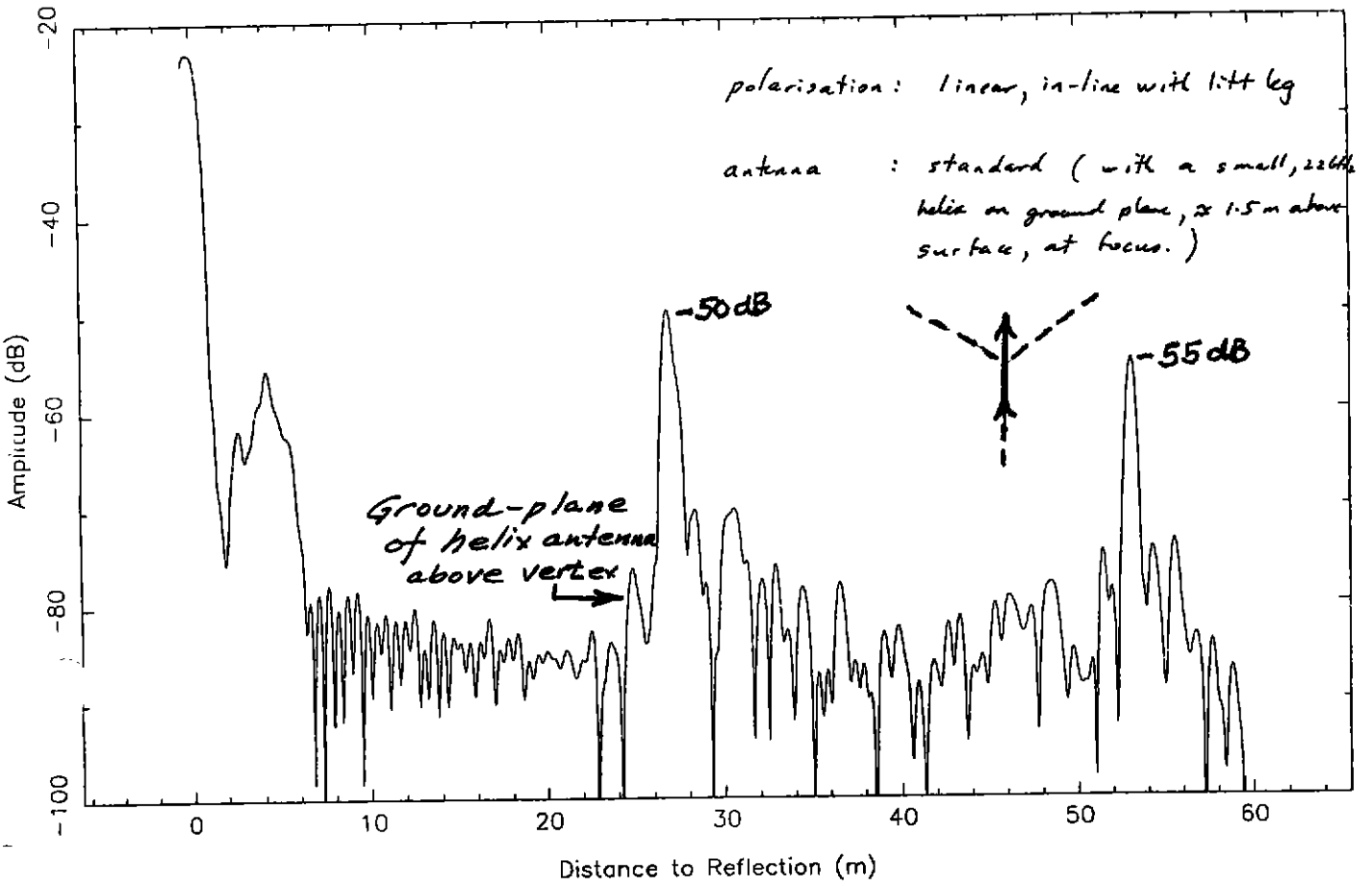

pks06.dat

Parkes Baseline Ripple Tests (Reflection Data)

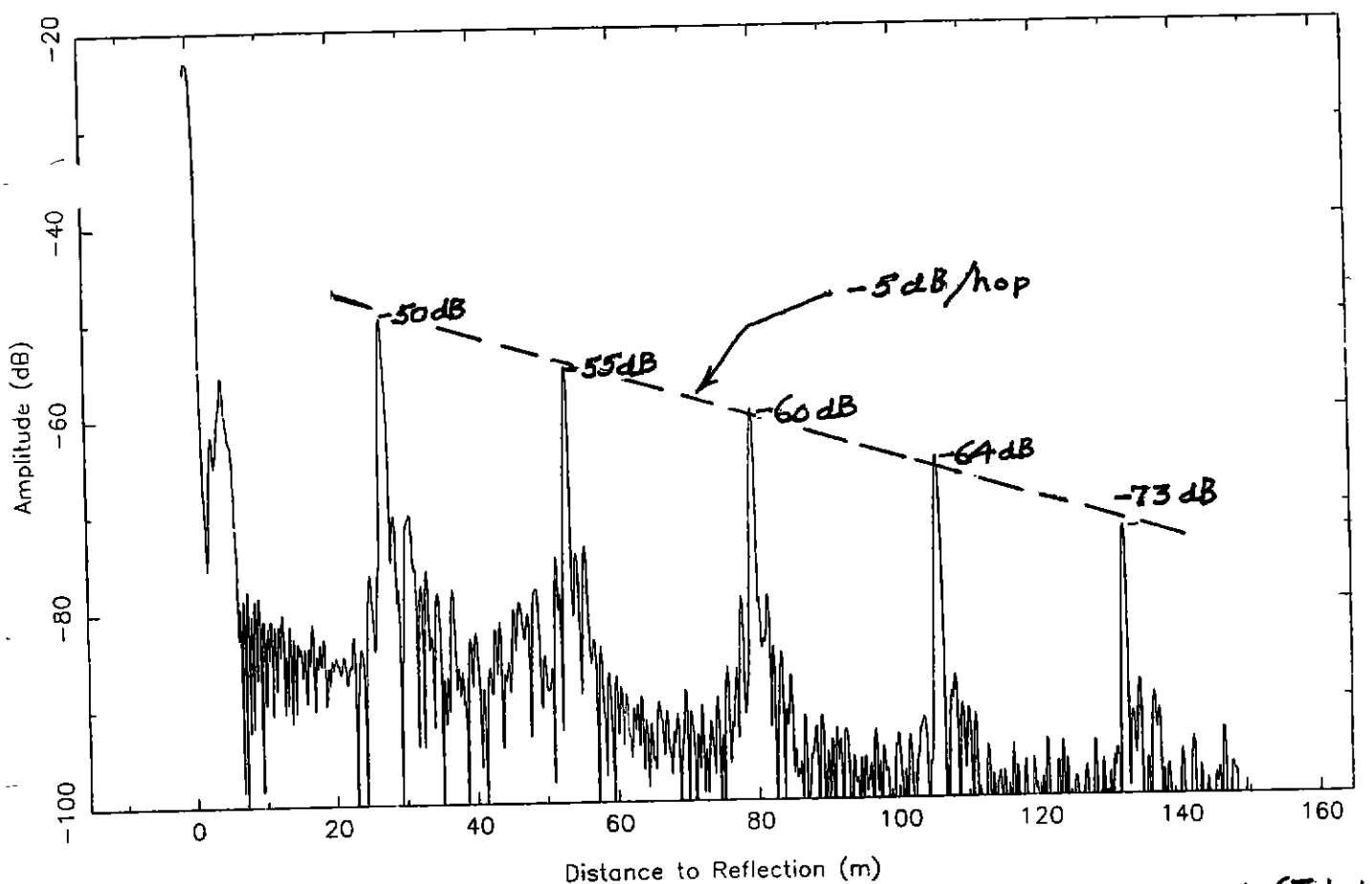

A1 (Feb 1998)

pks07.dat

Parkes Baseline Ripple Tests (Reflection Data)

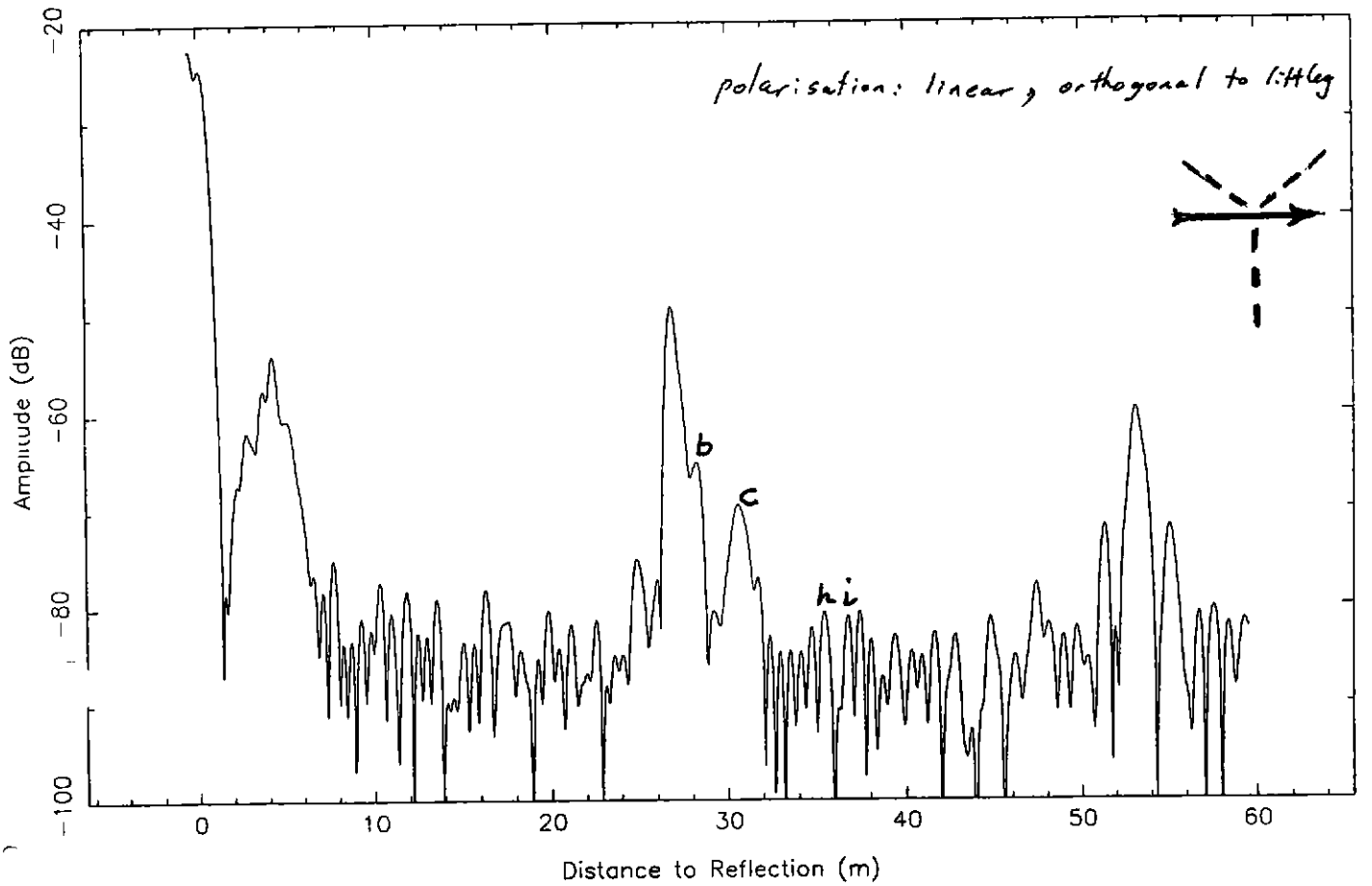

pks07.dat

Parkes Baseline Ripple Tests (Reflection Data)

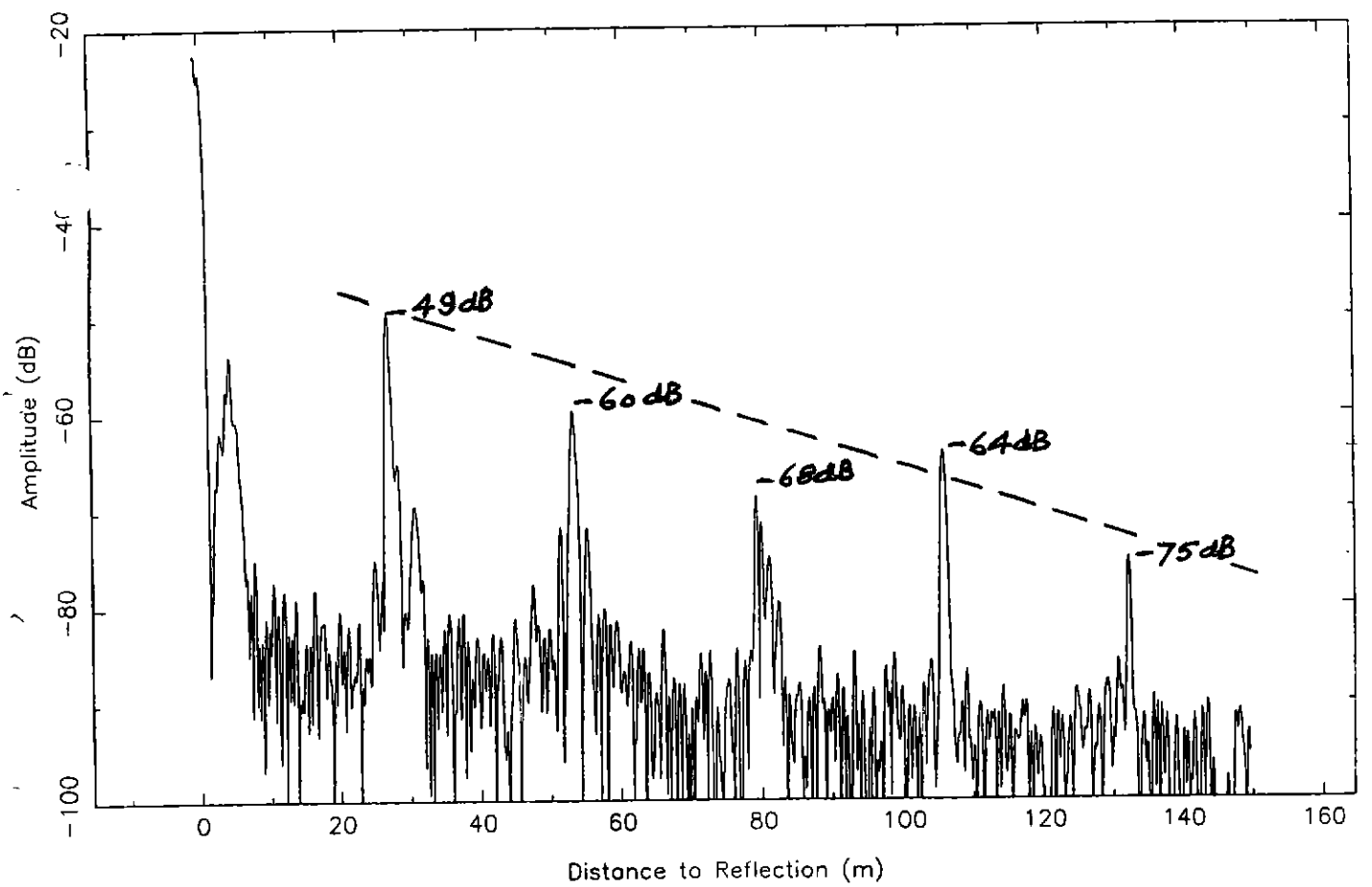

pks08.dat

Parkes Baseline Ripple Tests (Reflection Data)

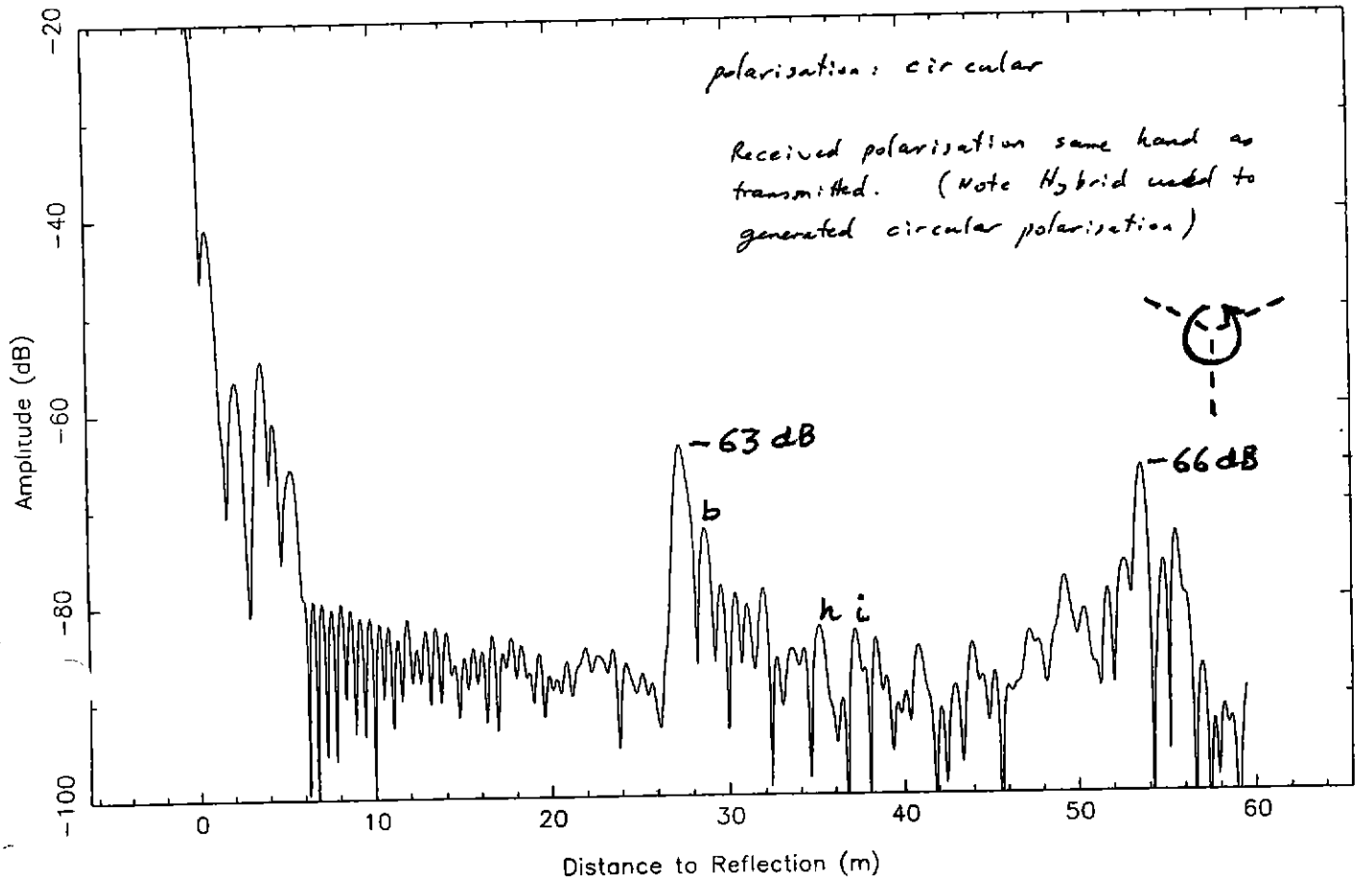

pks08.dat

Parkes Baseline Ripple Tests (Reflection Data)

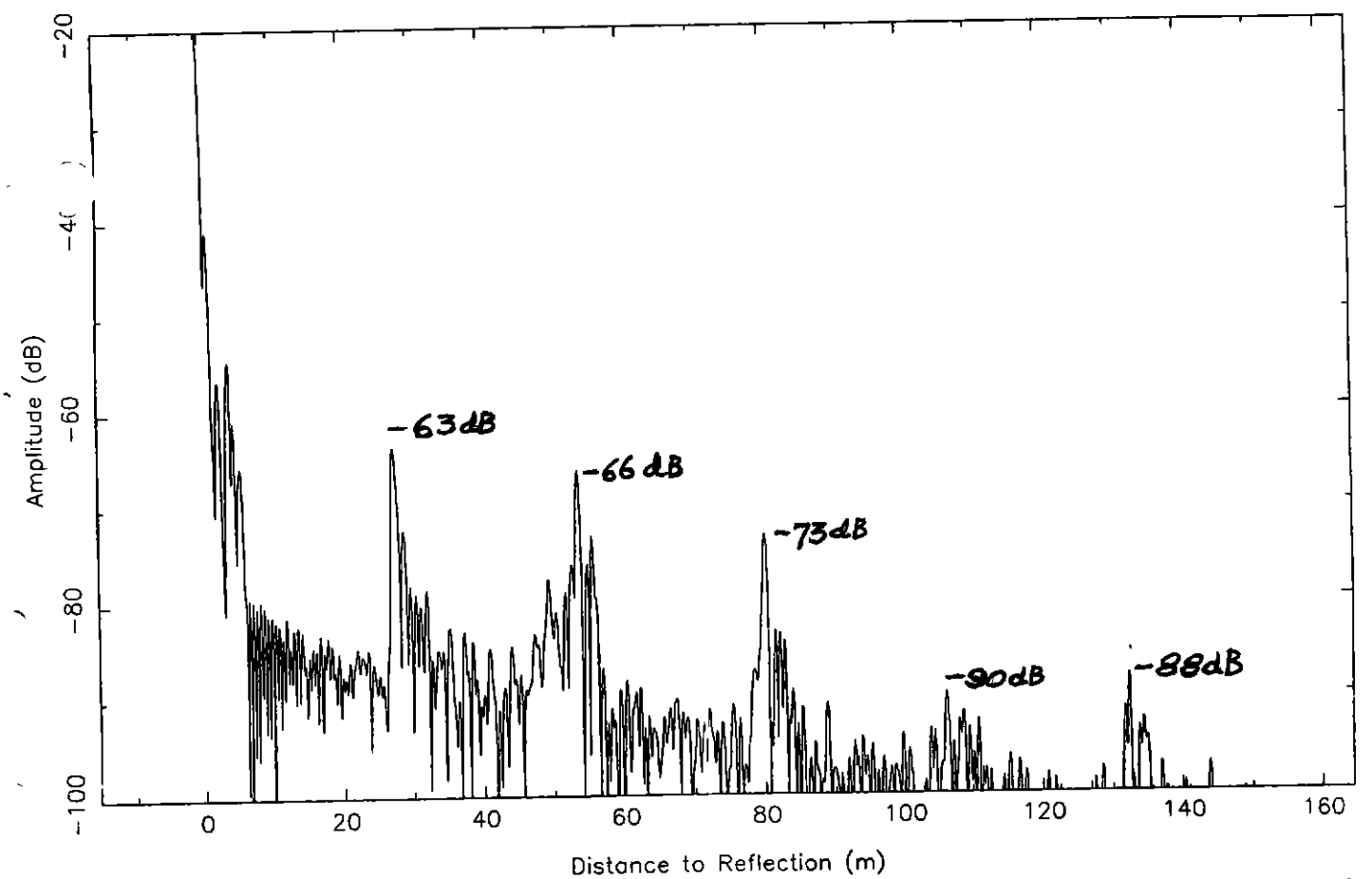

A3 (CP)

pksoq.dat

Parkes Baseline Ripple Tests (Reflection Data)

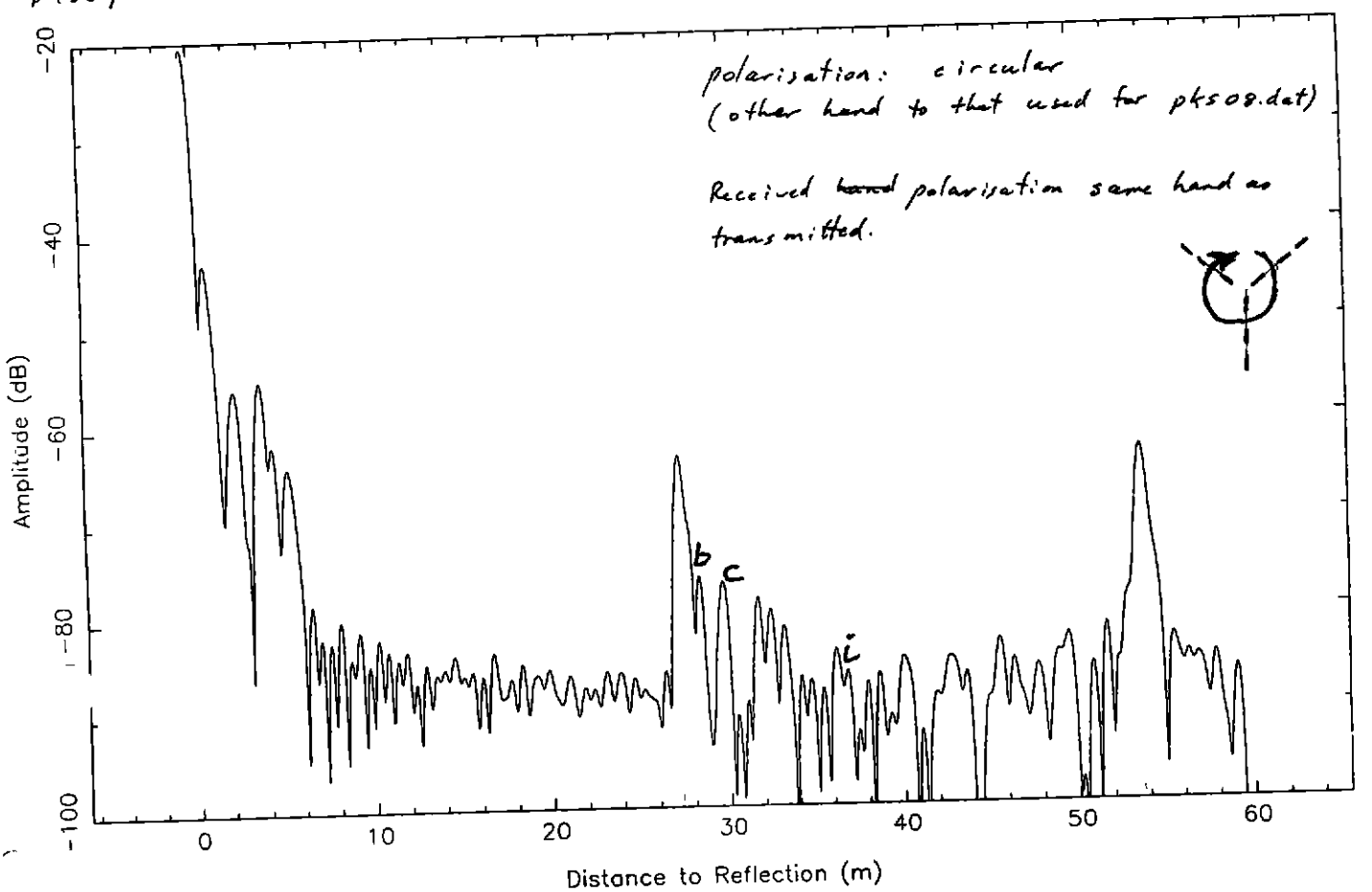

pksoq.dat

Parkes Baseline Ripple Tests (Reflection Data)

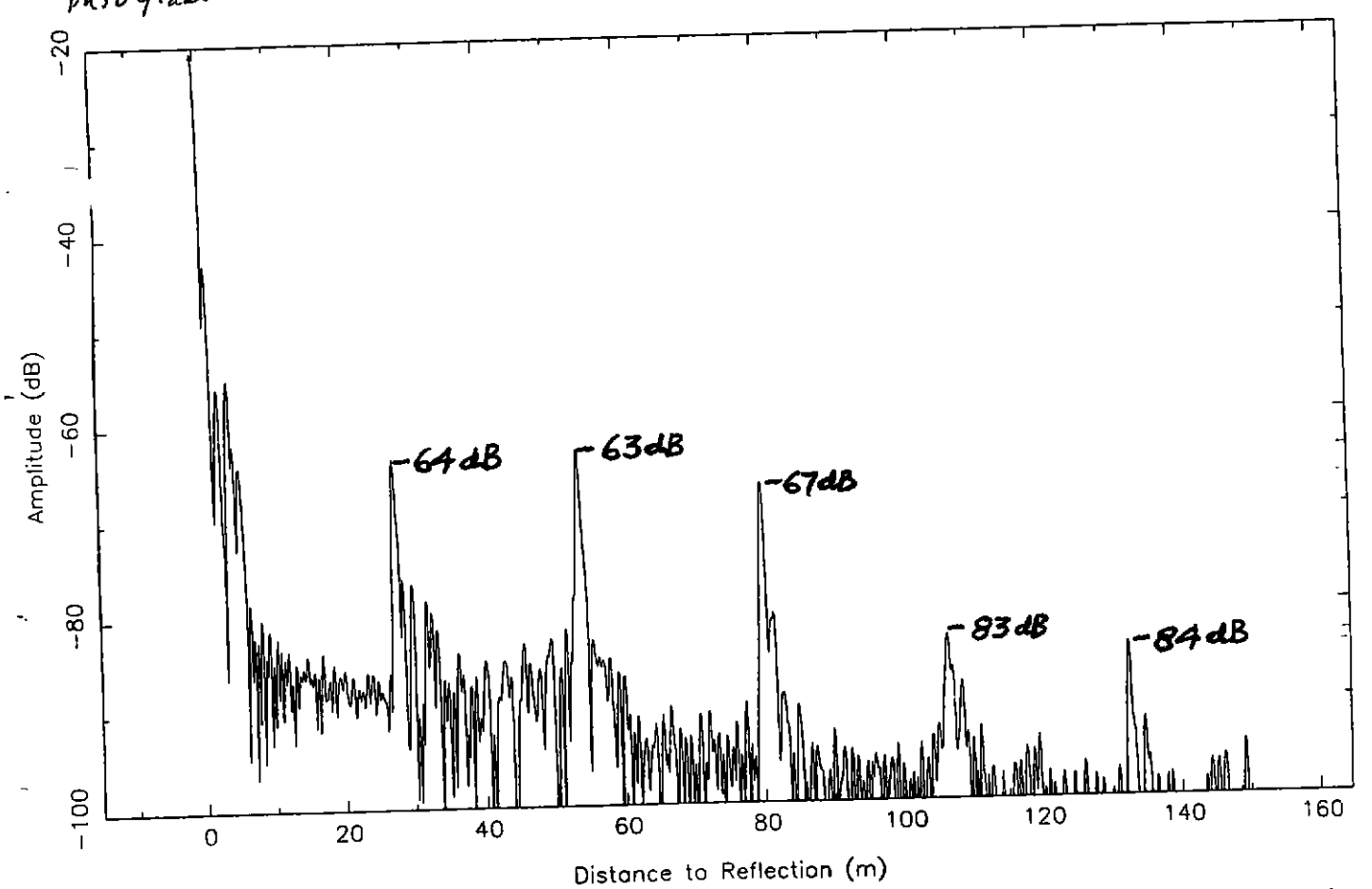

A4 (CP)

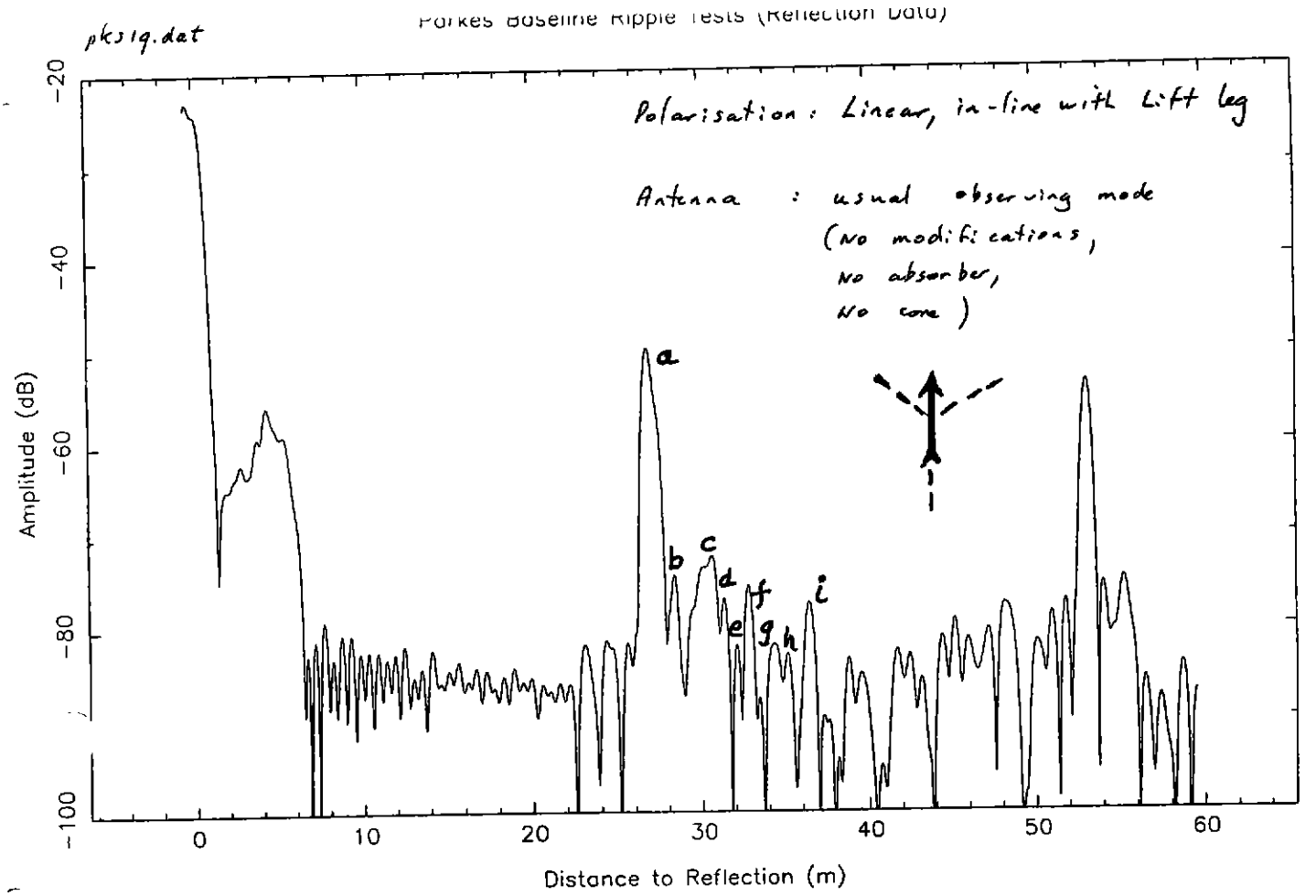
pks19.dat
Parkes Baseline Ripple Tests (Reflection Data)
Polarisation : Linear, in-line with Lift leg
Antenna : usual observing mode
(No modifications,
No absorber,
No cone)
a
b
c
d
e
f
g
h
i
Amplitude (dB)
-20
-40
-60
-80
-100
0
10
20
30
40
50
60
Distance to Reflection (m)

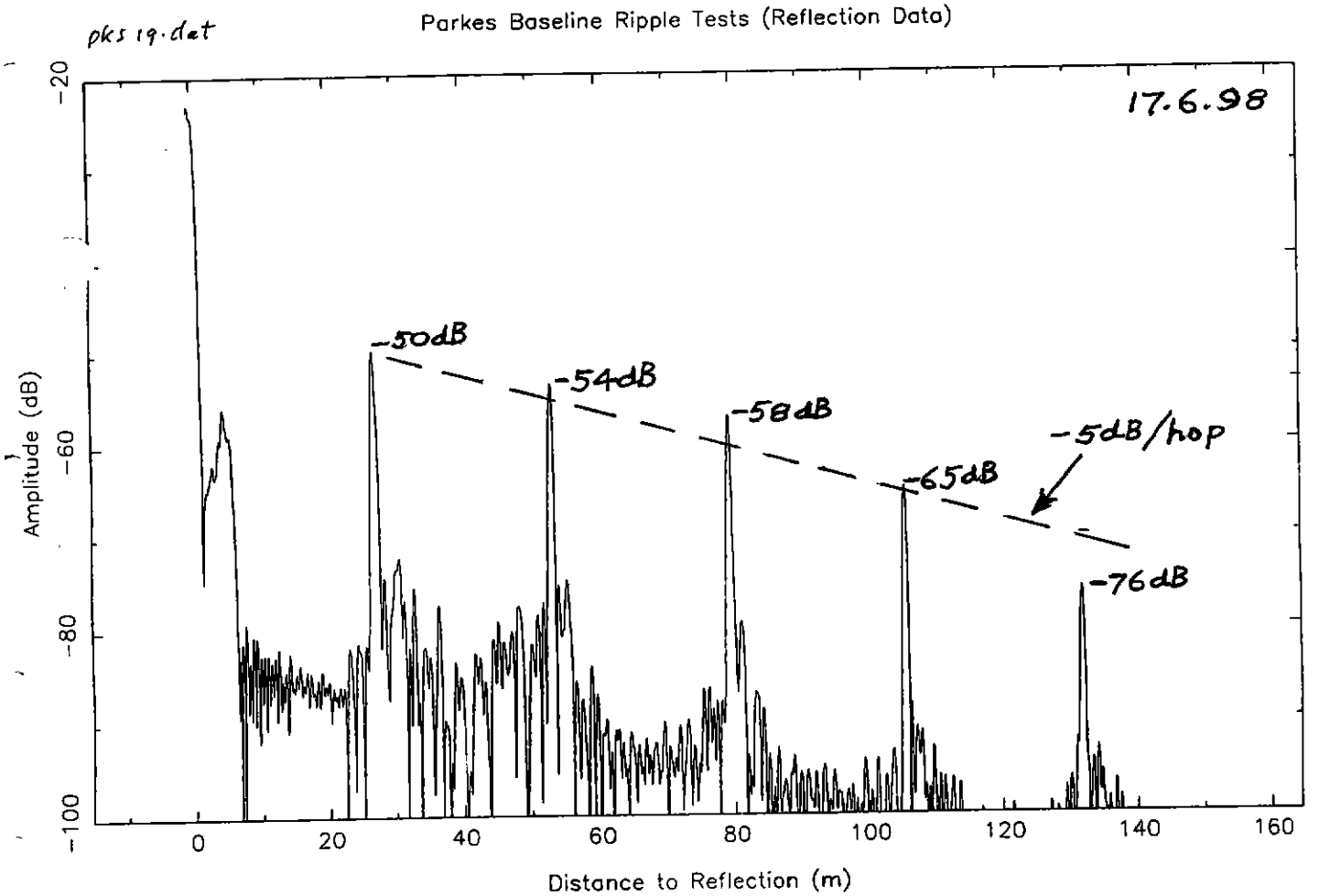
pks19.dat
Parkes Baseline Ripple Tests (Reflection Data)
17.6.98
-50dB
-54dB
-58dB
-65dB
-76dB
-5dB/hop
Amplitude (dB)
-20
-60
-80
-100
0
20
40
60
80
100
120
140
160
Distance to Reflection (m)

A5 (June 1998)

pks 10.dat

Parkes Baseline Ripple Tests (Reflection Data)

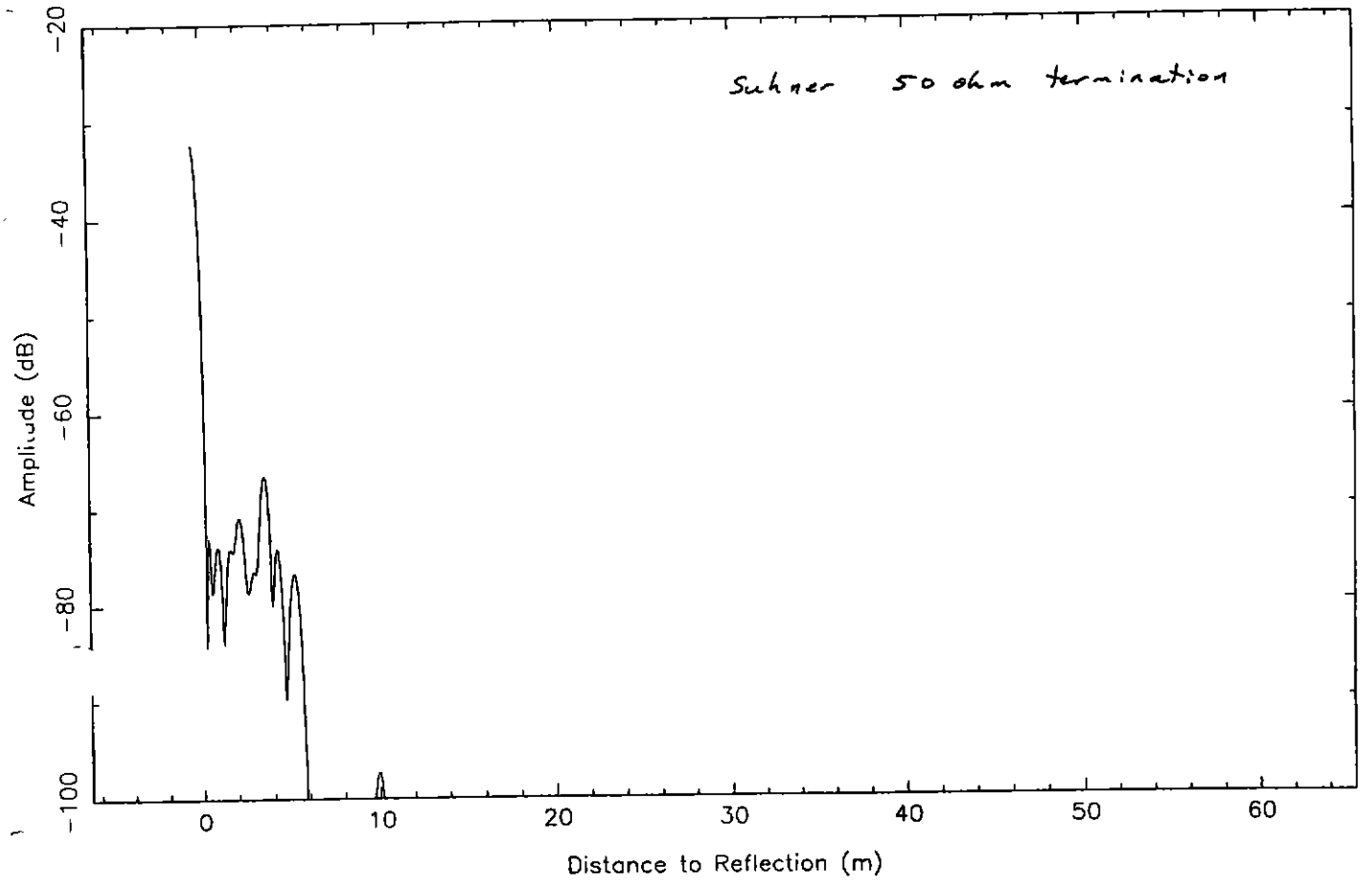

pks 10.dat

Parkes Baseline Ripple Tests (Reflection Data)

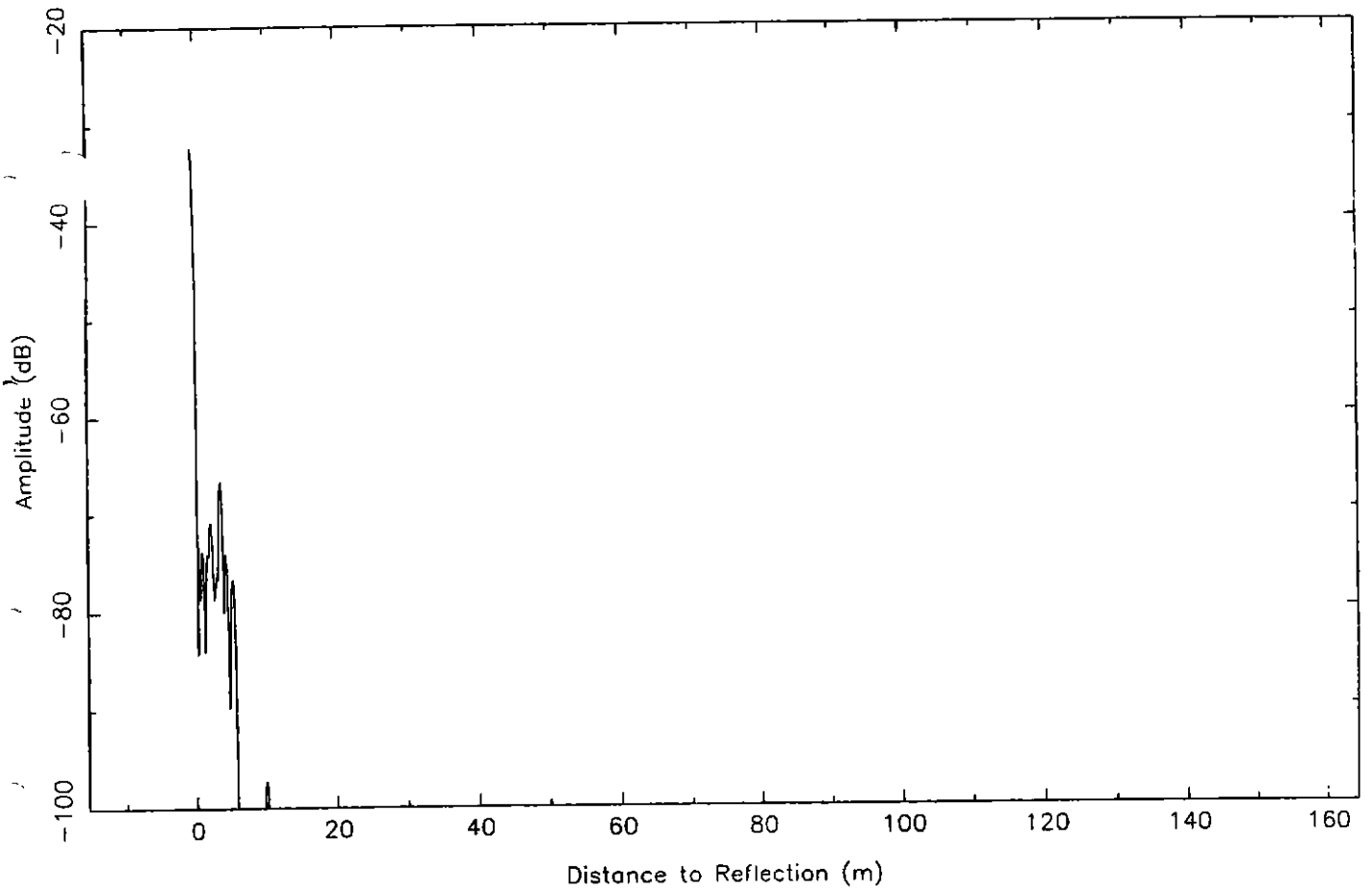

pks19.dat

Parkes Baseline Ripple Tests (Reflection Data)

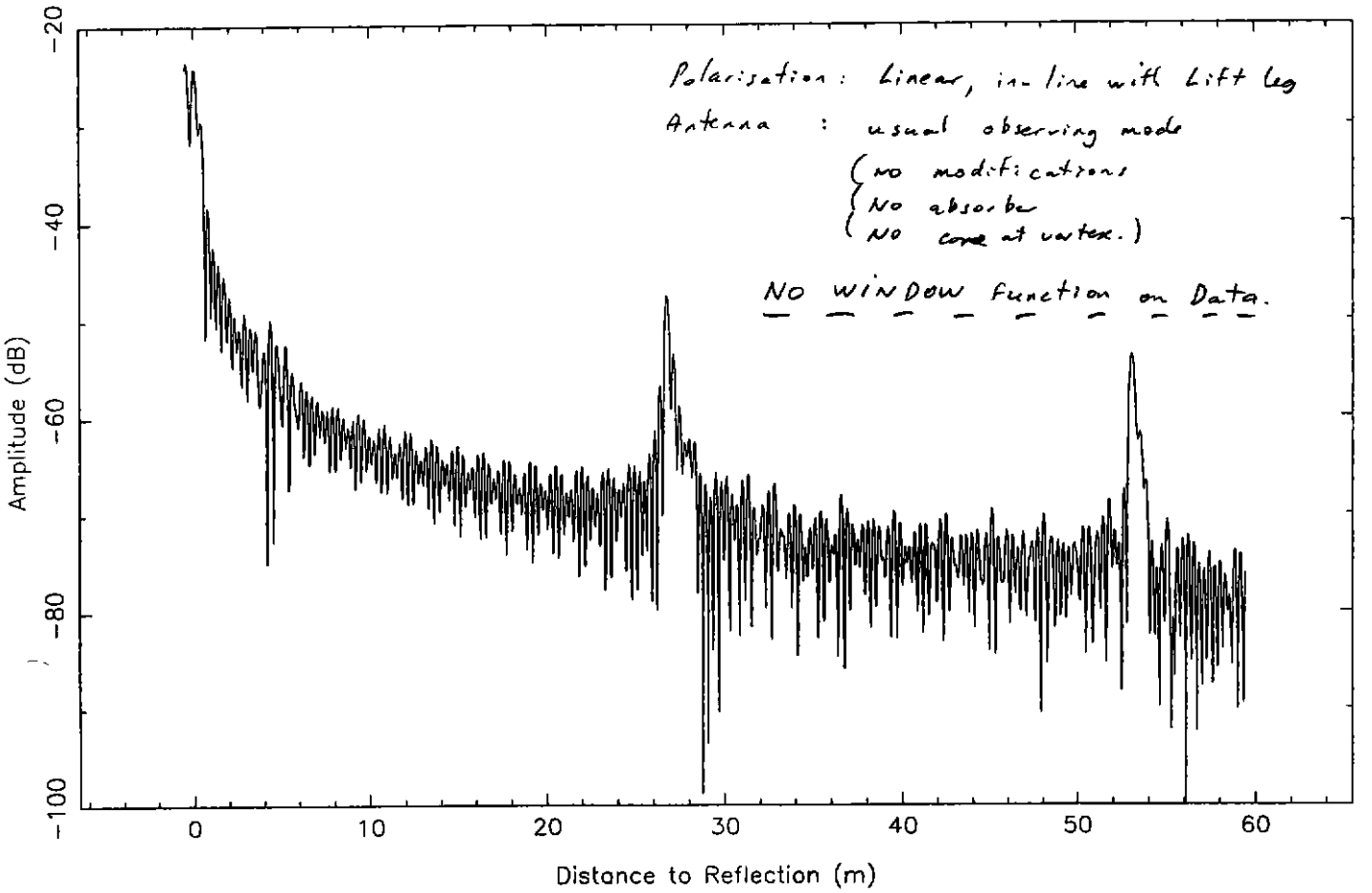

pks19.dat

Parkes Baseline Ripple Tests (Reflection Data)

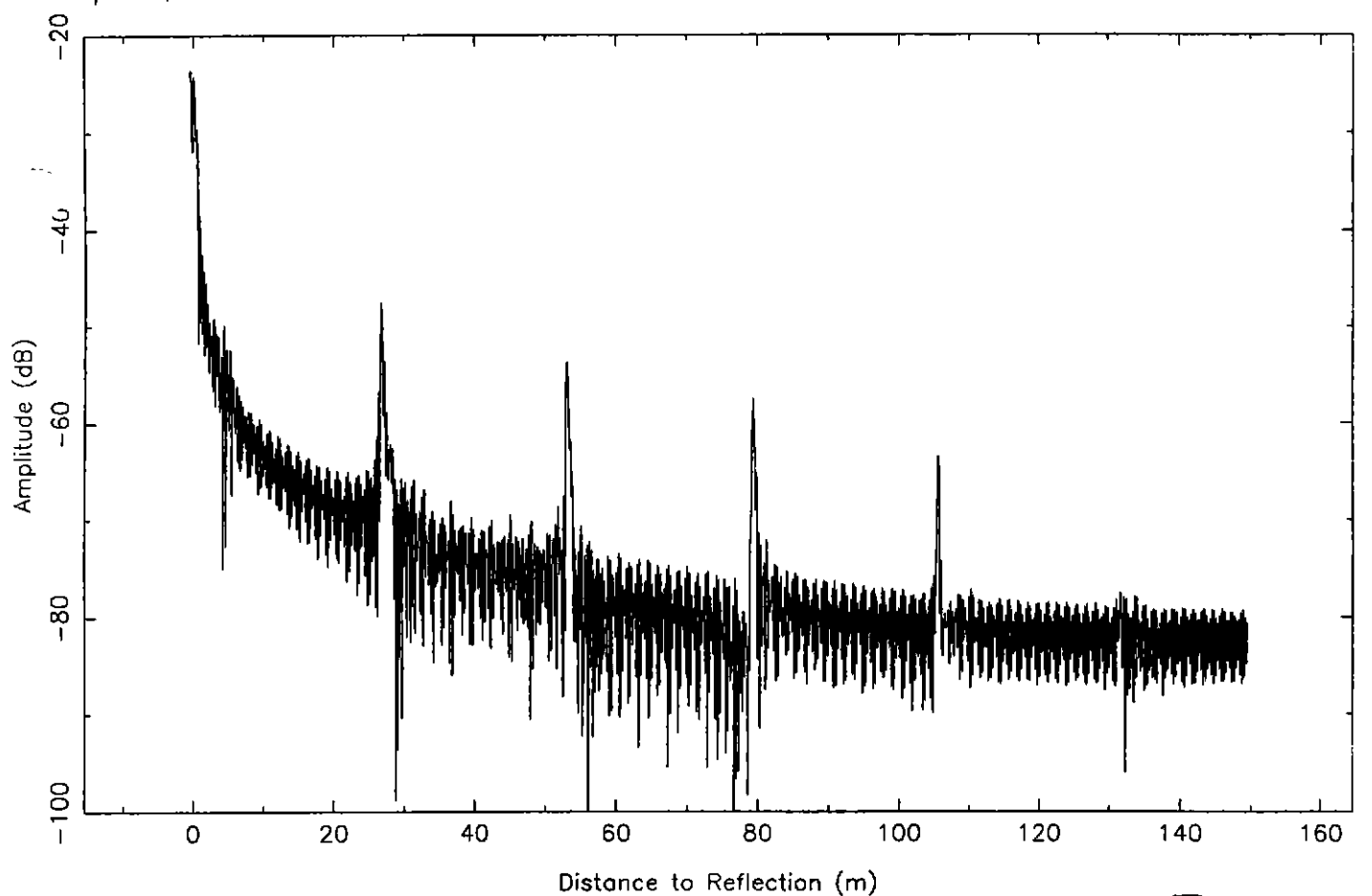

Pks 11. dat

Parkes Baseline Ripple Tests (Reflection Data)

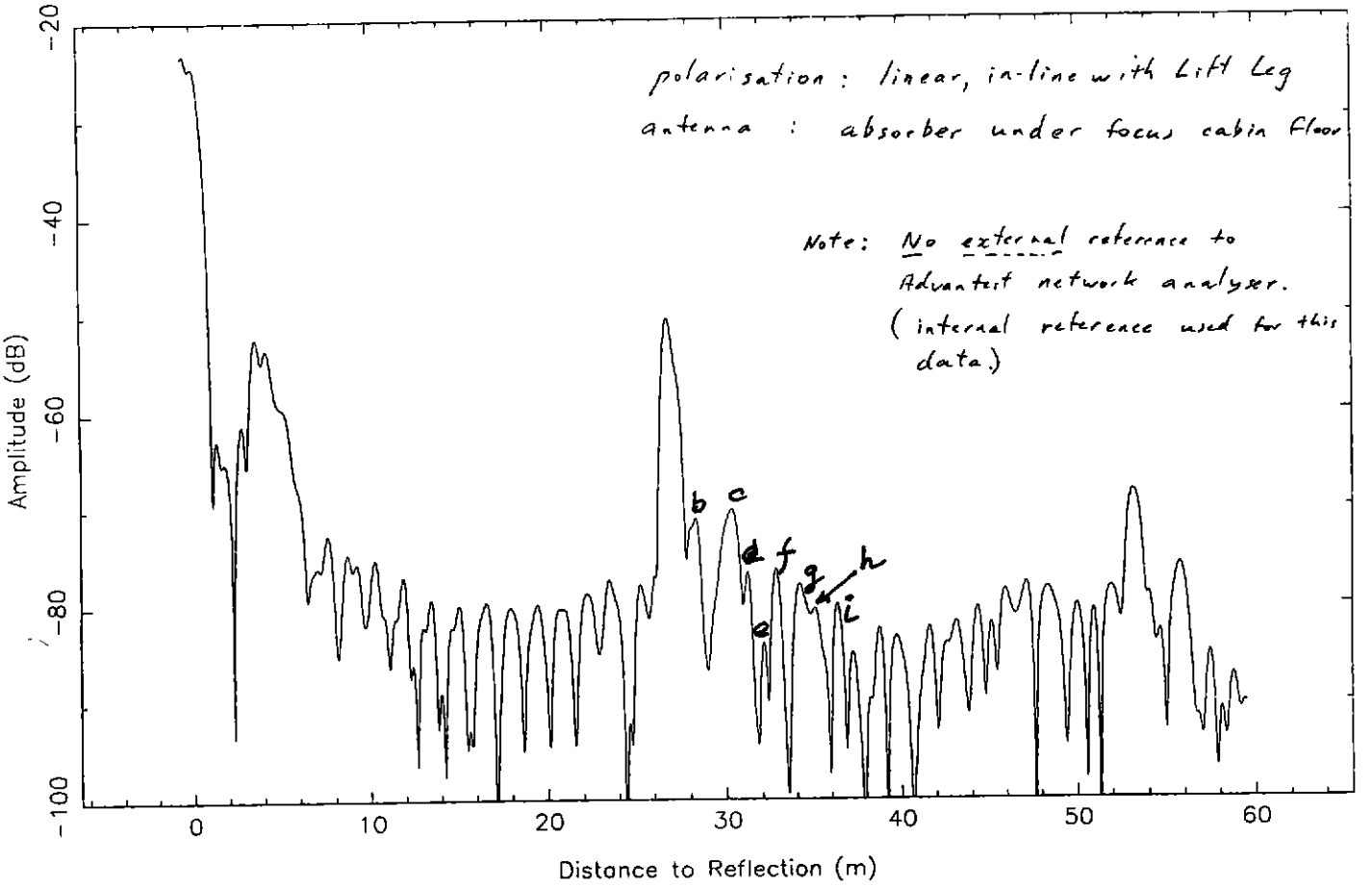

Pks 11. dat

Parkes Baseline Ripple Tests (Reflection Data)

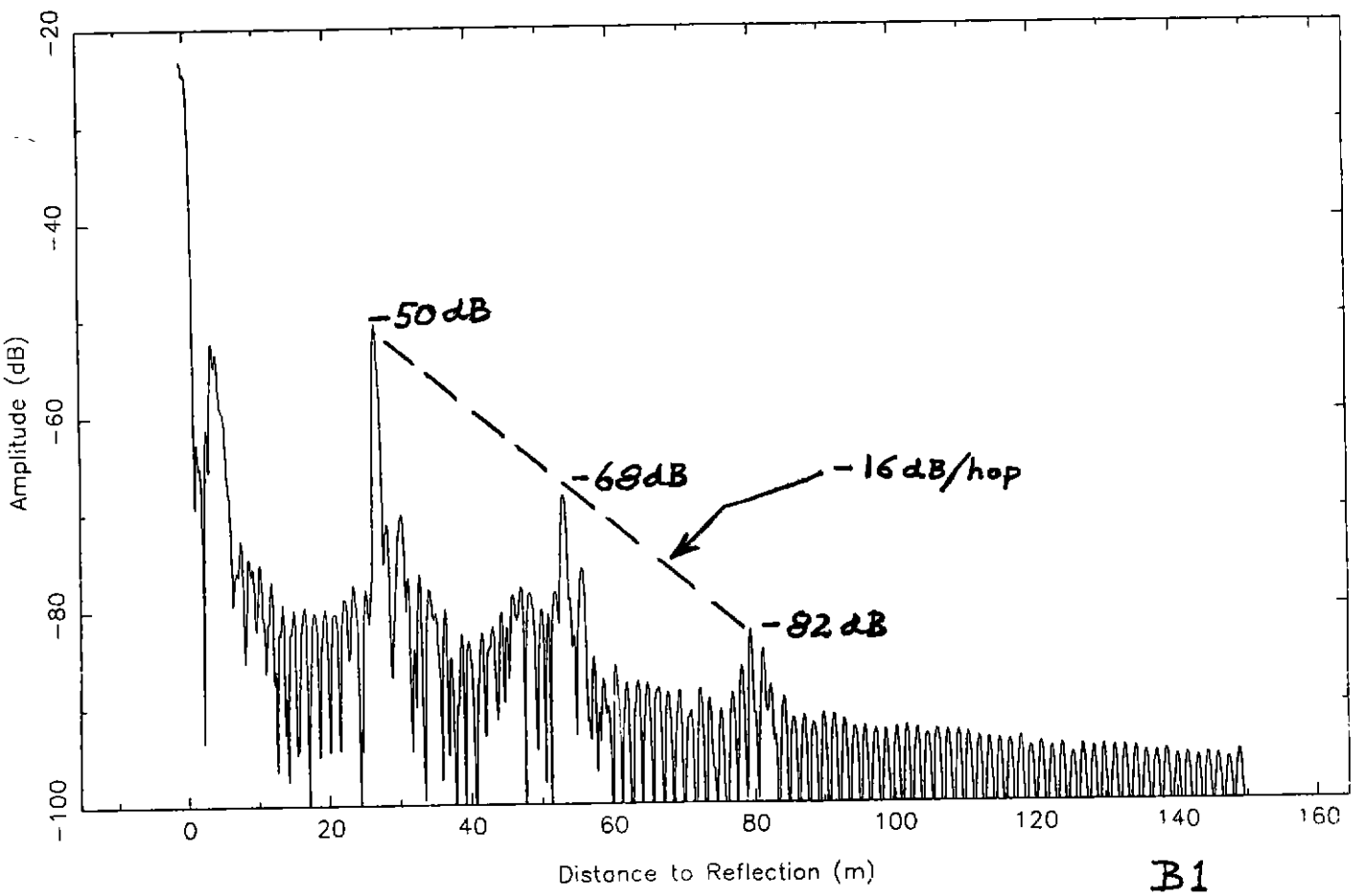

pks13.dat

Parkes Baseline Ripple Tests (Reflection Data)

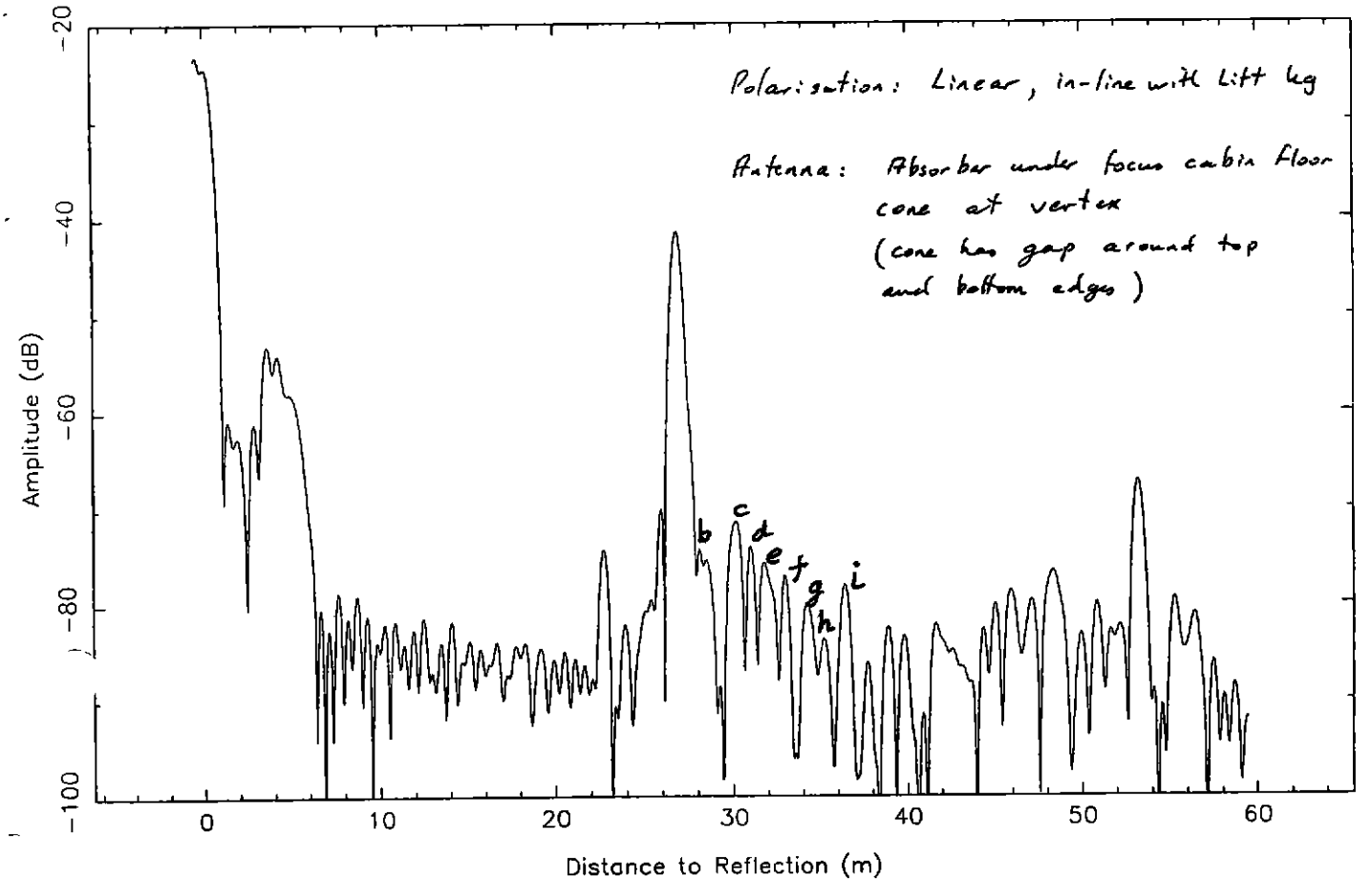

pks13.dat

Parkes Baseline Ripple Tests (Reflection Data)

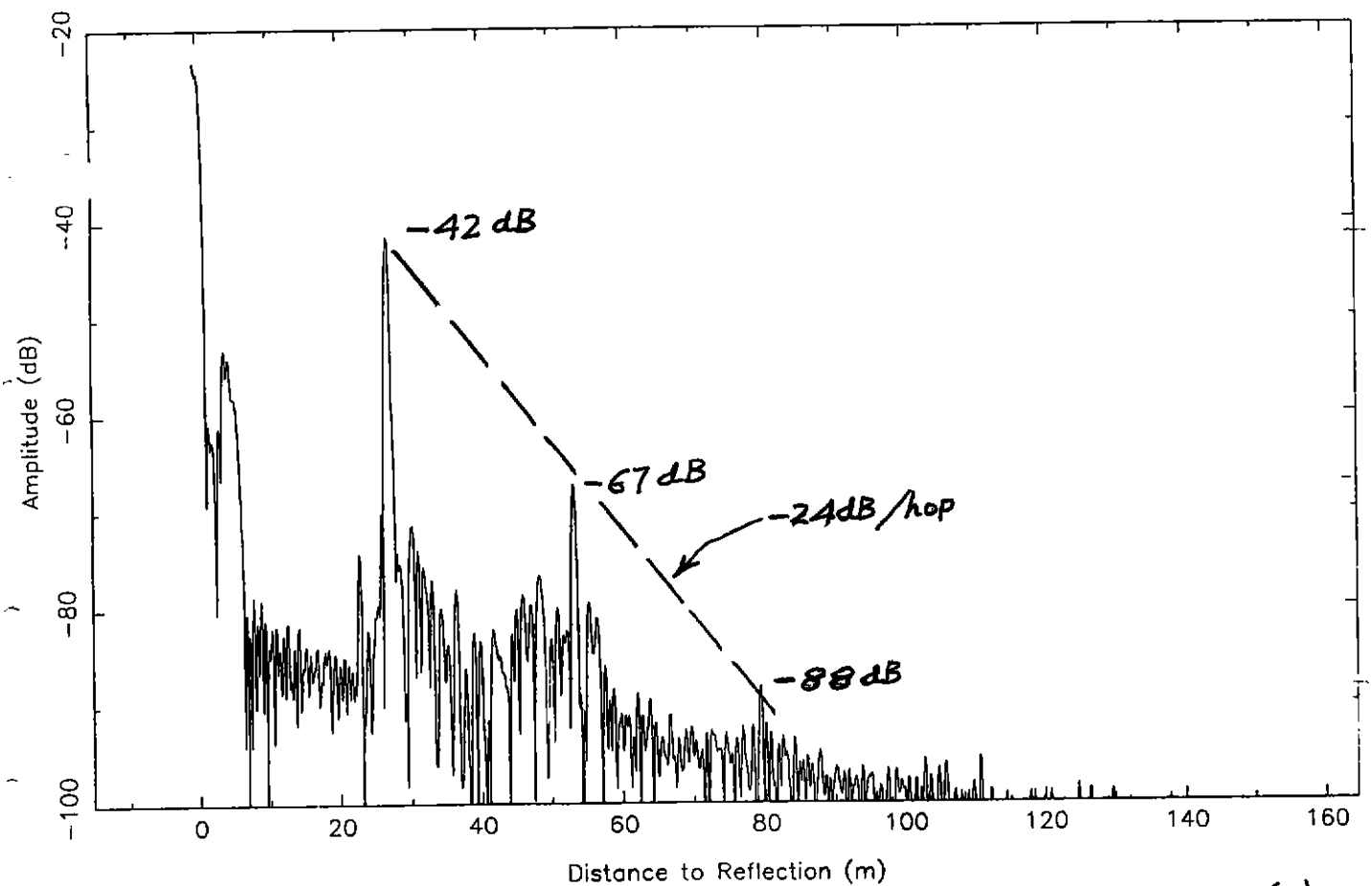

C1 (a)

pks 14.dat

Parkes Baseline Ripple Tests (Reflection Data)

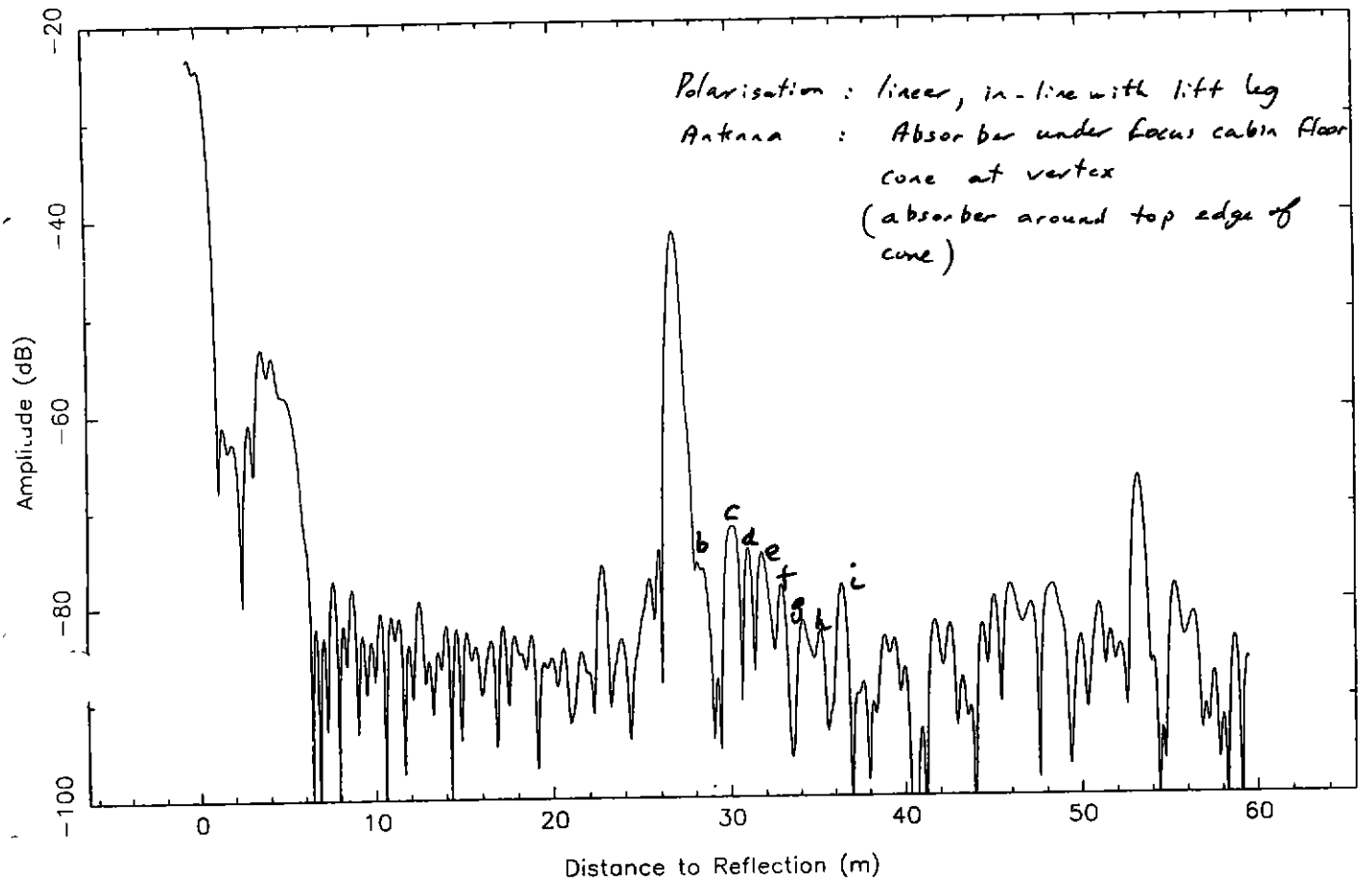

pks 14.dat

Parkes Baseline Ripple Tests (Reflection Data)

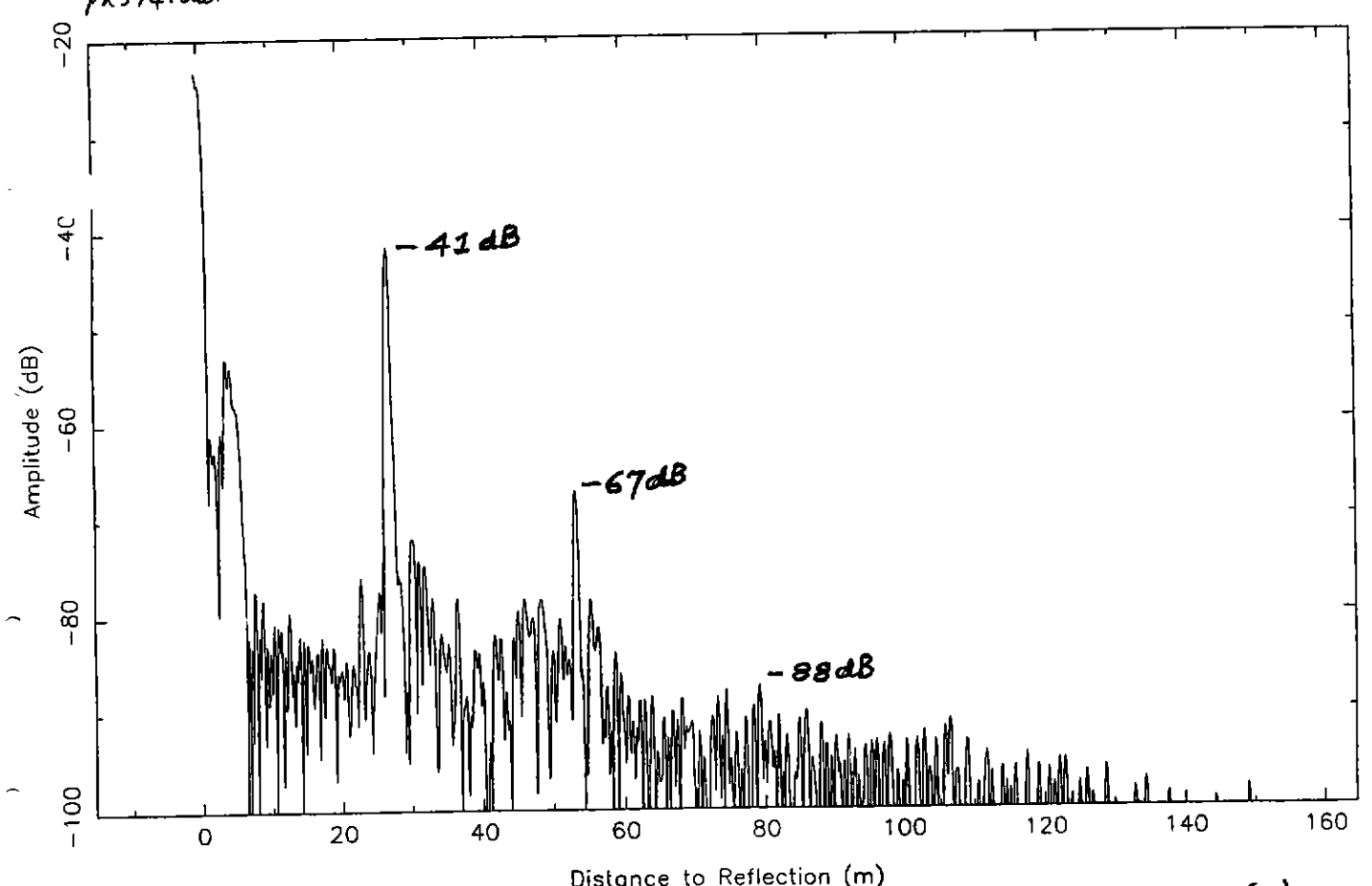

C1 (b)

pks15.dat

Parkes Baseline Ripple Tests (Reflection Data)

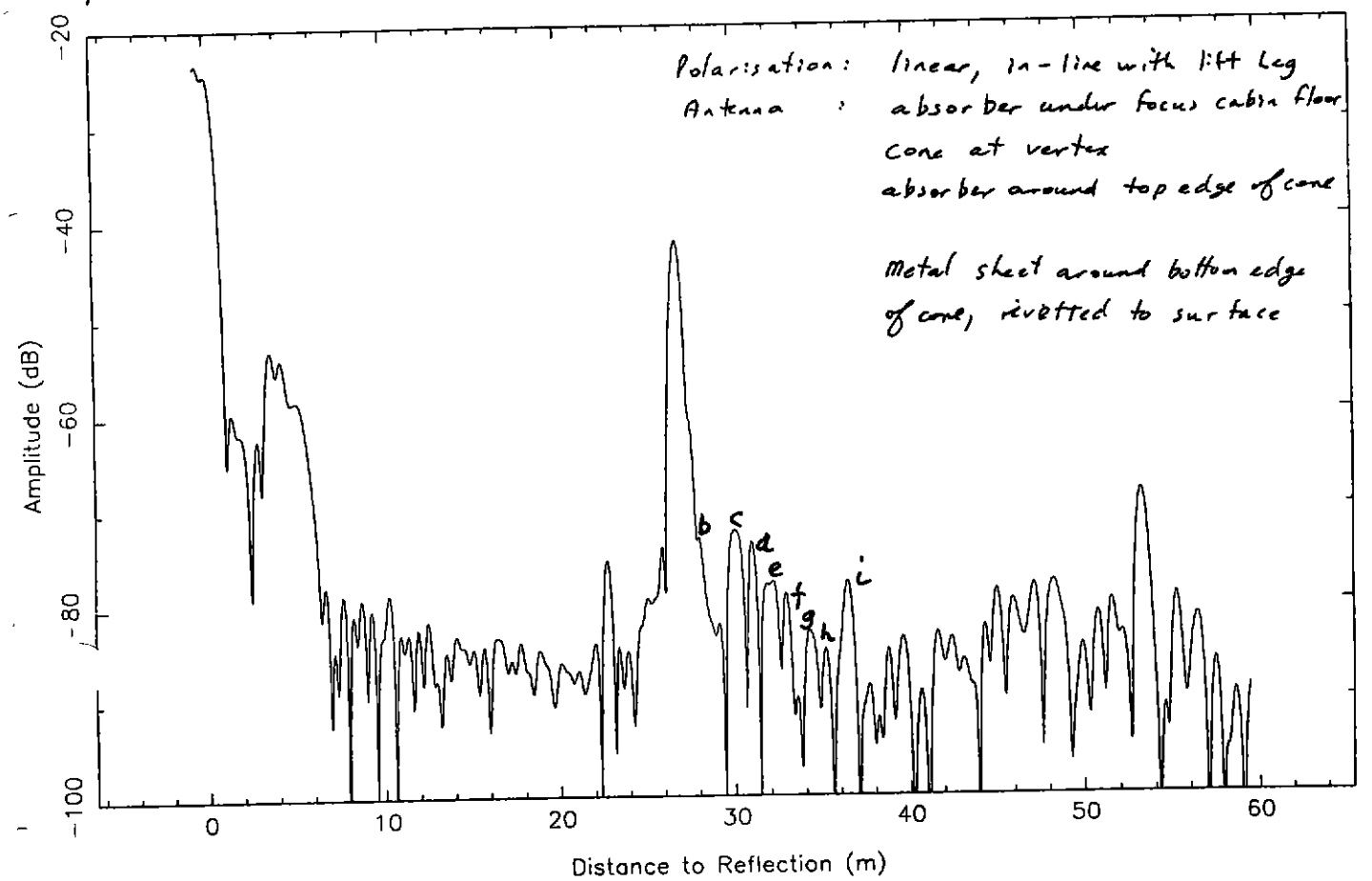

pks15.dat

Parkes Baseline Ripple Tests (Reflection Data)

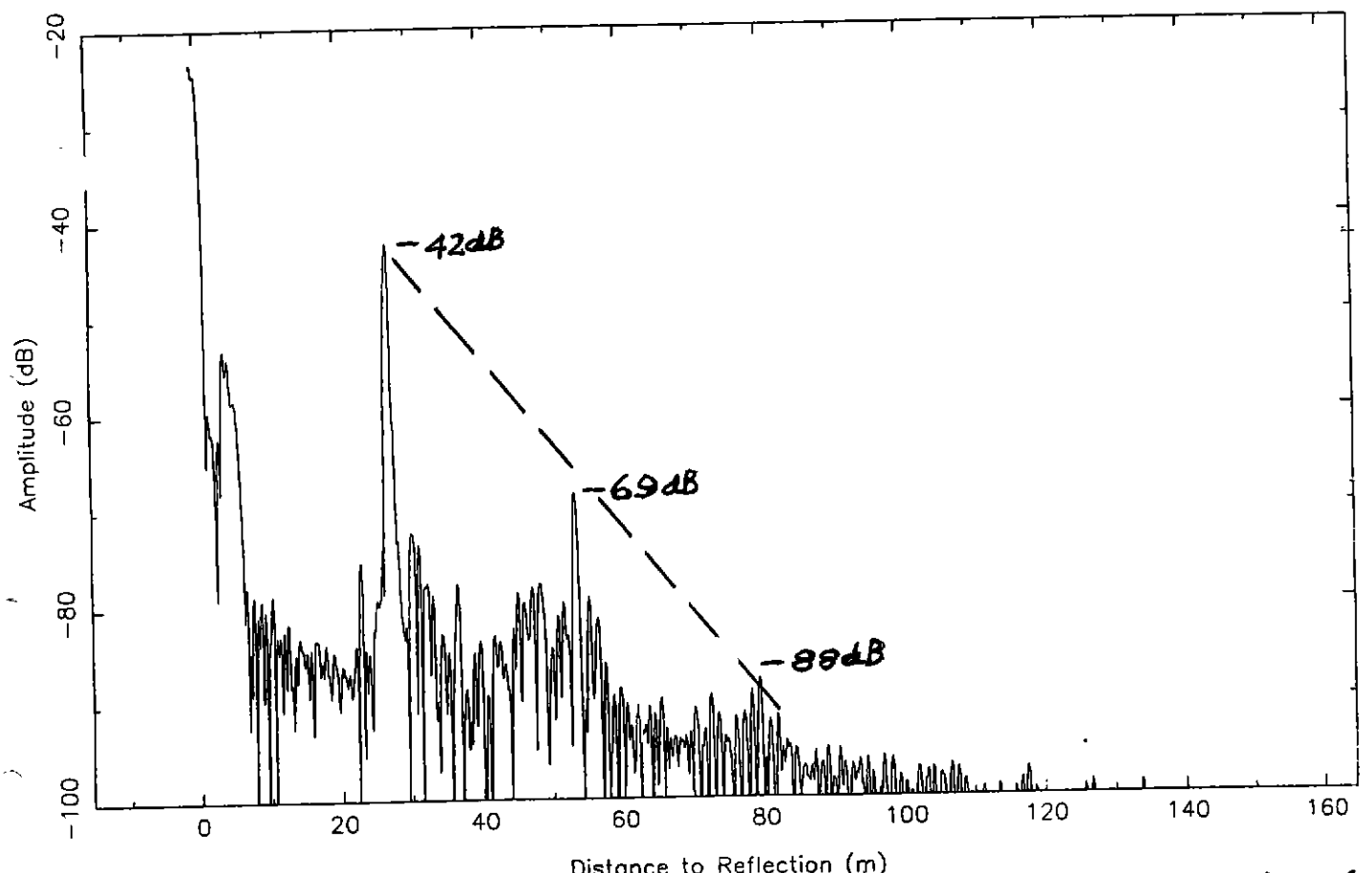

C1 (c) (i) - (LP)

pks 16.dat

Parkes Baseline Ripple Tests (Reflection Data)

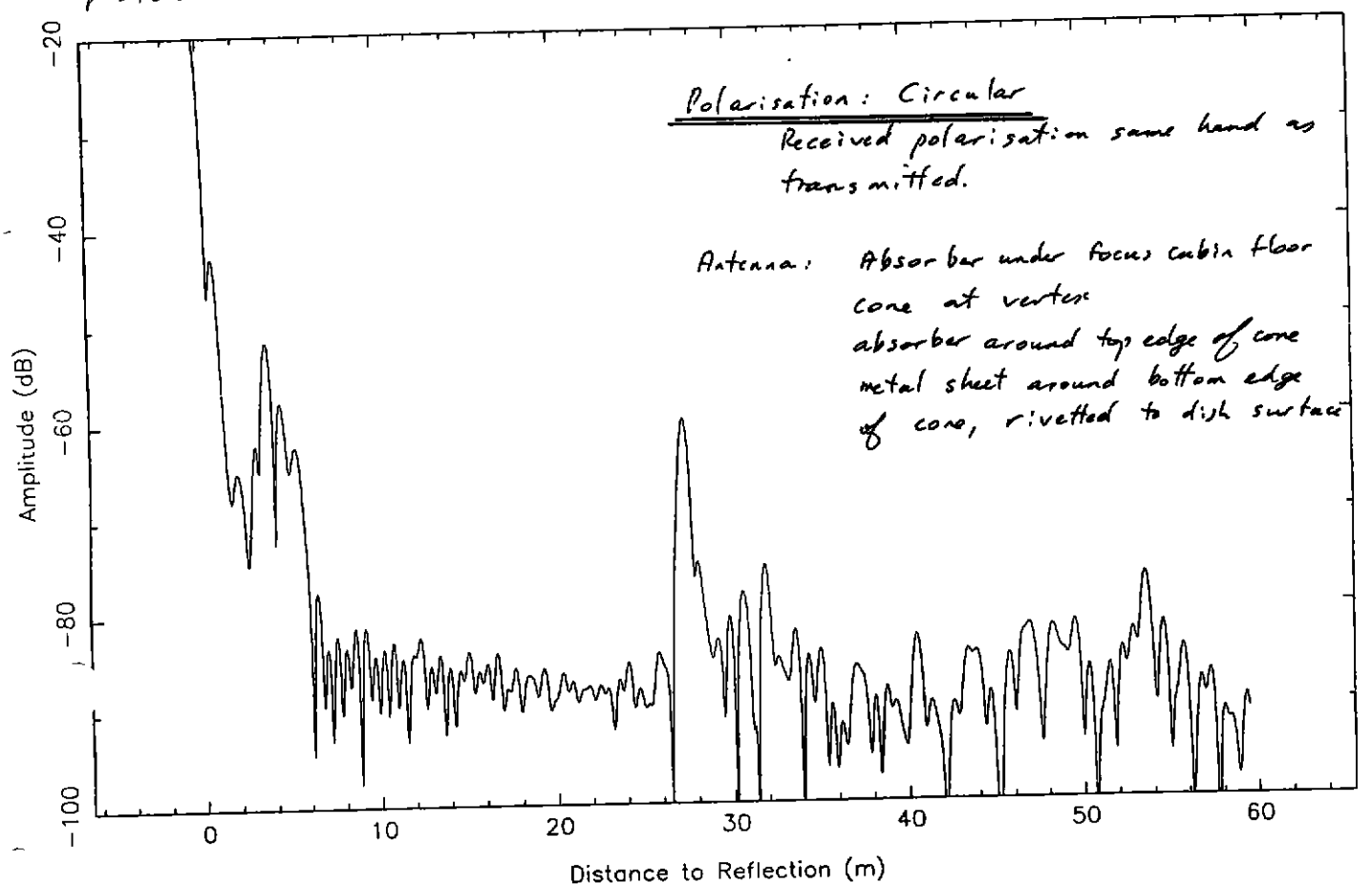

Polarisation: Circular
Received polarisation same hand as transmitted.

Antenna: Absorber under focus cabin floor
cone at vertex
absorber around top edge of cone
metal sheet around bottom edge of cone, rivetted to dish surface

pks 16.dat

Parkes Baseline Ripple Tests (Reflection Data)

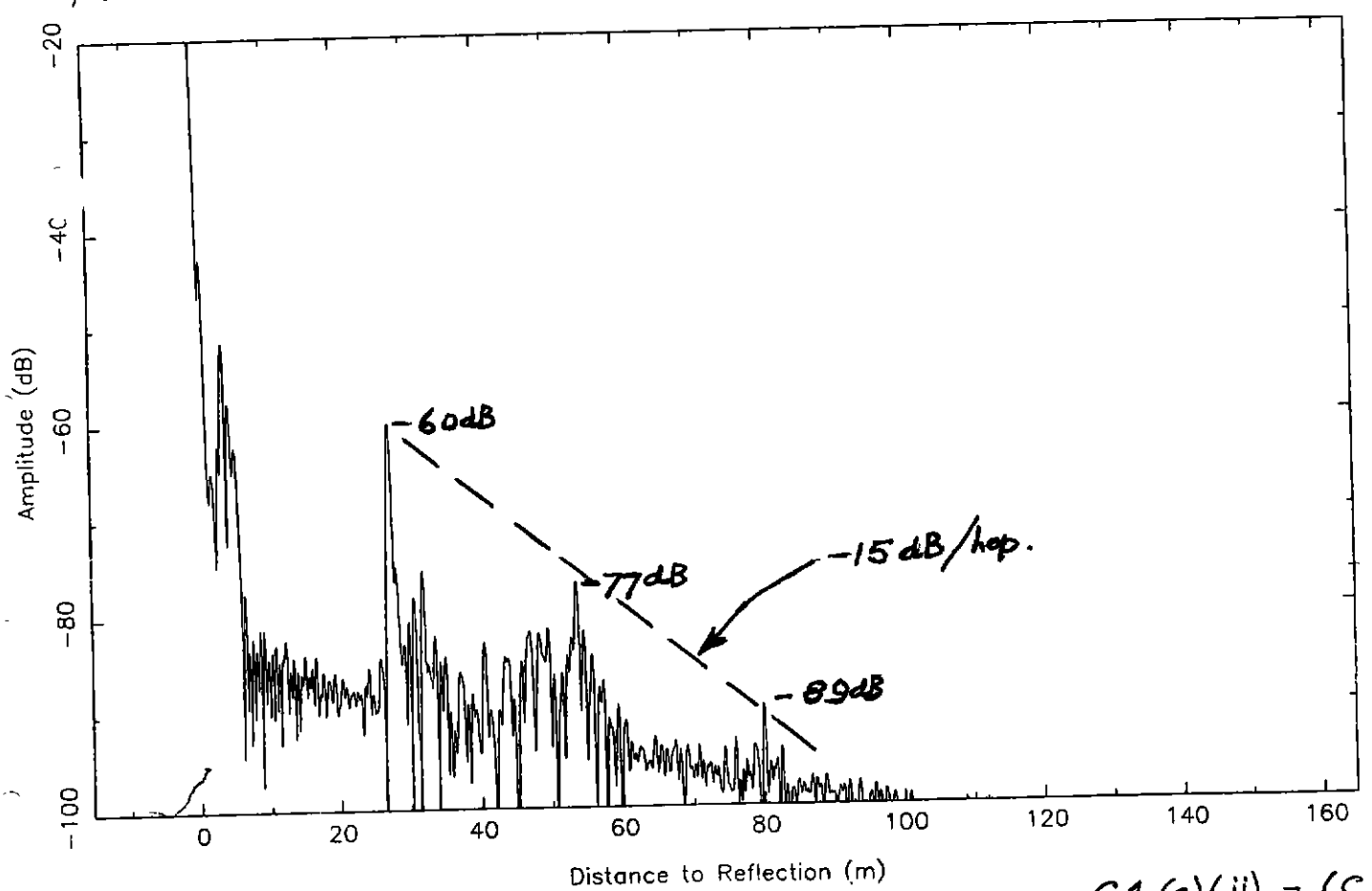

C1(c)(ii) - (CP)

pks 17.dat

Parkes Baseline Ripple Tests (Reflection Data)

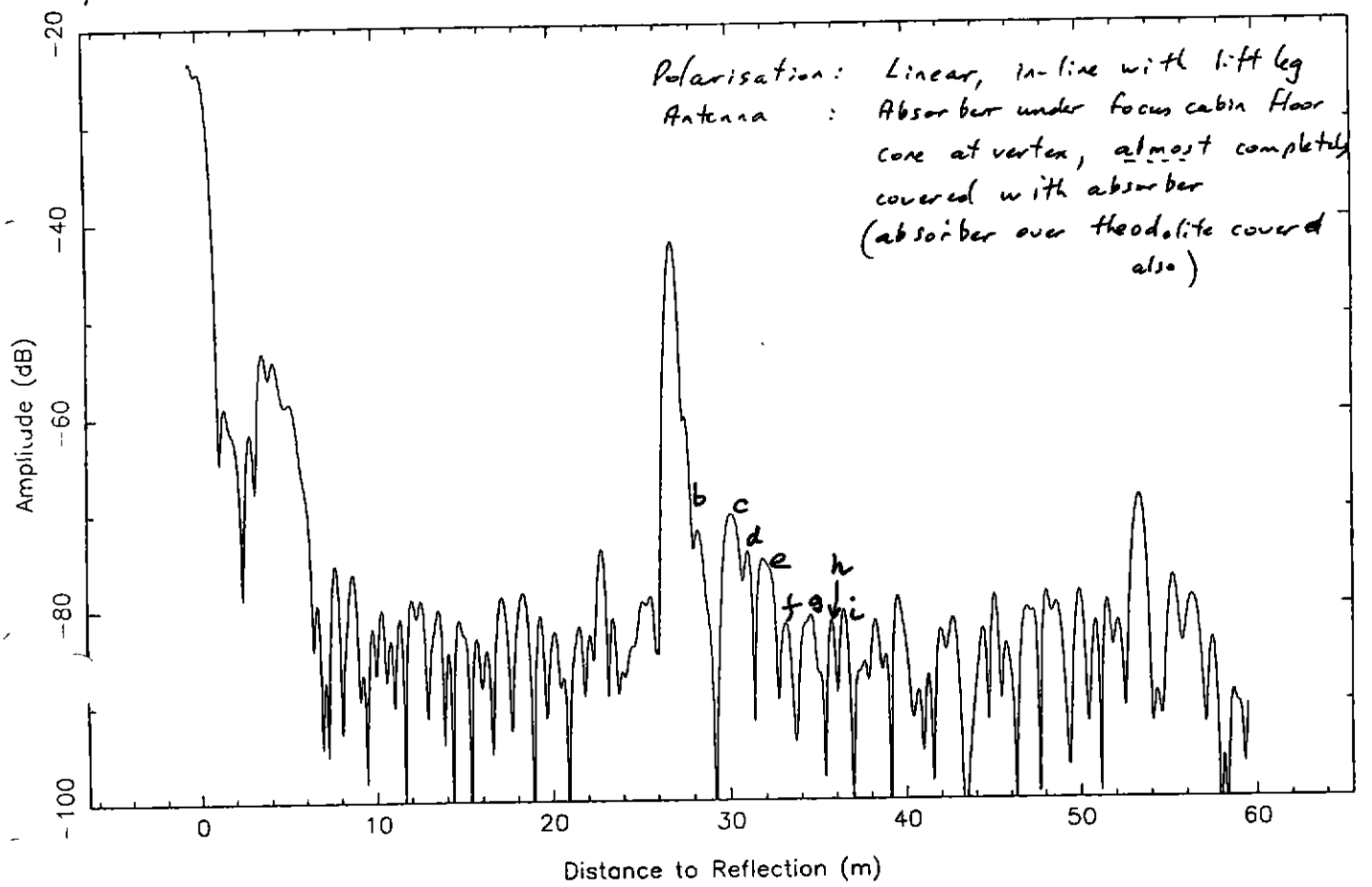

pks 17.dat

Parkes Baseline Ripple Tests (Reflection Data)

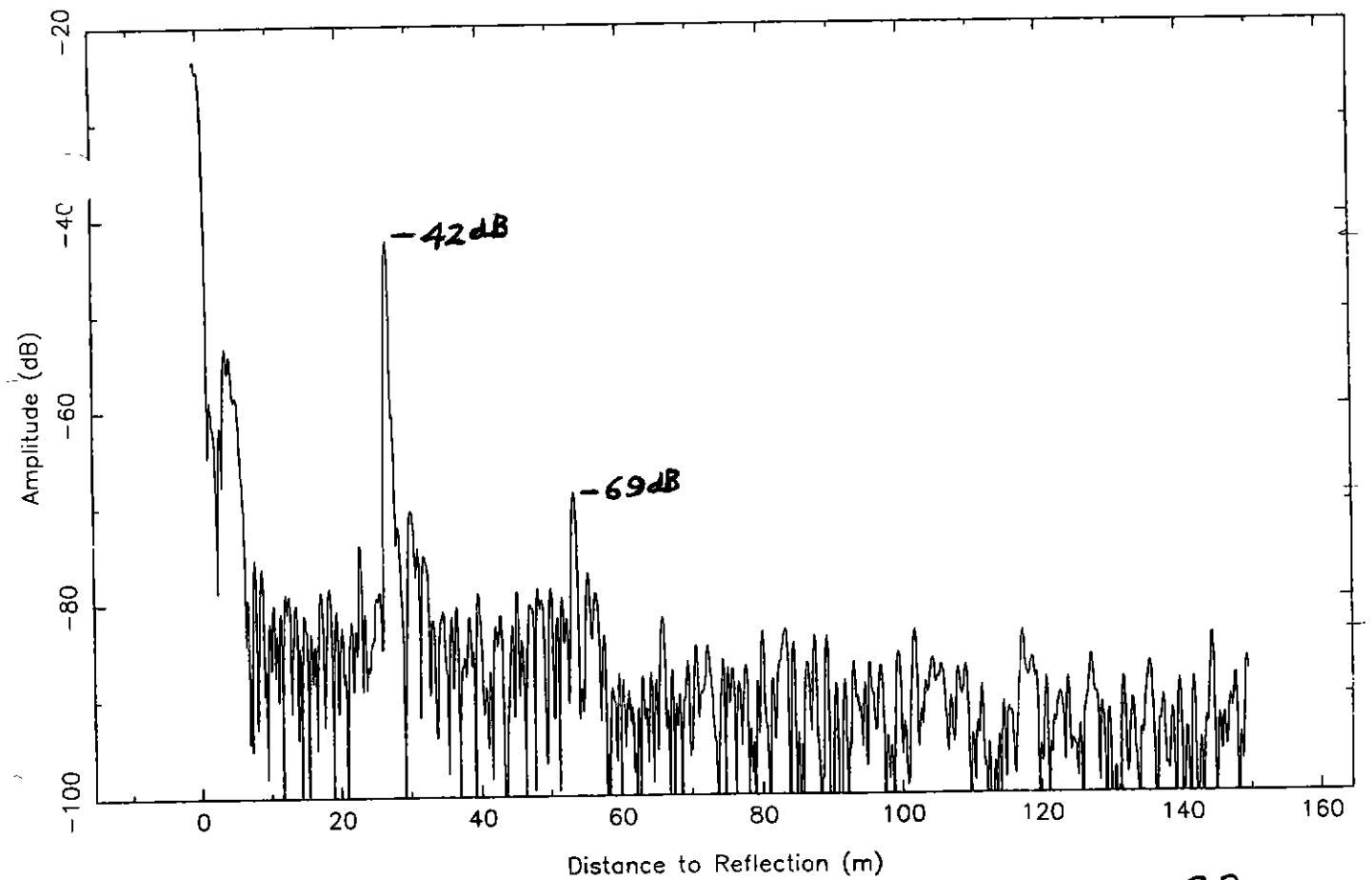

C2

pks 18.dat

Parkes Baseline Ripple Tests (Reflection Data)

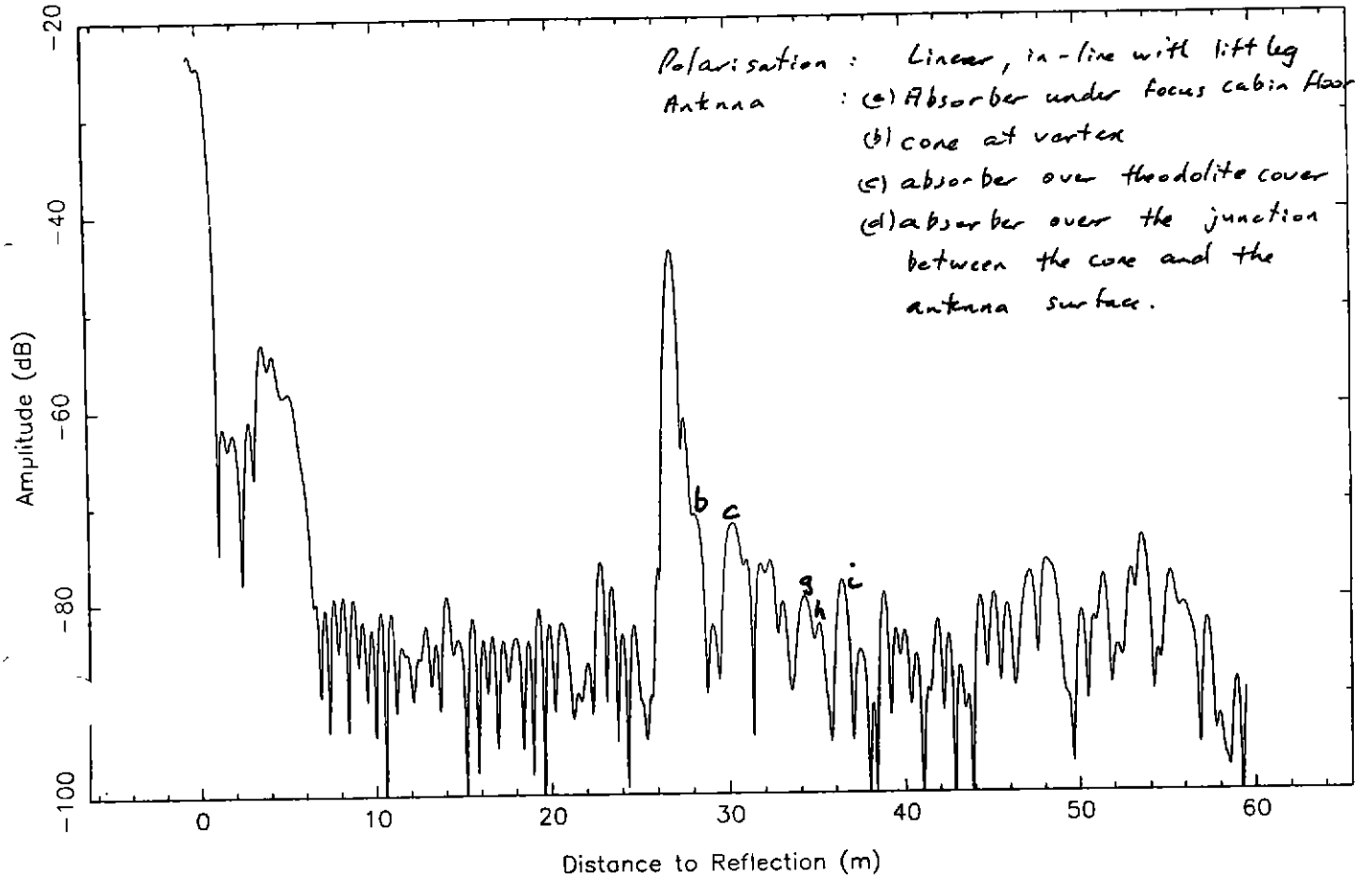

pks 18.dat

Parkes Baseline Ripple Tests (Reflection Data)

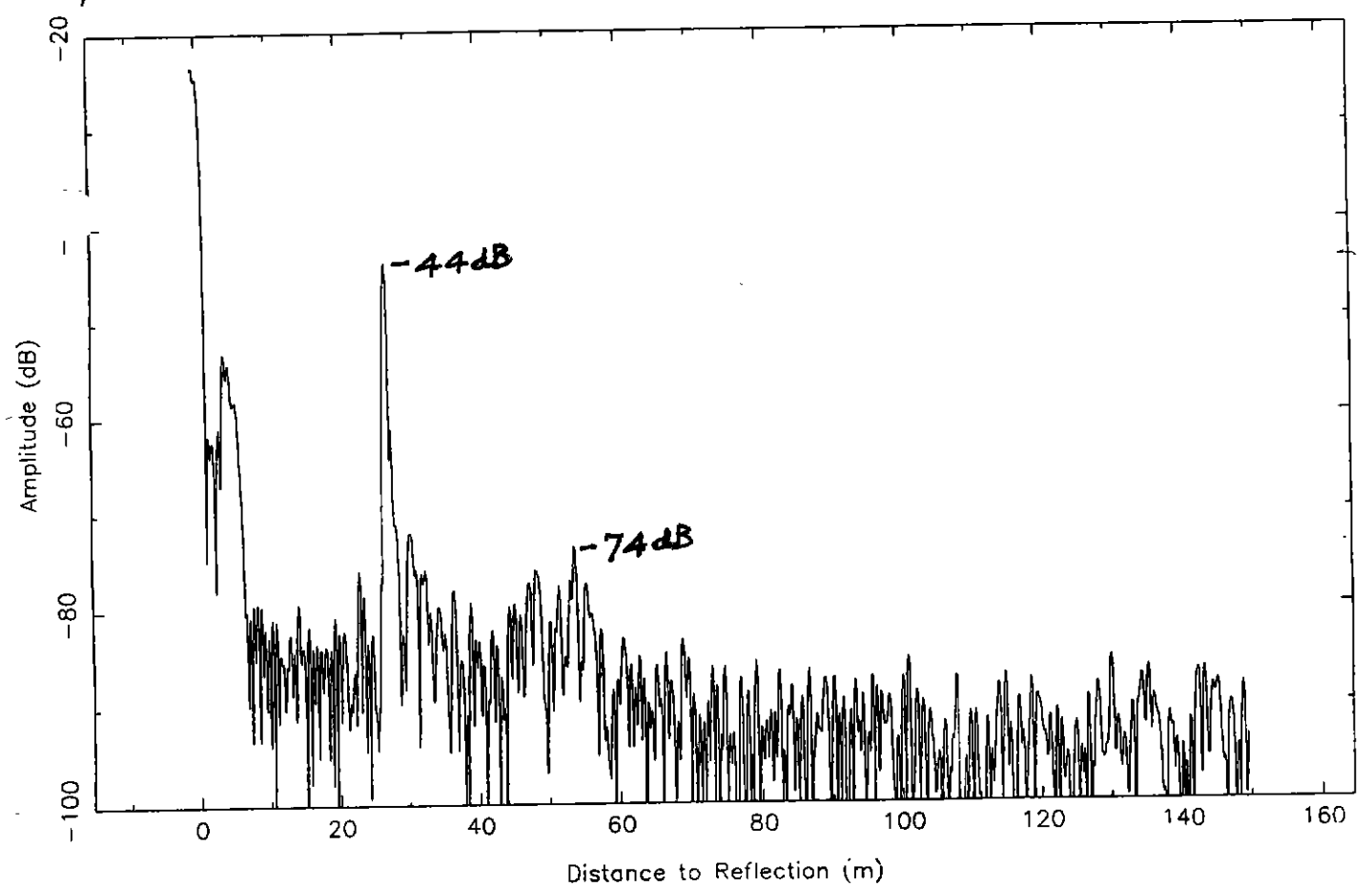

ATTACHMENT B

Day-Time Baseline-Ripple
Frequency-Intensity Scan Displays

June 1998

From data supplied by L. Staveley-Smith & M.J. Kesteven

Day-Time Baseline-Ripple Frequency-Intensity Scan Displays

1. Introduction

The drive of the Parkes radio telescope was modified so that solar scans could be made, either across one, or two closely-spaced strut sidelobes, between ("parallel" to) two closely-spaced strut sidelobes, or in an area remote from the strut sidelobes.

Standard displays for the H-line multibeam receiver system were used to enable comparisons to be made of indicative magnitude of the baseline-ripple for the following antenna configurations (see also Table A):

- REF A: Antenna in normal configuration.
- REF B: Absorber on focal-plane (covering focus-cabin under-floor area).
- REF C1: Addition of experimental metal cone at vertex.

2. Results and Conclusions

Total power measurements were also recorded. In particular, these results showed that for "radial" angles (θ) closer than about 10° from antenna main-beam, the strut sidelobe levels increased rapidly, being approximately 12dB higher in level at $\theta = 6°$ compared to far-out lobes, decreasing to about 3dB at $\theta = 12°$.

An aspect of using absorber on the focal plane (Ref B and C1) is that the system temperature is increased, since some percentage of feed spillover will see the absorber at 300K. For the feed design used with the multibeam receiver, an additional 3.5K was observed. This component is expected to be less with hybrid-mode feeds used on other receivers. Any permanent application of absorber on the focal-plane would require detailed investigation of use of low-profile weather-proof absorber.

Samples of the frequency-intensity scan displays are attached. Note that for the first three sets, data is available for the antenna configurations Ref A, B and C1, whereas for the second five sets, data is available only for configurations Ref A and B.

It should be noted that it was not always possible to carry out repeat scans for the different antenna configurations at the same time on consecutive days. (The antenna/strut-lobe/sun location plots given in the attached results are shown for Ref A only). Also some scans were done close to the period when the sun was setting.

In Table A, the comparison in performance for the various antenna configurations for each scan type is summarised. In general, the results are superior (i.e. reduced baseline ripple) when the absorber is used on the focal-plane. In all cases, high levels of ripple occur on or close to a strut-lobe where θ is small (for the measurement cases, $\theta = 6°$ and 12°). for more-distant strut-lobes, the lobe is evident, but the region either side of the strut-lobe is cleaner when absorber is used. Interestingly, for these further out regions, antenna configuration C1 gives significant levels of interference which could be due to the reception of sun through the vertex cone scatter lobes (see Fig 2.2 of main text).

TABLE A

Frequency-Intensity Scan Displays - Across Strut-Lobes, and Distant from Strut-Lobes

Scan Ref.	Radial Angle from Main-beam, θ	Corres. azimuth angle	Scan Description	Comments (see notes below re definition of A,B, C1)
P	6°	240° → 290°	Crosses strut-lobe	C1 better than B, both considerably better than A.
Q	30° → 55°	210°	Does not cross strut-lobe	B better than A; C1 could be affected by concentrated cone radiation (see Fig. 2.2 of main report)
R	30° → 55°	240°	Does not cross strut-lobe	Comments as for Q
S	6°	120° → 180°	Crosses strut-lobe	B better than A
T	12°	140° → 195°	Crosses strut-lobe	Comments as for S
U	35° → 55°	180°	Crosses junction of 2 strut-lobes	B marginally better than A
V	35° → 60°	150°	Does not cross strut-lobe	Similar
W	15° → 30°	180°	Scan between 2 strut-lobes	B better than A.

Notes to Table A:

1. Scans were made in each case (P-W) for the following antenna configurations:

   - Ref A: normal antenna configuration.
   - Ref B: absorber on focal-plane.

   In the case of scans (P-R), additional scans were obtained for the following antenna configuration:

   - Ref C1: addition of experimental metal cone at vertex.

PGPLOT Window 1

980613_0241 #36 6°, 240° → 300°, one leg sidelobe

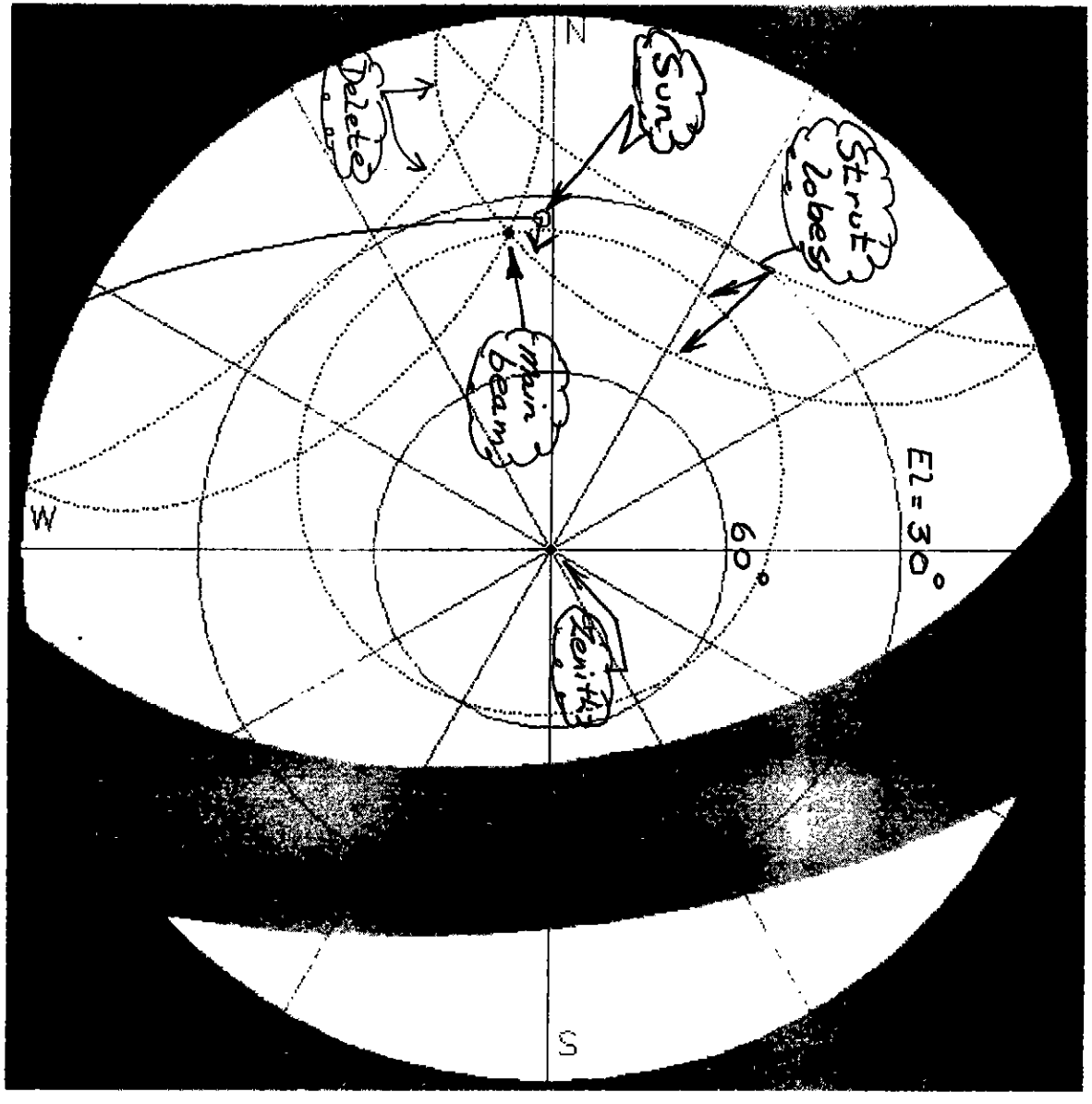

Compiled from lobo_slave_6.

Local date: 13 Jun 98
Local time: 12:13:16

Az of dish: 352.1 deg.
Ze of dish: 54.2 deg.

Tracks starting within the next 2.0 hrs are plotted.

.04 days since last satellite data update.

Clock rate: 10

Forecast map resolution:
40 by 30

o Sun
▪ GPS
▪ Glonass

Type help for cmd summary.

I (a)

980613_0211 #36

Beam Number: 1

Polarization A

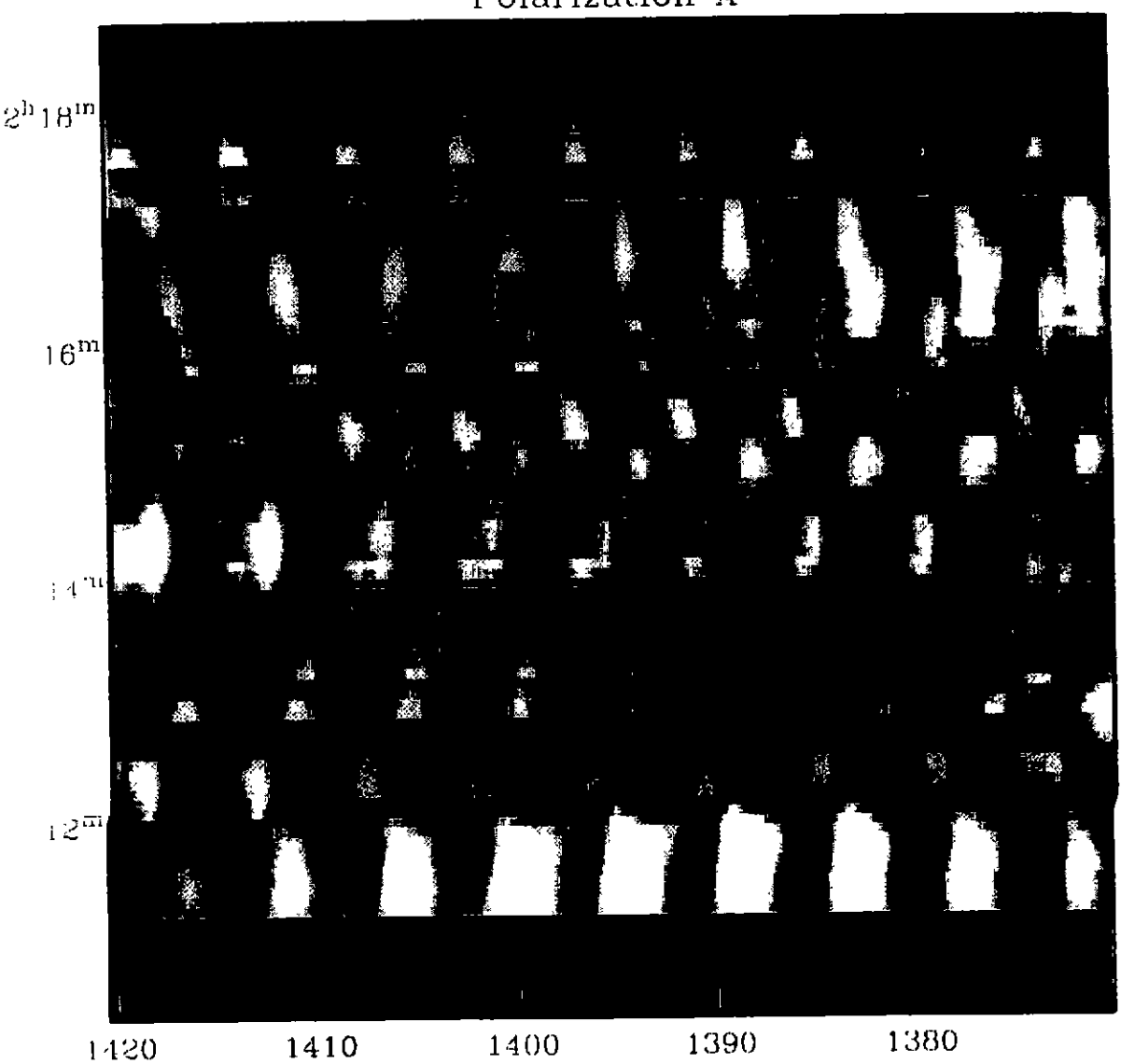

P(A)

#82

Part Number 1

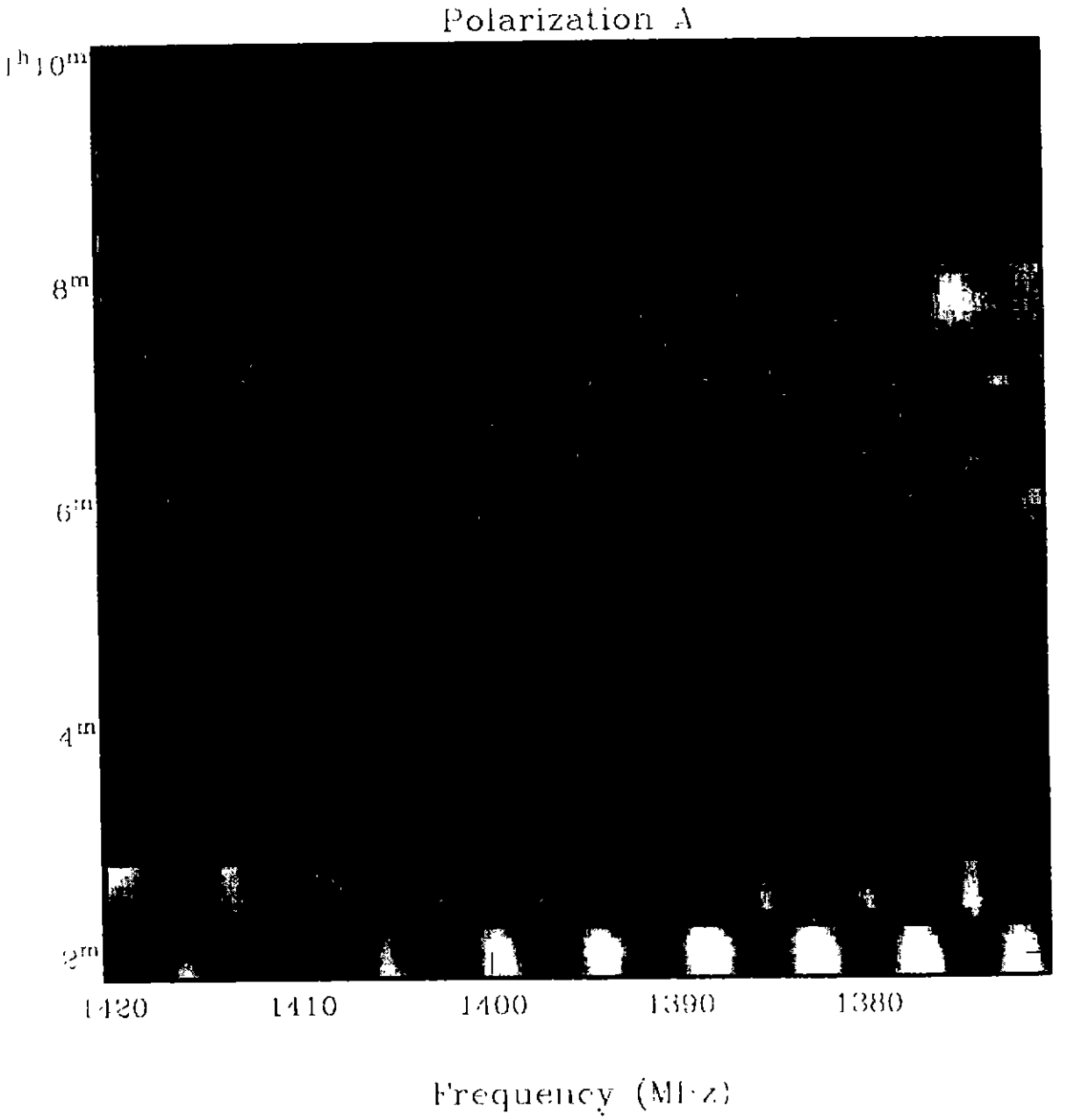

P(B)

#111

Beam Number 1

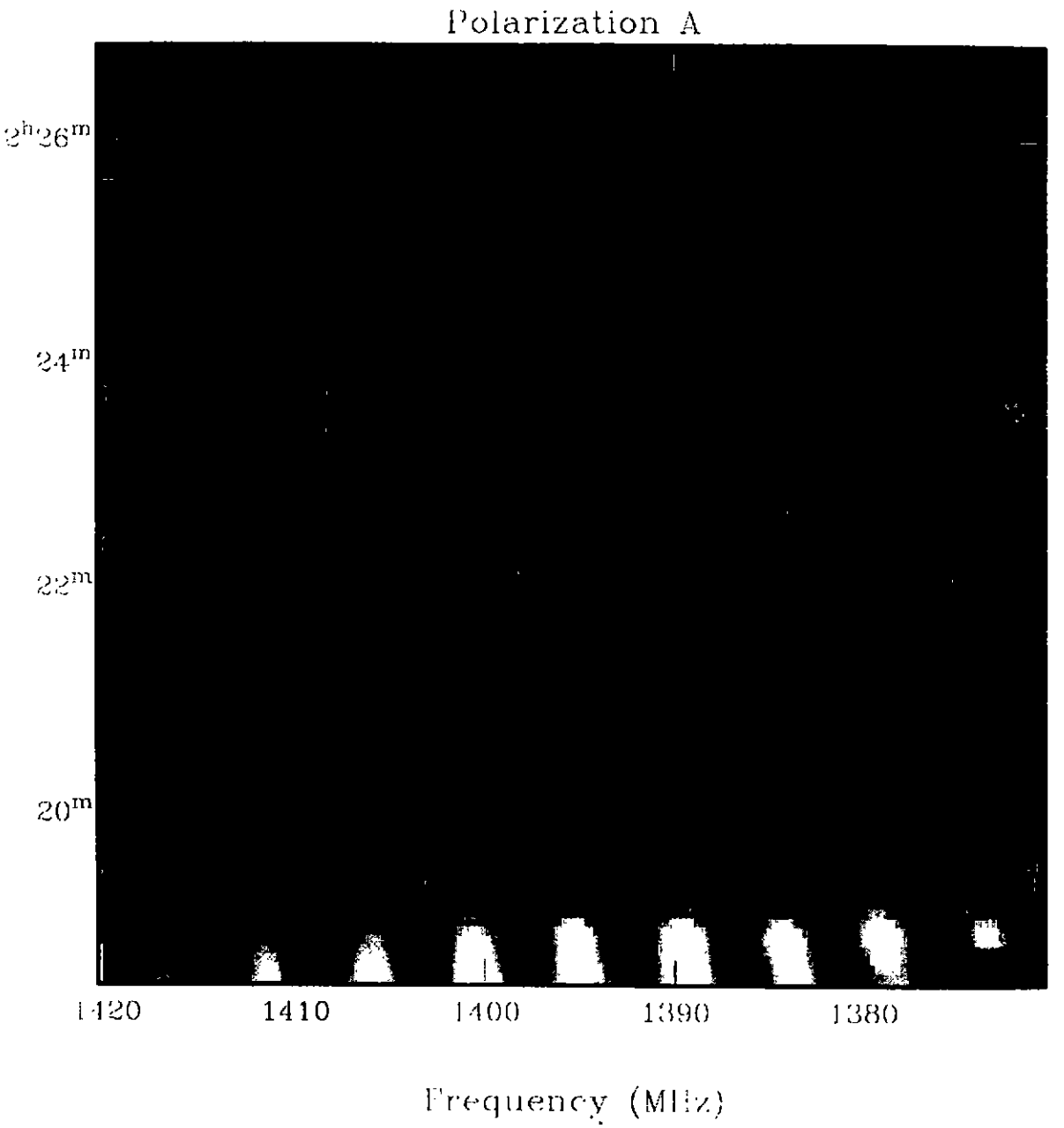

P(C1)

PGPLOT Window 1

980613_0612 #53 START

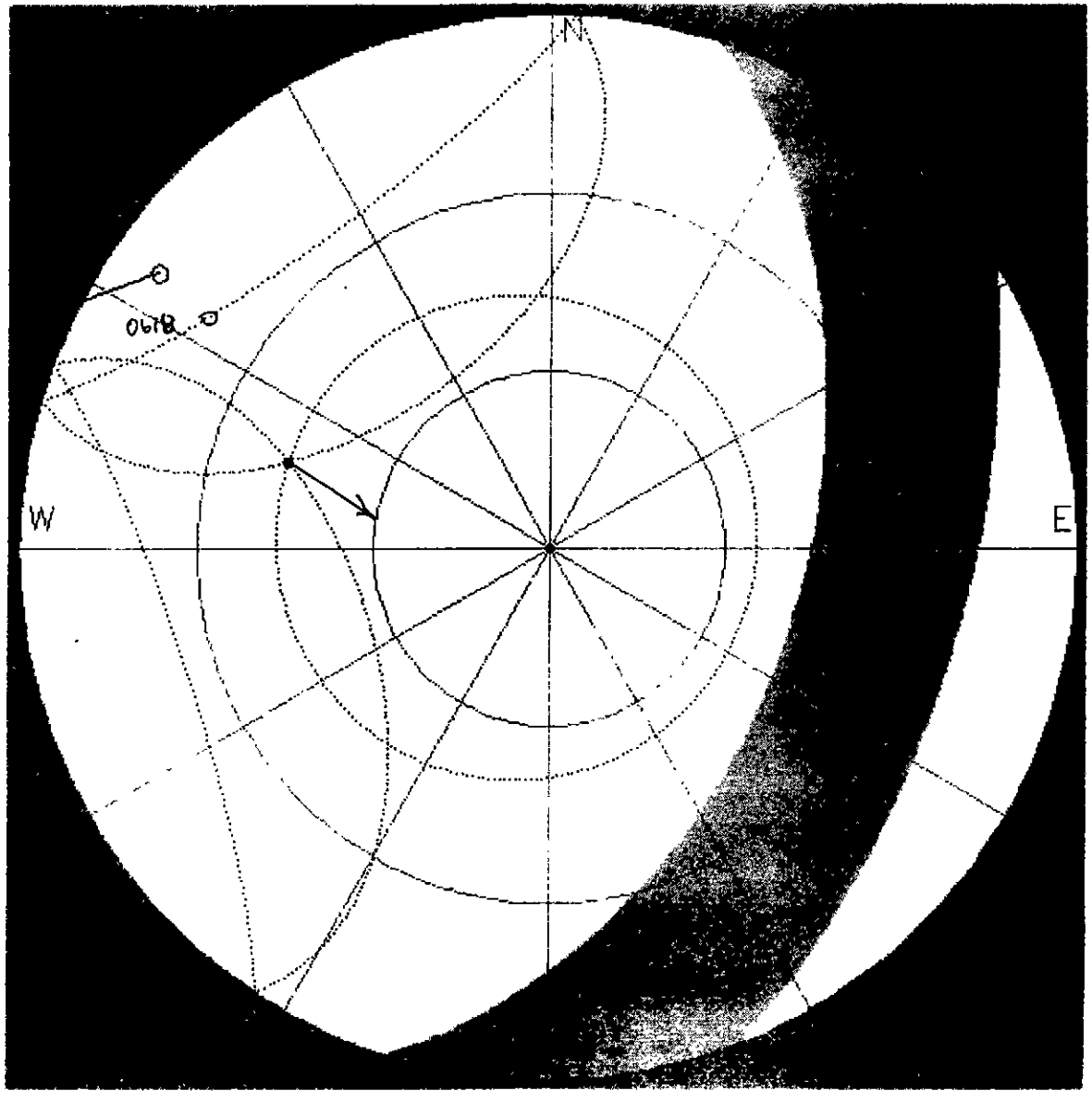

Compiled from lobo_slave_6.

Local date: 13 Jun 98
Local time: 16:13:39

Az of dish: 288.2 deg.
Ze of dish: 46.9 deg.

Tracks starting within the next 2.0 hrs are plotted.

0.20 days since last satellite data update.

Clock rate: 10

Forecast map resolution:
40 by 30

o Sun
▪ GPS
▪ Glonass

Type help for cmd summary.

(4) 2

980613_062 #53

Beam Number 1

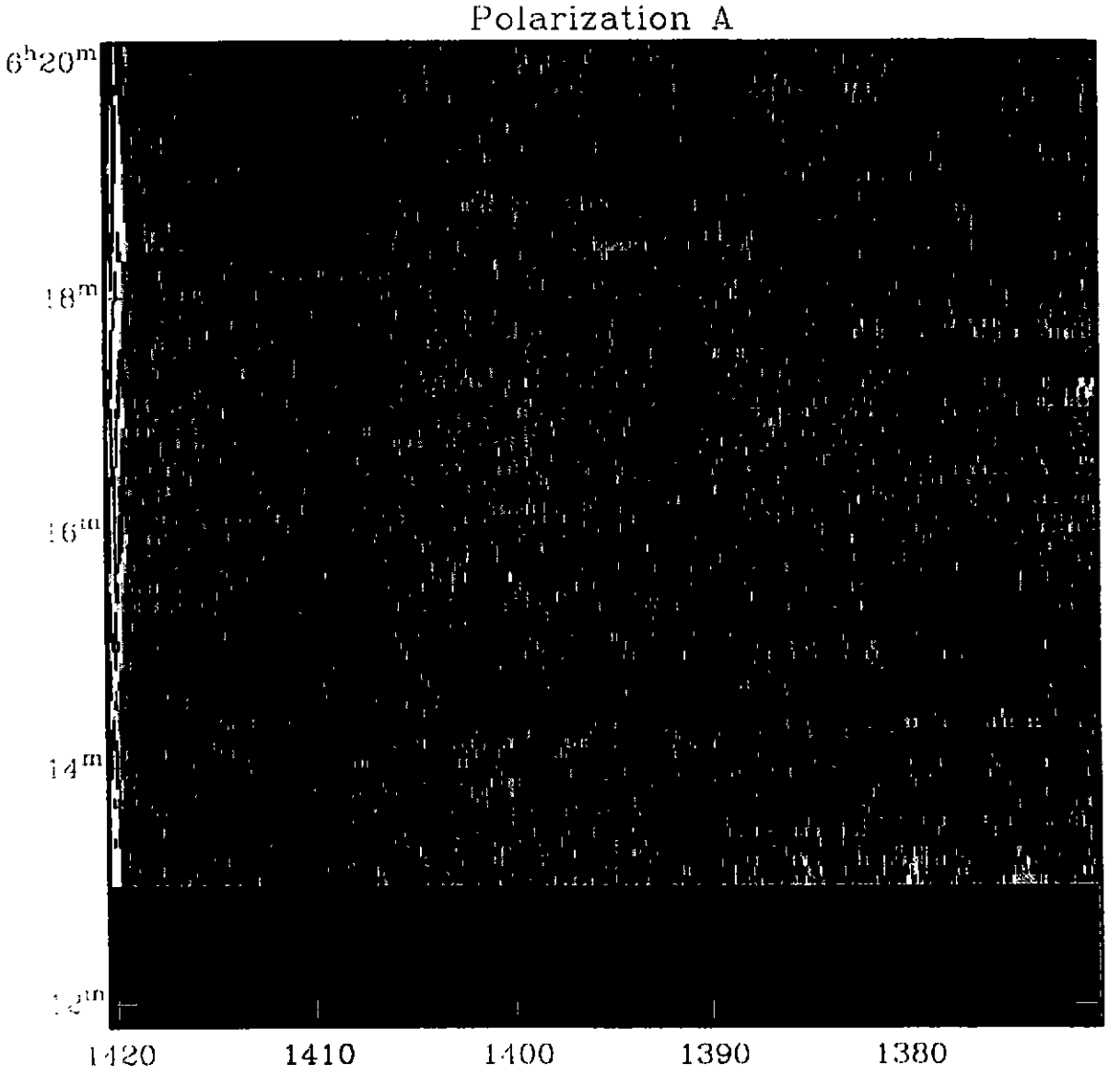

Q (A)

76

Chart Number 1

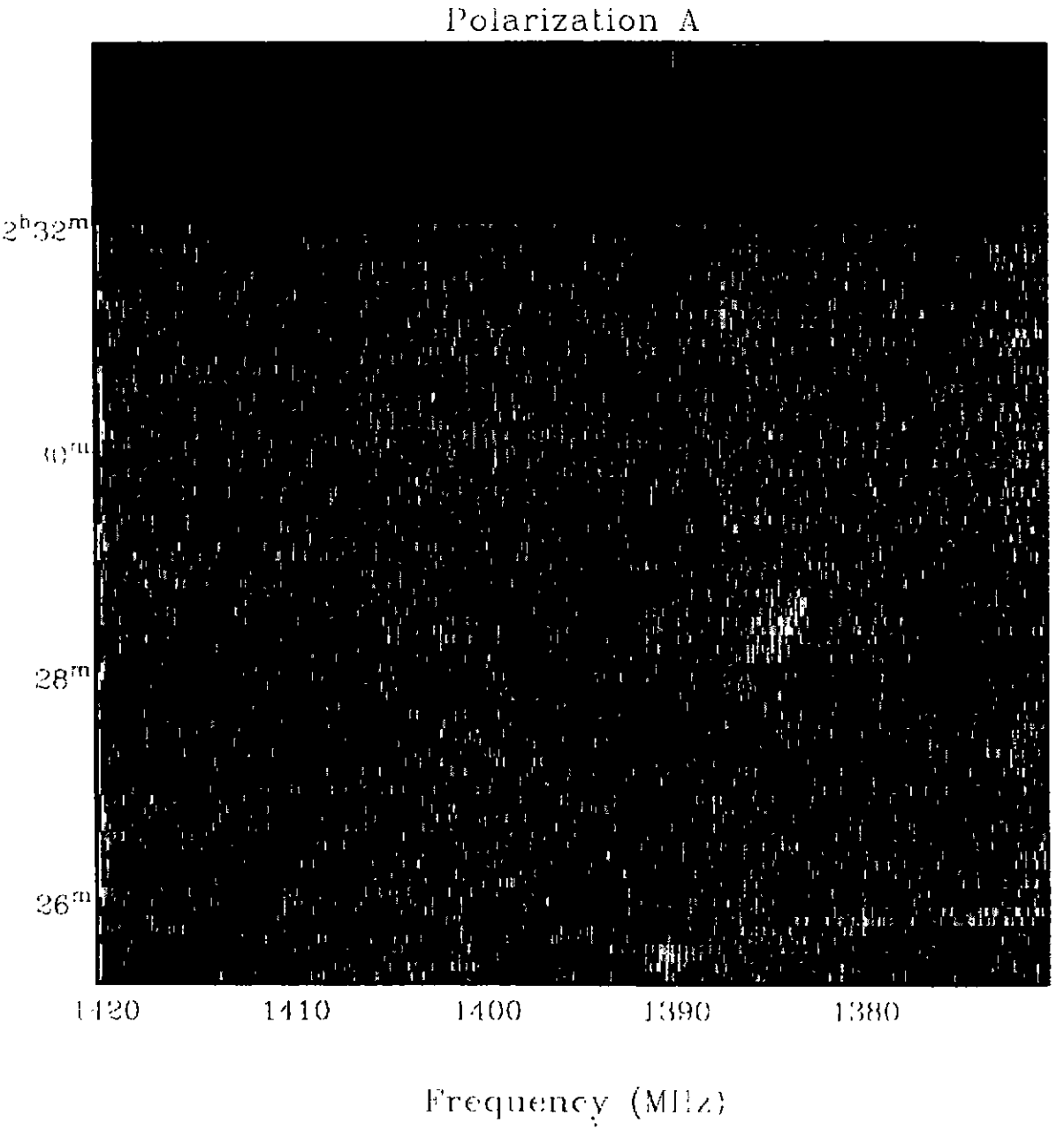

Q (B)

#113

Beam Number: 1

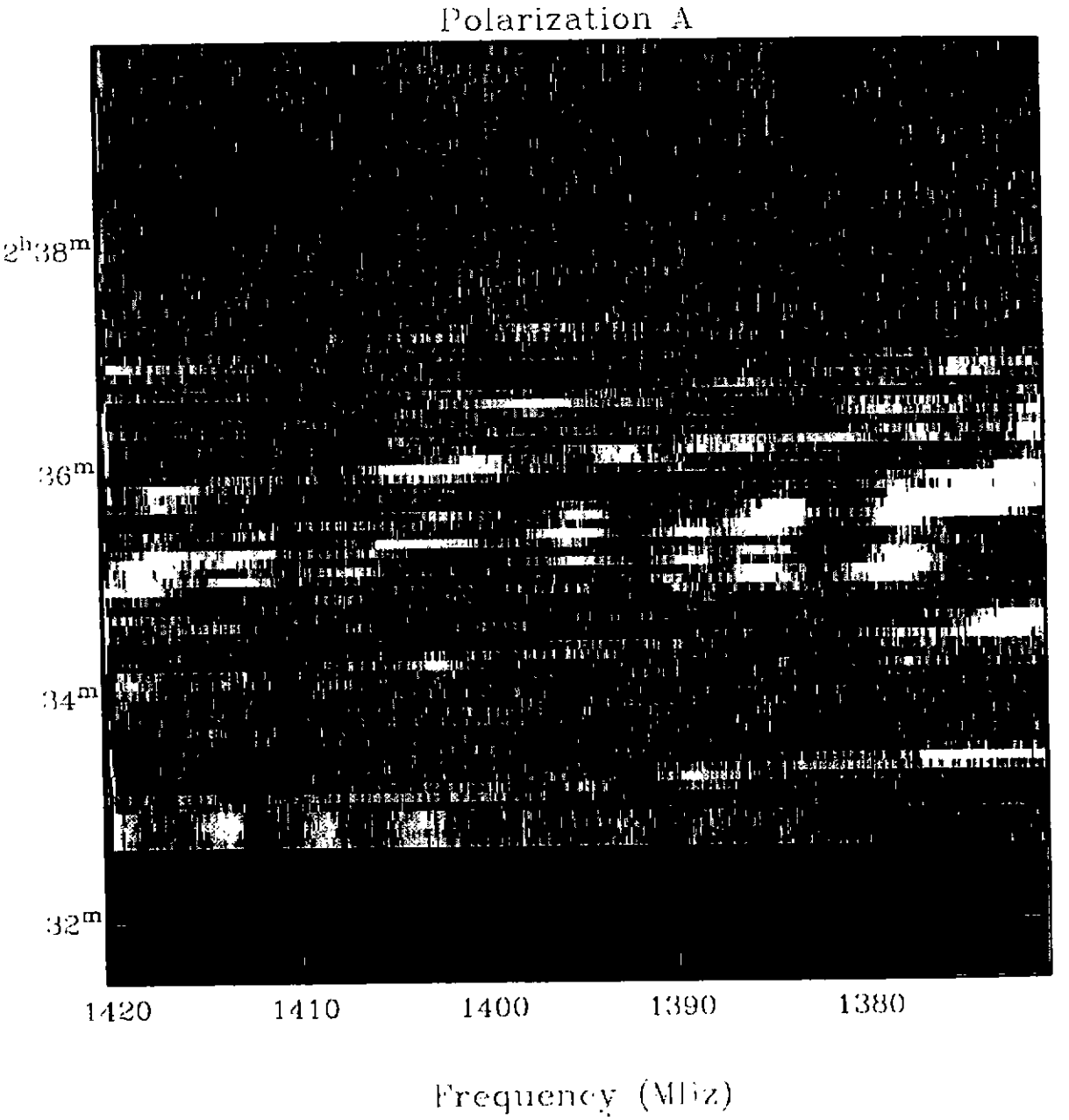

Q (CI)

PGPLOT Window 1

980613_0625 #55 SORT

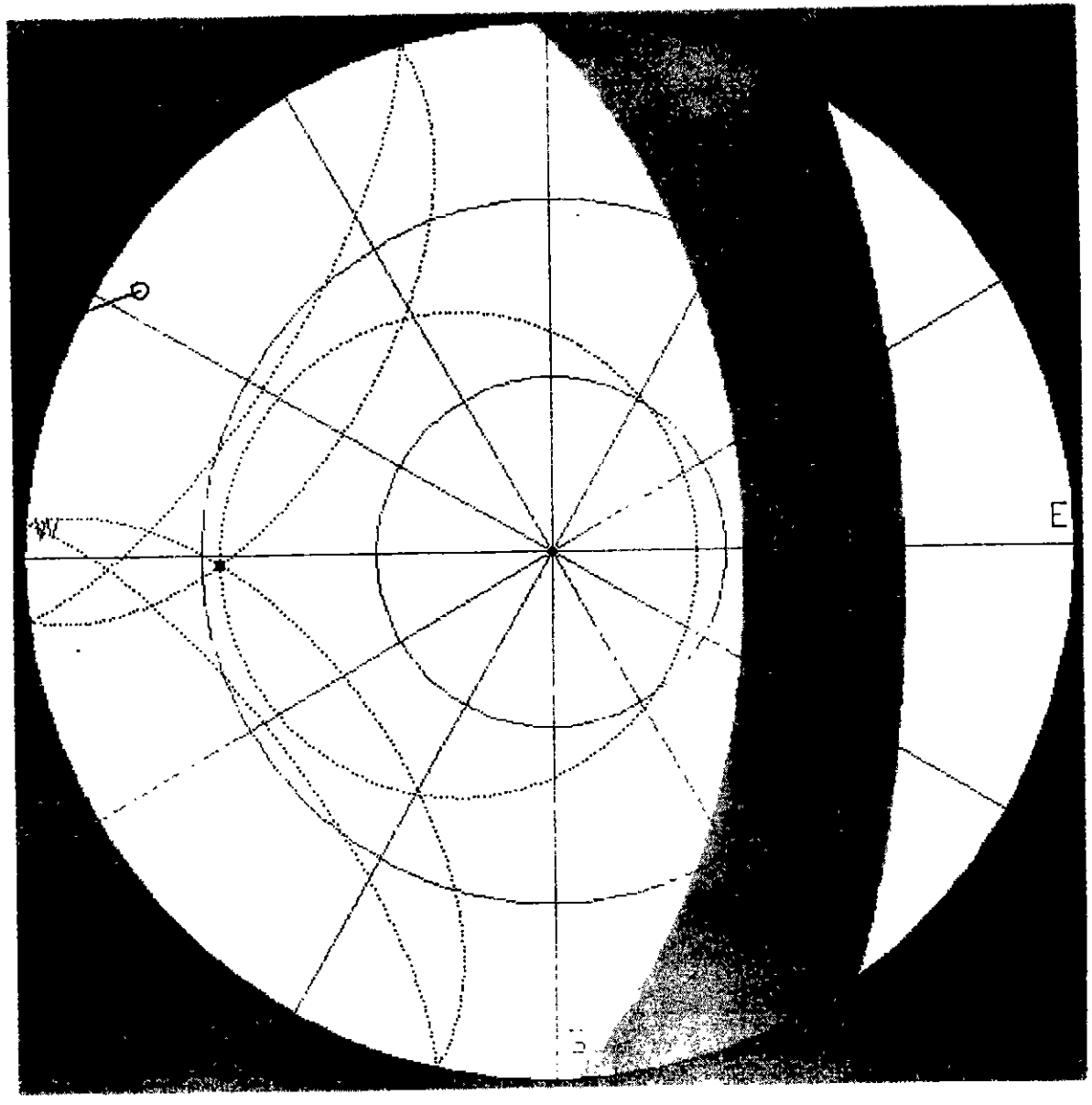

Compiled from lobo_slave_6.

Local date: 13 Jun 98
Local time: 16:26:30

Az of dish: 268.5 deg.
Ze of dish: 56.9 deg.

Tracks starting within the next 2.0 hrs are plotted.

0.21 days since last satellite data update.

Clock rate: 10

Forecast map resolution:
40 by 30

o Sun
▪ GPS
▪ Glonass

Type help for cmd summary.

R (4)

980613_0825 #55

Beam Number: 1

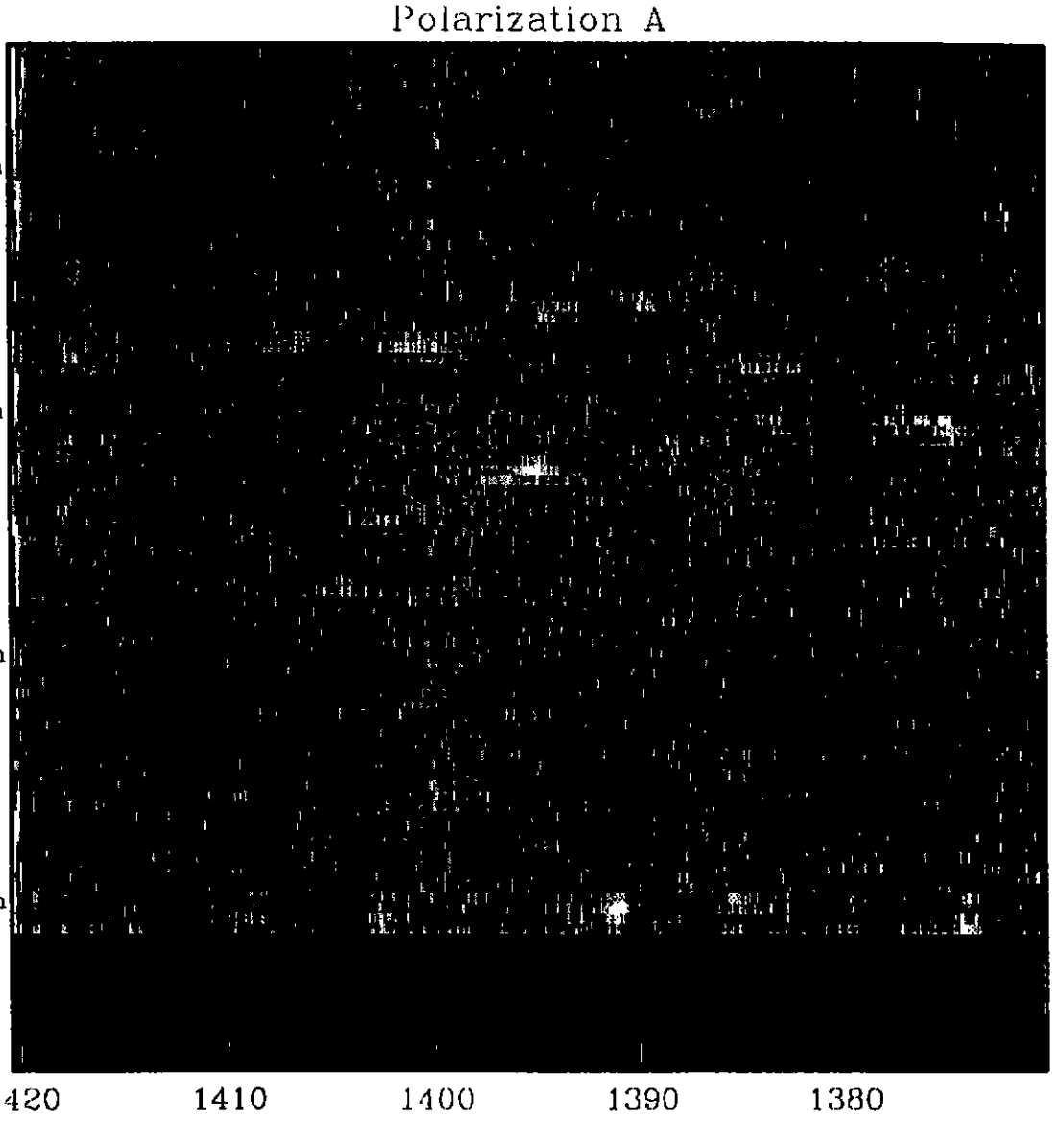

R (A)

#98

Scan Number 1

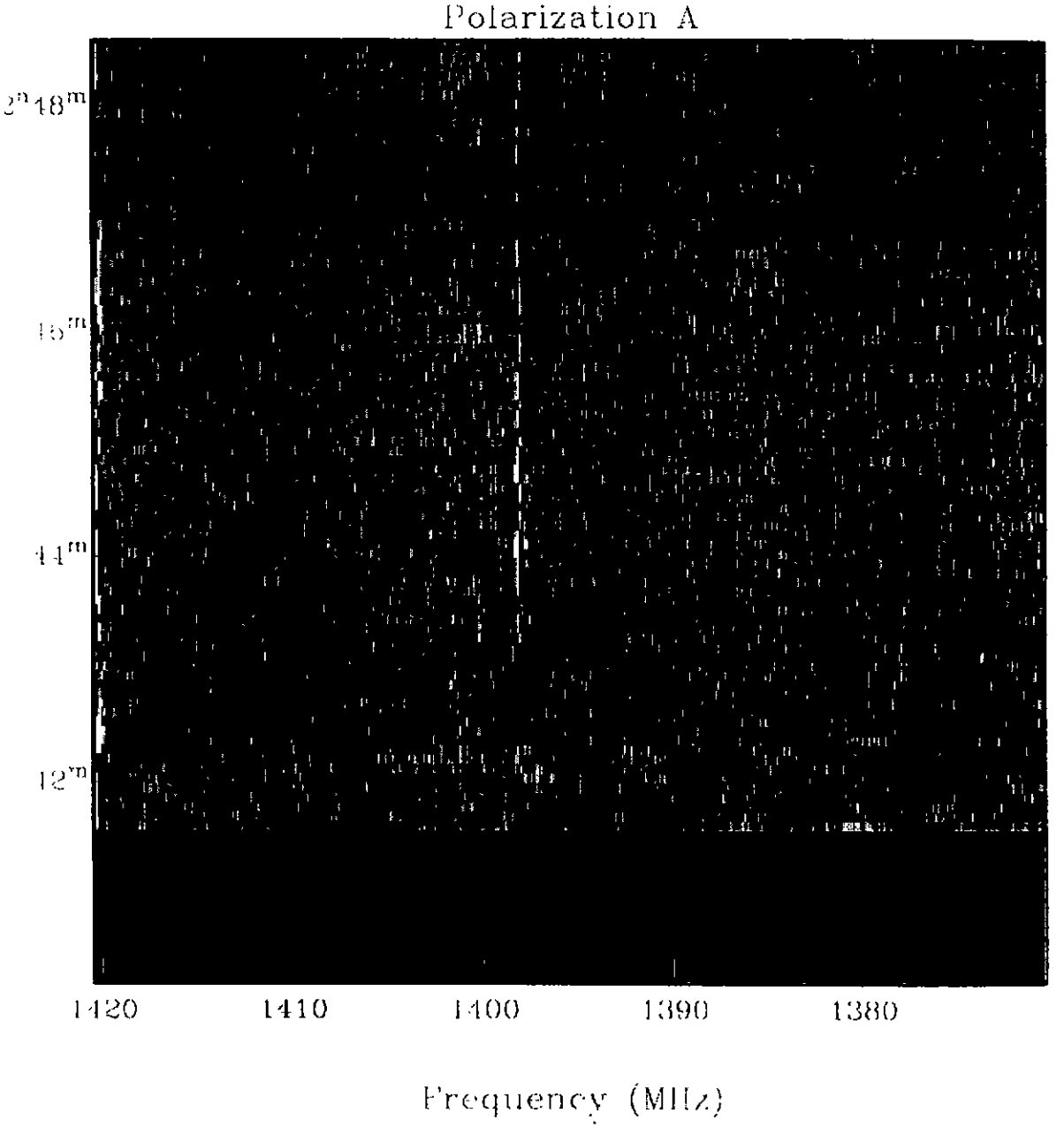

R (B)

#115

Beam Number: 1

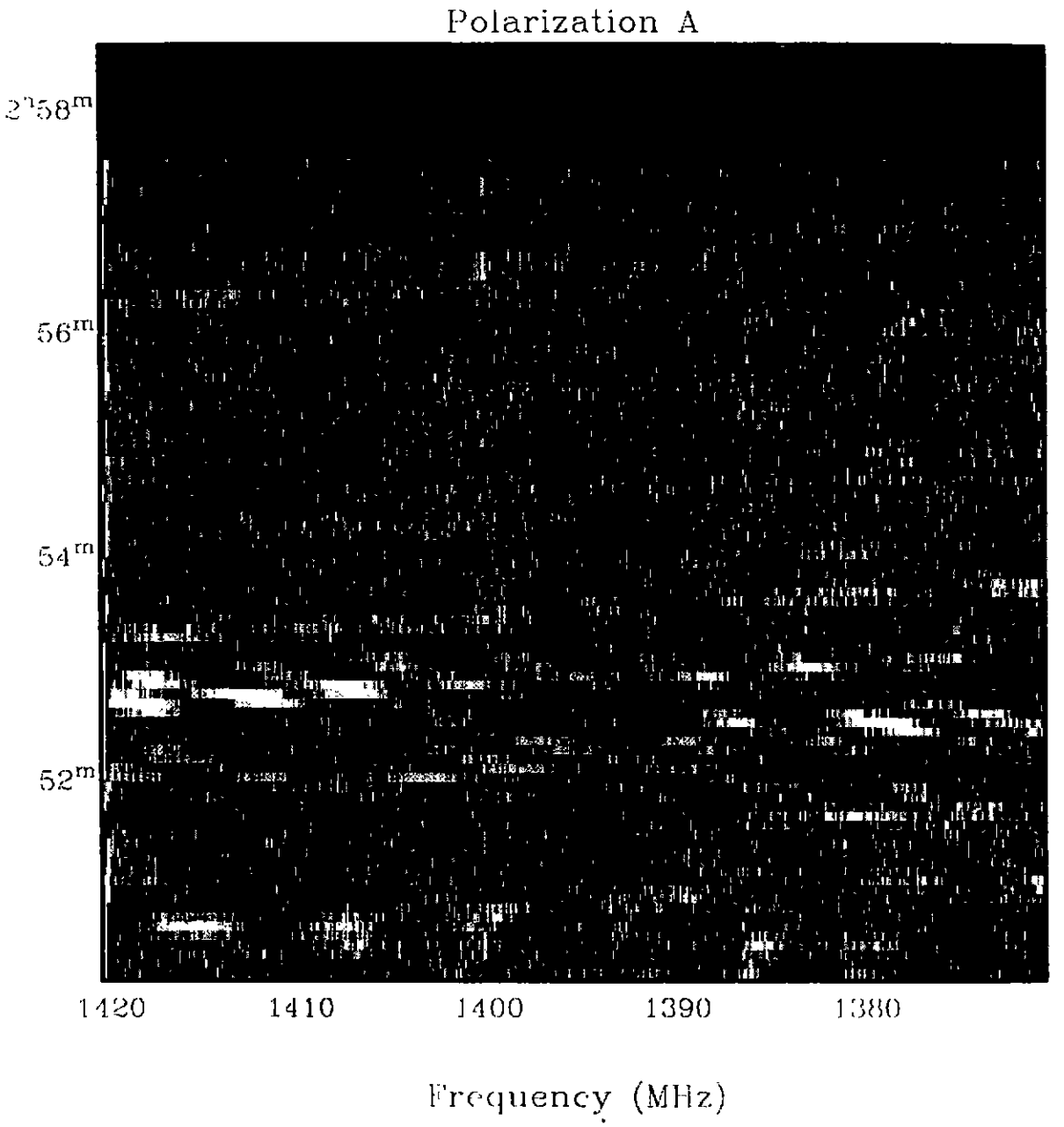

R (C1)

PGPLOT Window 1

980613_0157 #34

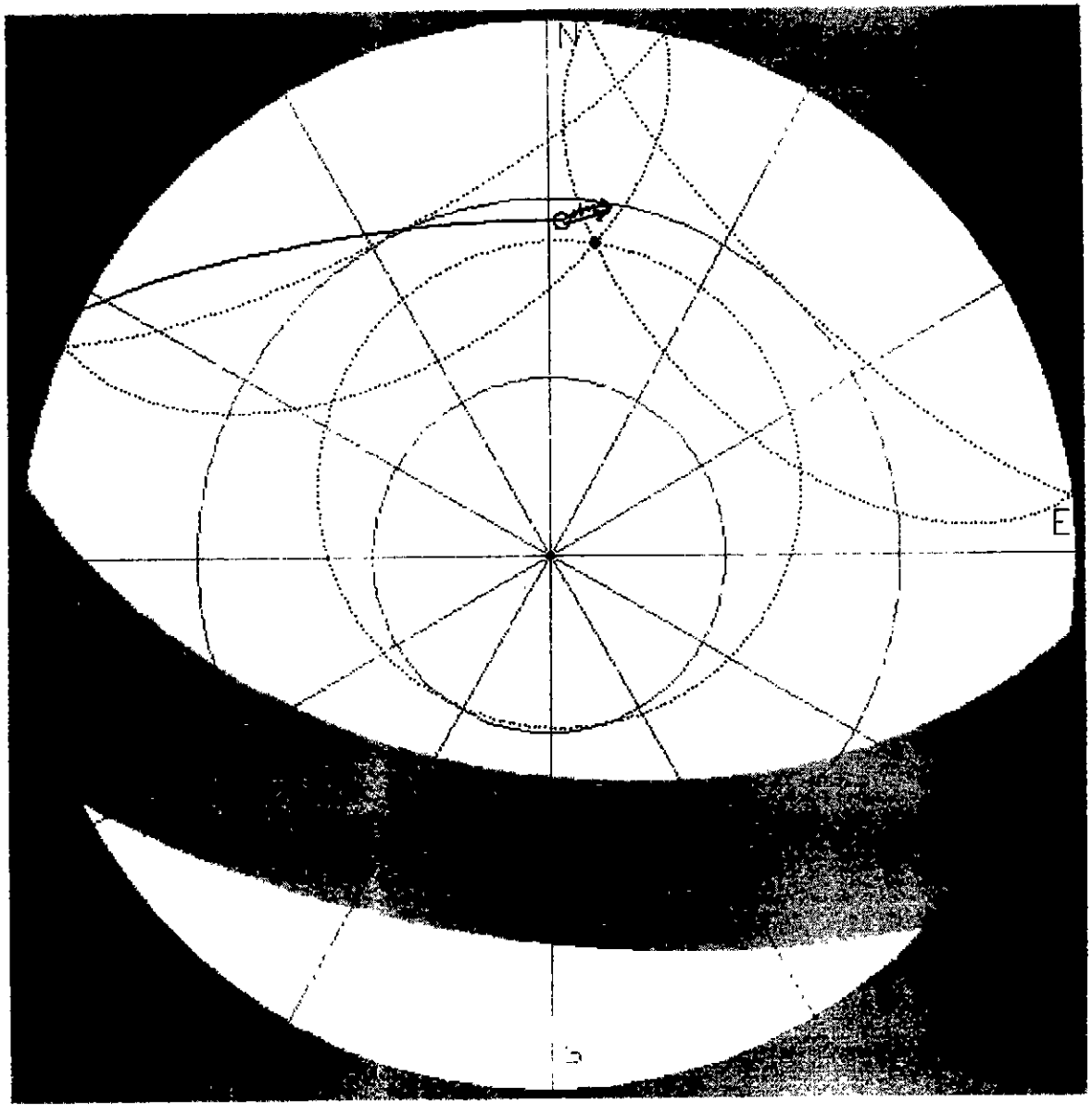

Compiled from lobo_slave_6.

Local date: 13 Jun 98
Local time: 11:57:51

Az of dish: 8.6 deg.
Ze of dish: 52.9 deg.

Tracks starting within the next 2.0 hrs are plotted.

.03 days since last satellite data update.

Clock rate: 10

Forecast map resolution:
40 by 30

o Sun
▪ GPS
▪ Glonass

Type help for cmd summary.

S (A)

9806B #34

Beam Number: 1

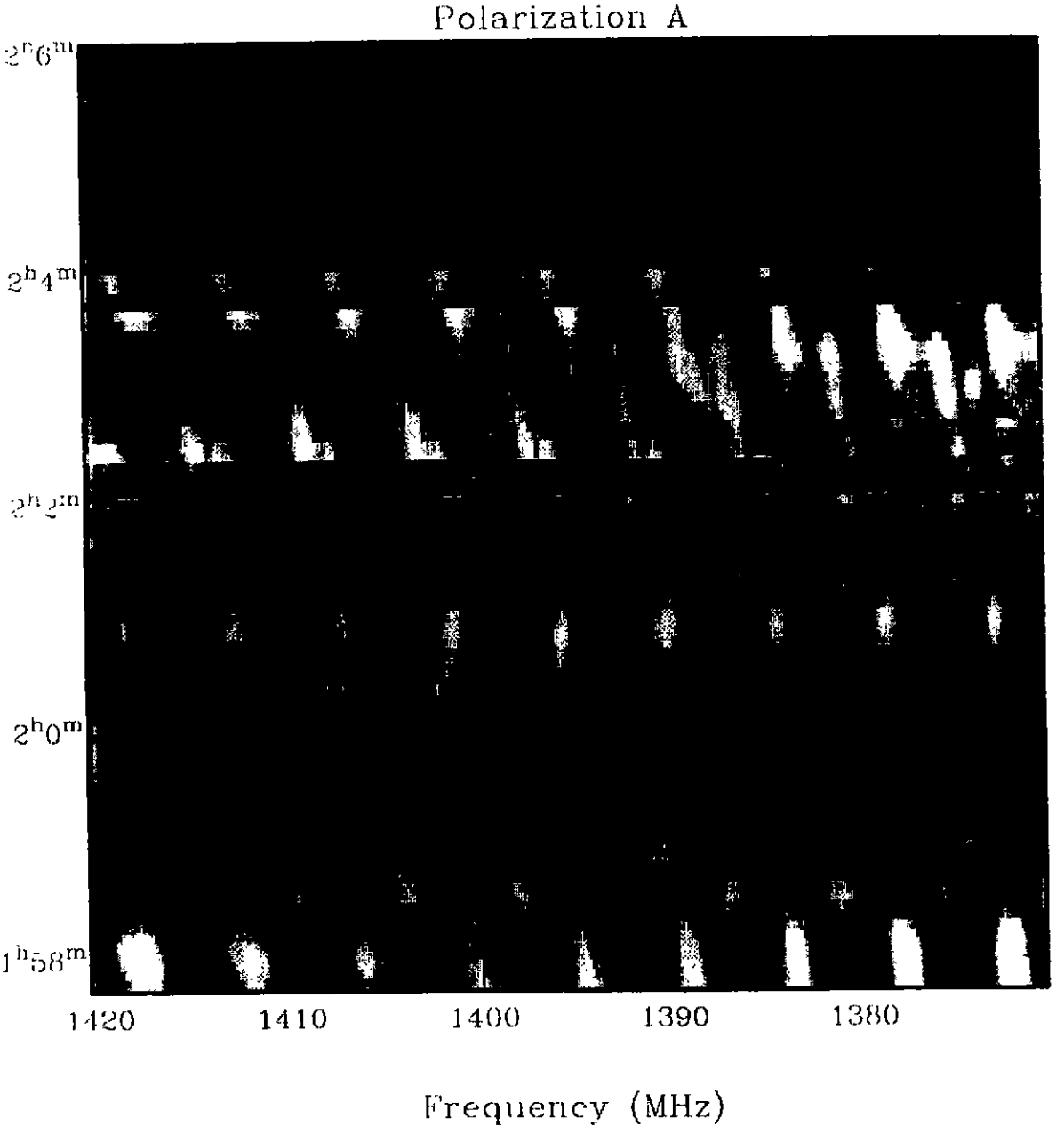

S (A)

#75

ar. Number: 1

Polarization A

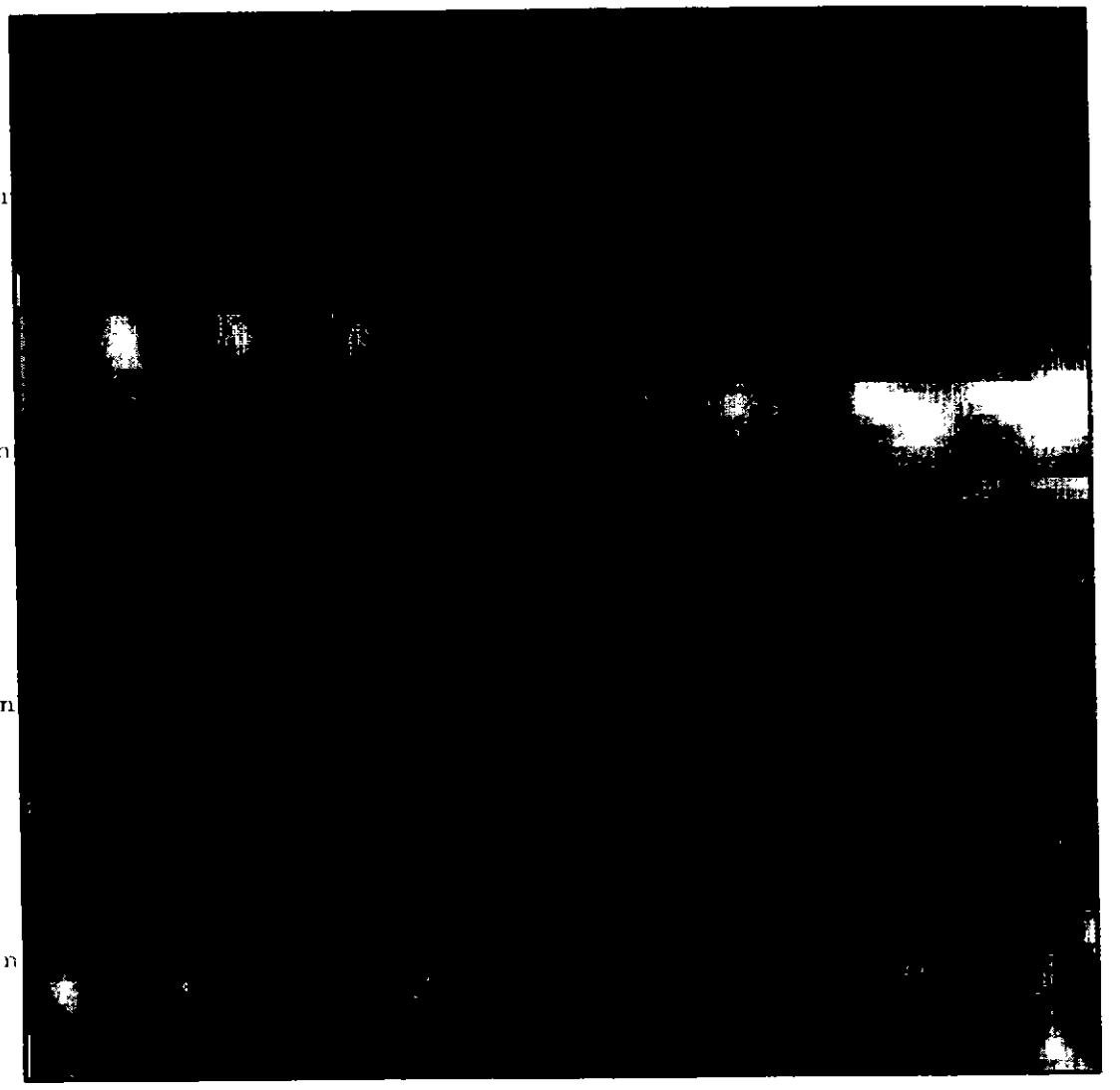

S(B)

PGPLOT Window 1

980613_0142 #31

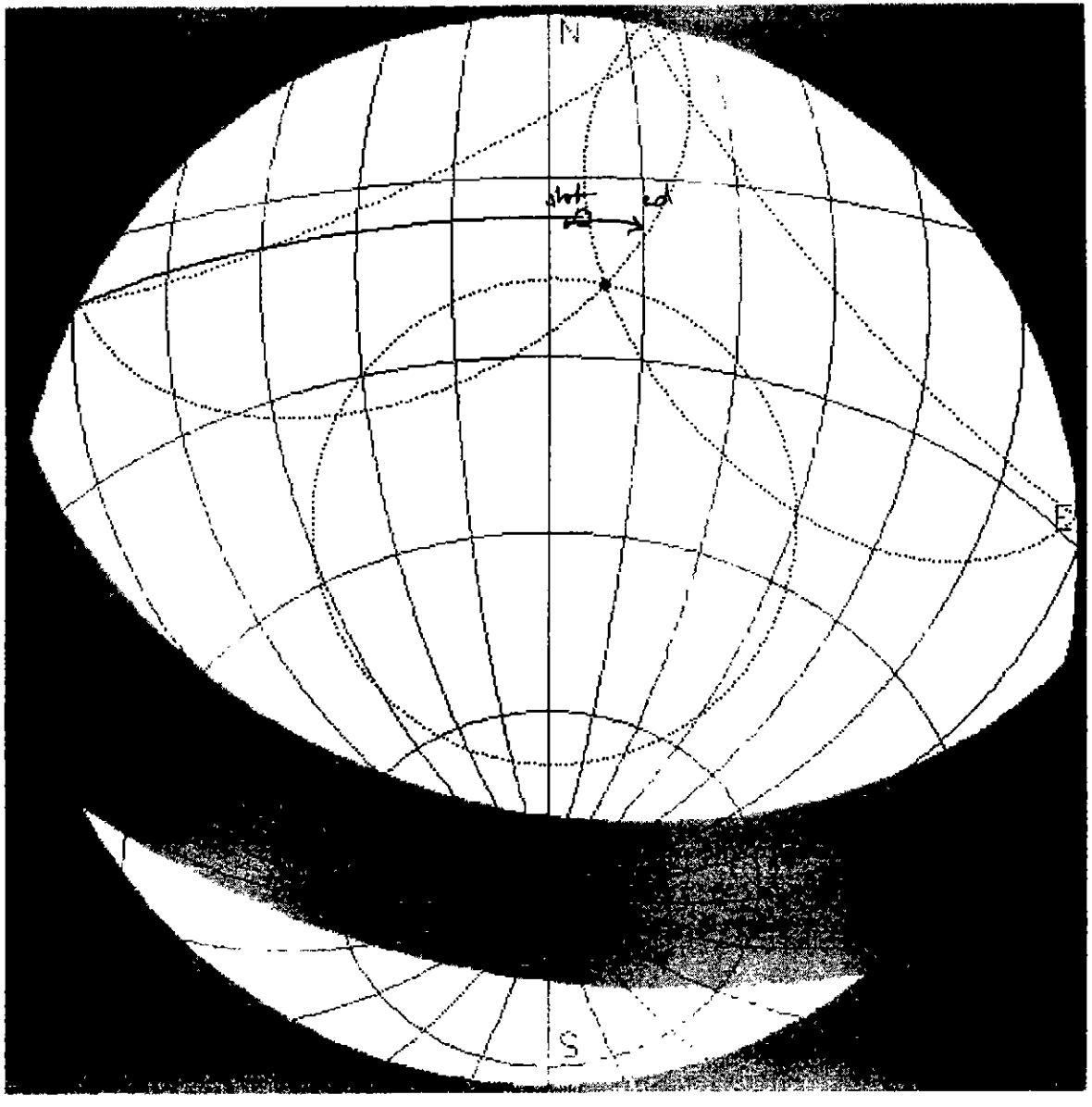

Compiled from lobo_slave_6.

Local date: 13 Jun 98
Local time: 11:44:44

Az of dish: 12.1 deg.
Ze of dish: 46.0 deg.

Tracks starting within the next 2.0 hrs are plotted.

.02 days since last satellite data update.

Clock rate: 10

Forecast map resolution:
40 by 30

- o Sun
- ▪ GPS
- ▪ Glonass

Type help for cmd summary.

T (A)

980613_0142 #31

Beam Number: 1

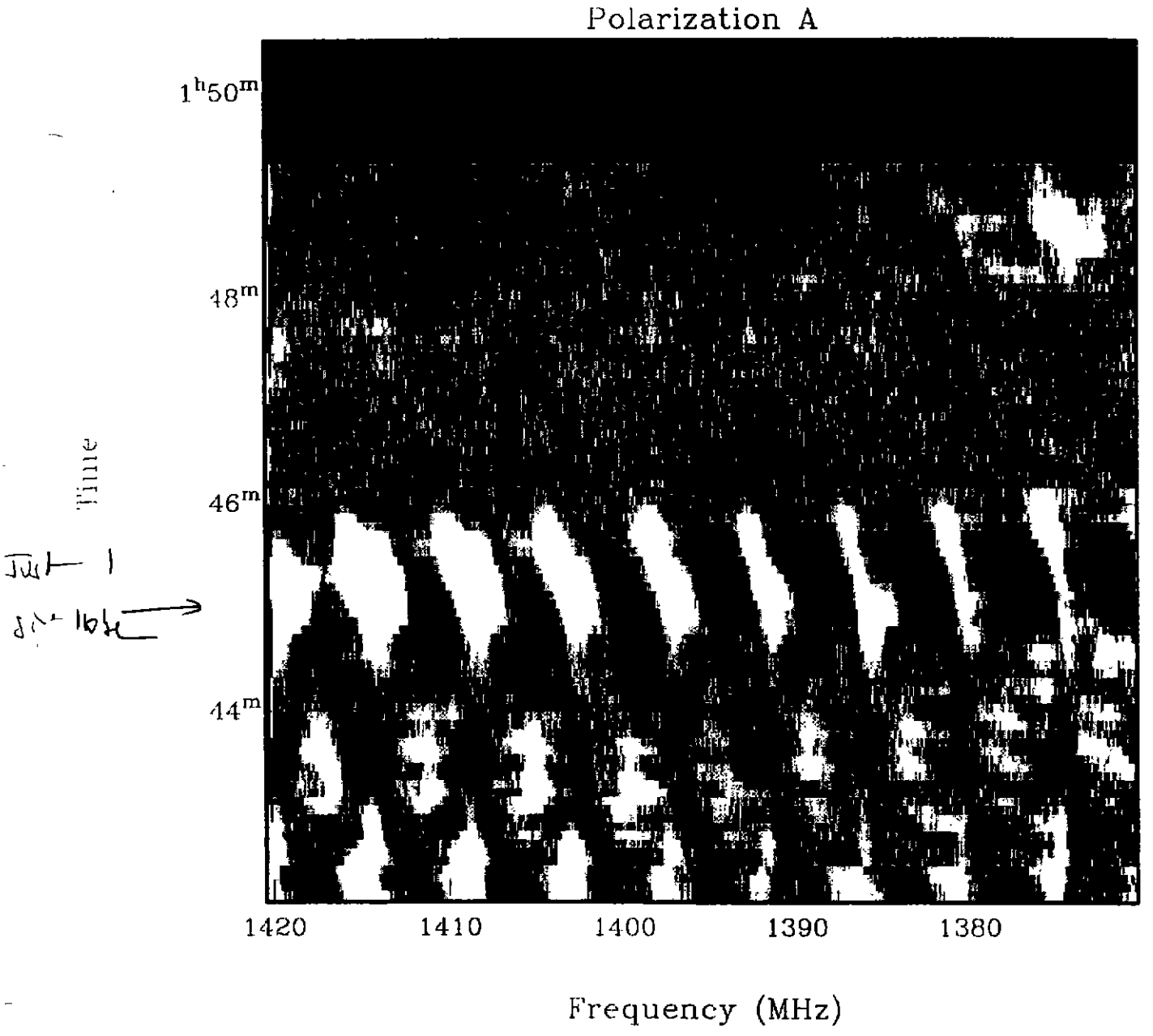

T(A)

980614_2358 #73

Scan Number 1

Polarization A

Frequency (MHz)

T(B)

PGPLOT Window 1

#50 start.

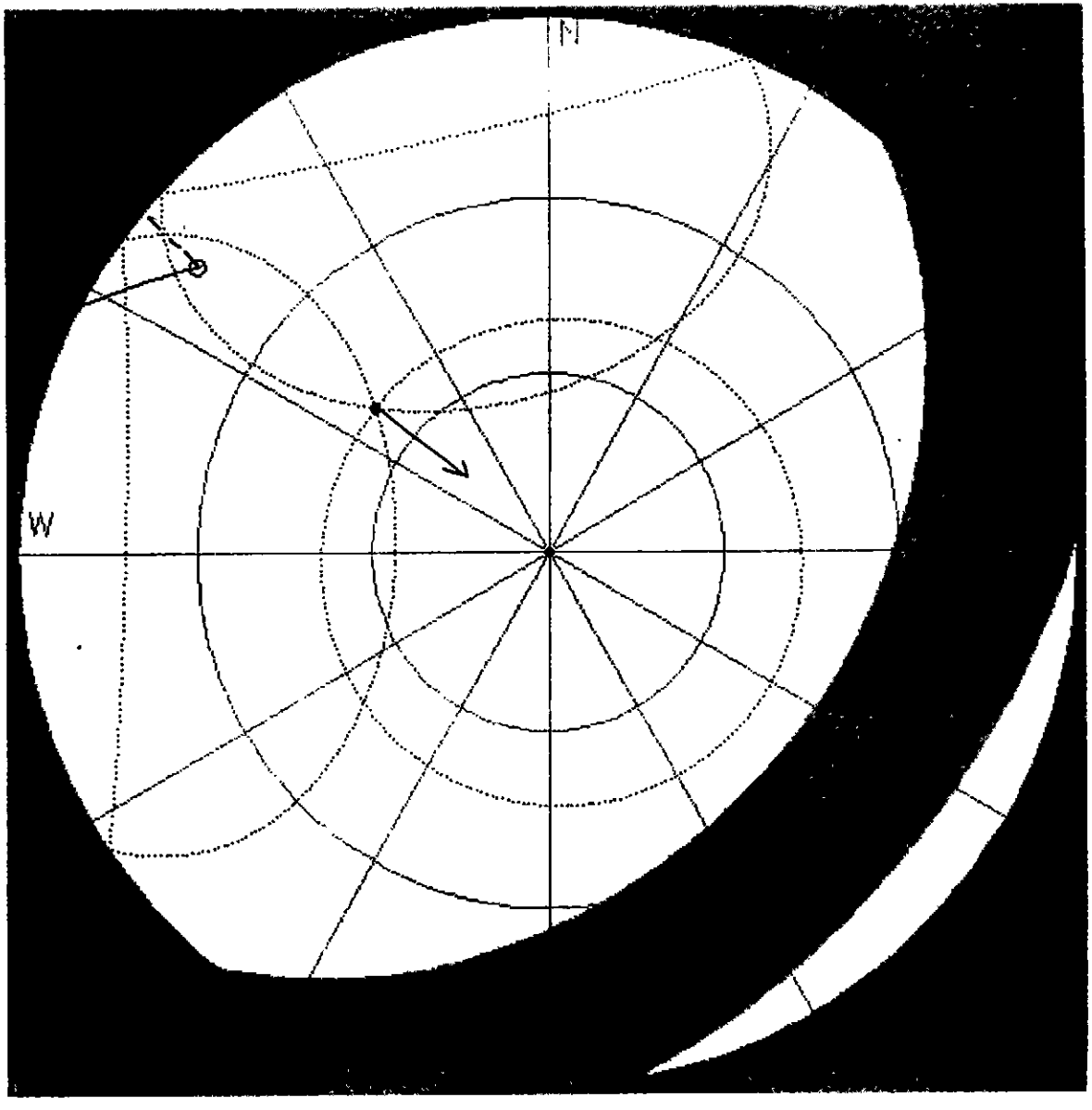

Compiled from lobo_slave_6.

Local date: 13 Jun 98
Local time: 15:48:45

Az of dish: 309.5 deg.
Ze of dish: 38.0 deg.

Tracks starting within the next 2.0 hrs are plotted.

0.19 days since last satellite data update.

Clock rate: 10

Forecast map resolution:
40 by 30

o Sun
▪ GPS
▪ Glonass

Type help for cmd summary.

U (A)

#50 980613_0547

Beam Number: 1

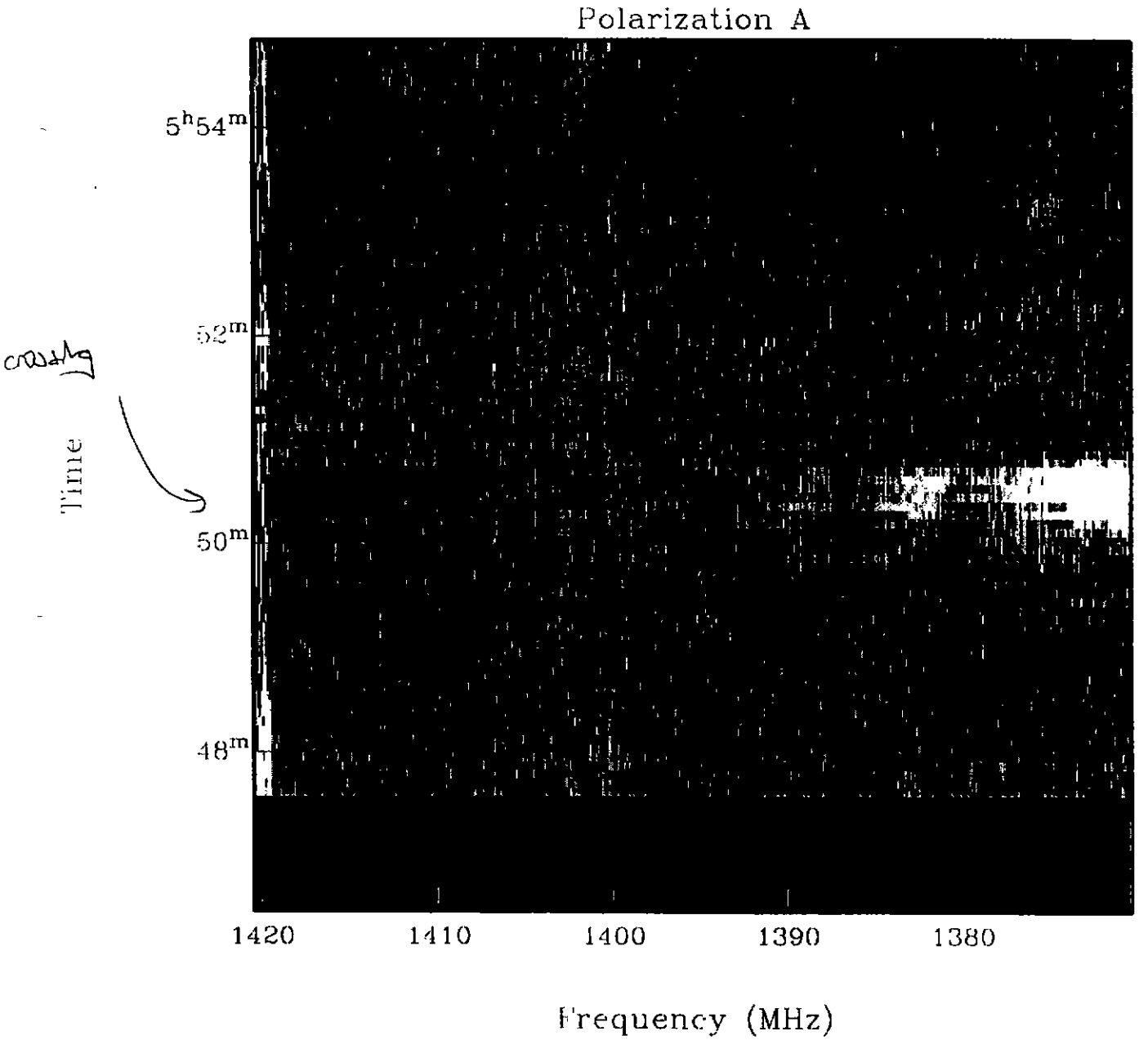

U (A)

#86

Beam Number 1

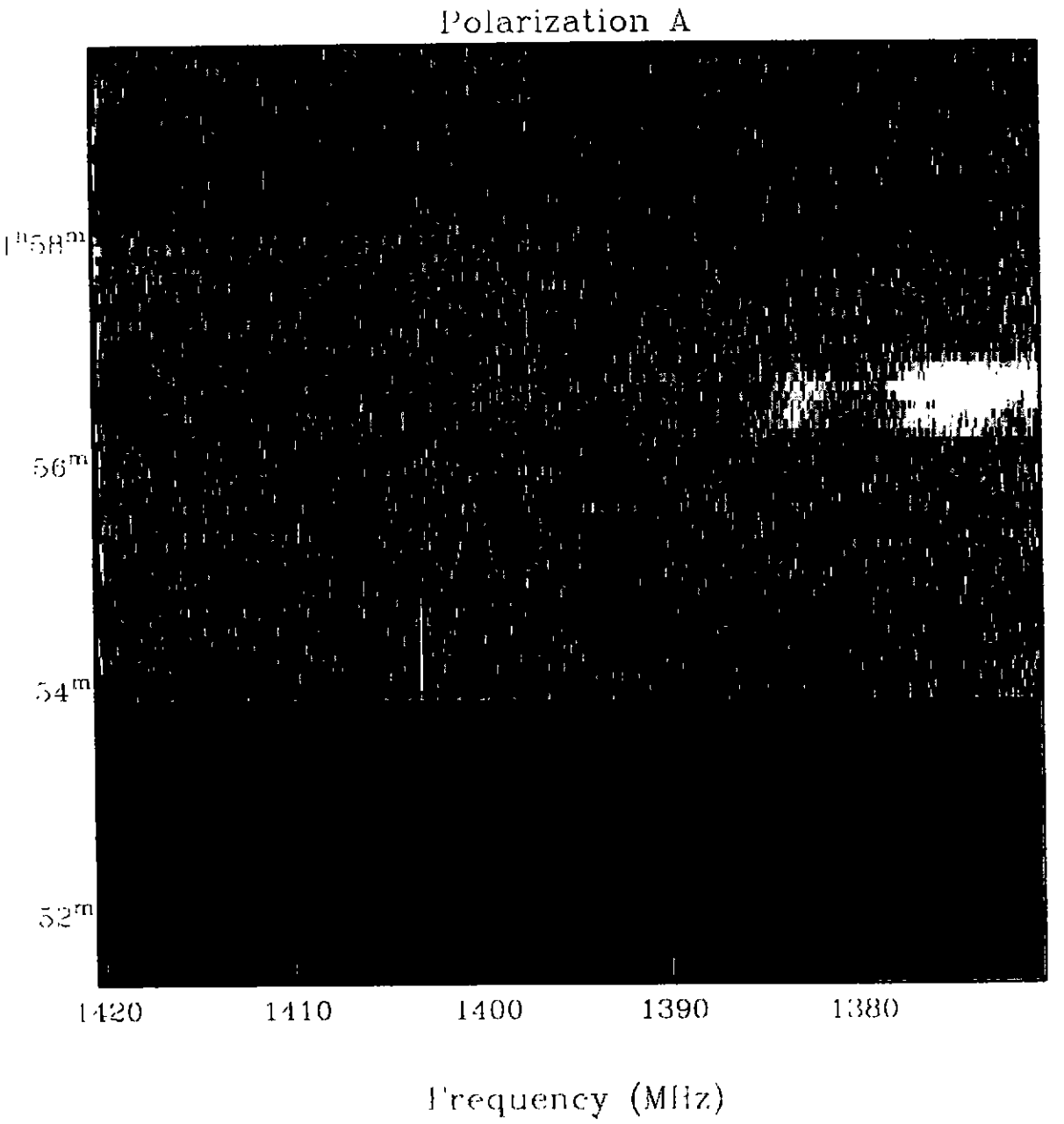

U (B)

PGPLOT Window 1

980613_0559 #51 START

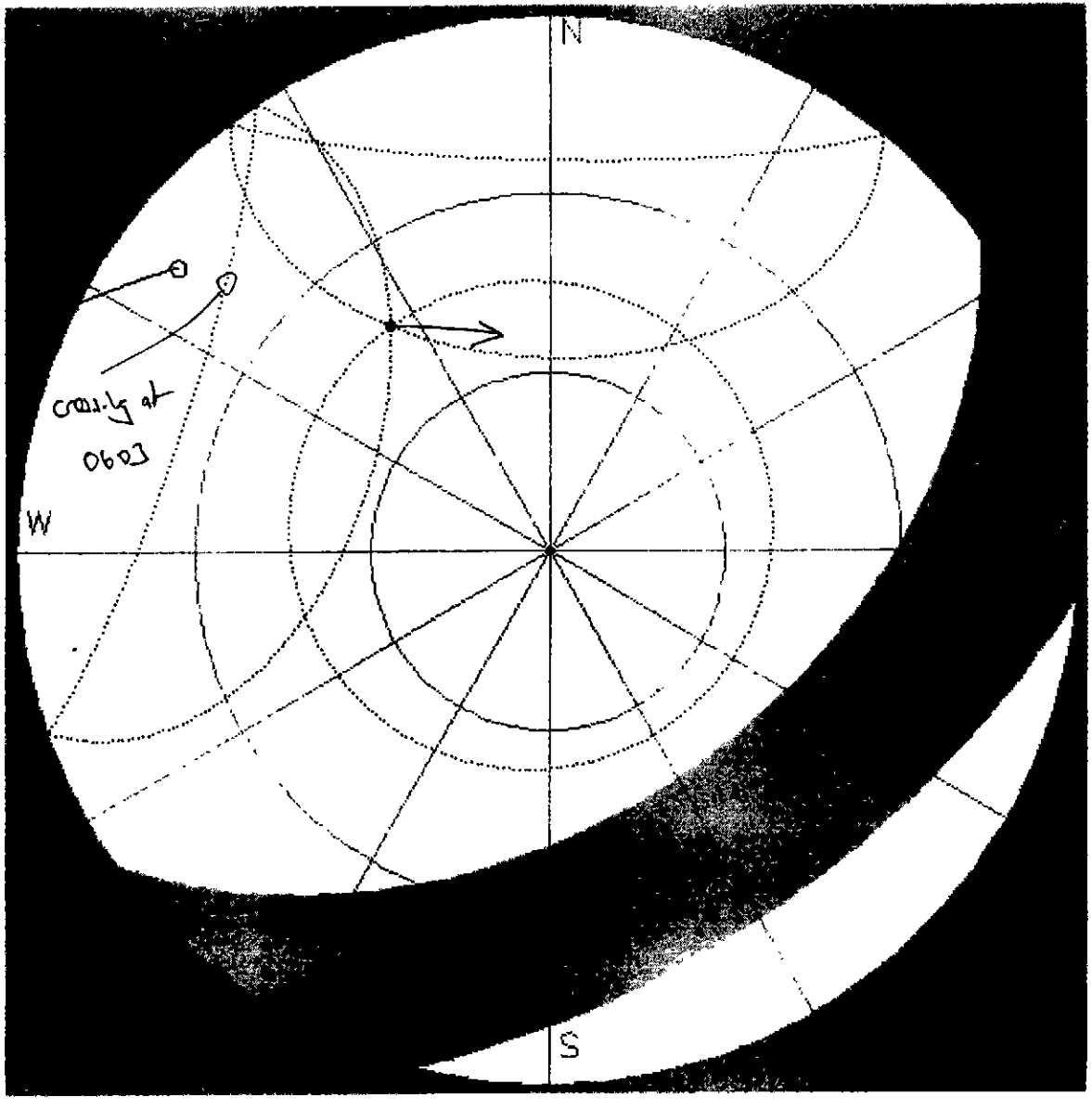

Compiled from lobo_slave_6.

Local date: 13 Jun 98
Local time: 15:59:33

Az of dish: 324.7 deg.
Ze of dish: 46.2 deg.

Tracks starting within the next 2.0 hrs are plotted.

0.19 days since last satellite data update.

Clock rate: 10

Forecast map resolution:
40 by 30

o Sun
▪ GPS
▪ Glonass

Type help for cmd summary.

(A) V

980613_0559 #51

Beam Number: 1

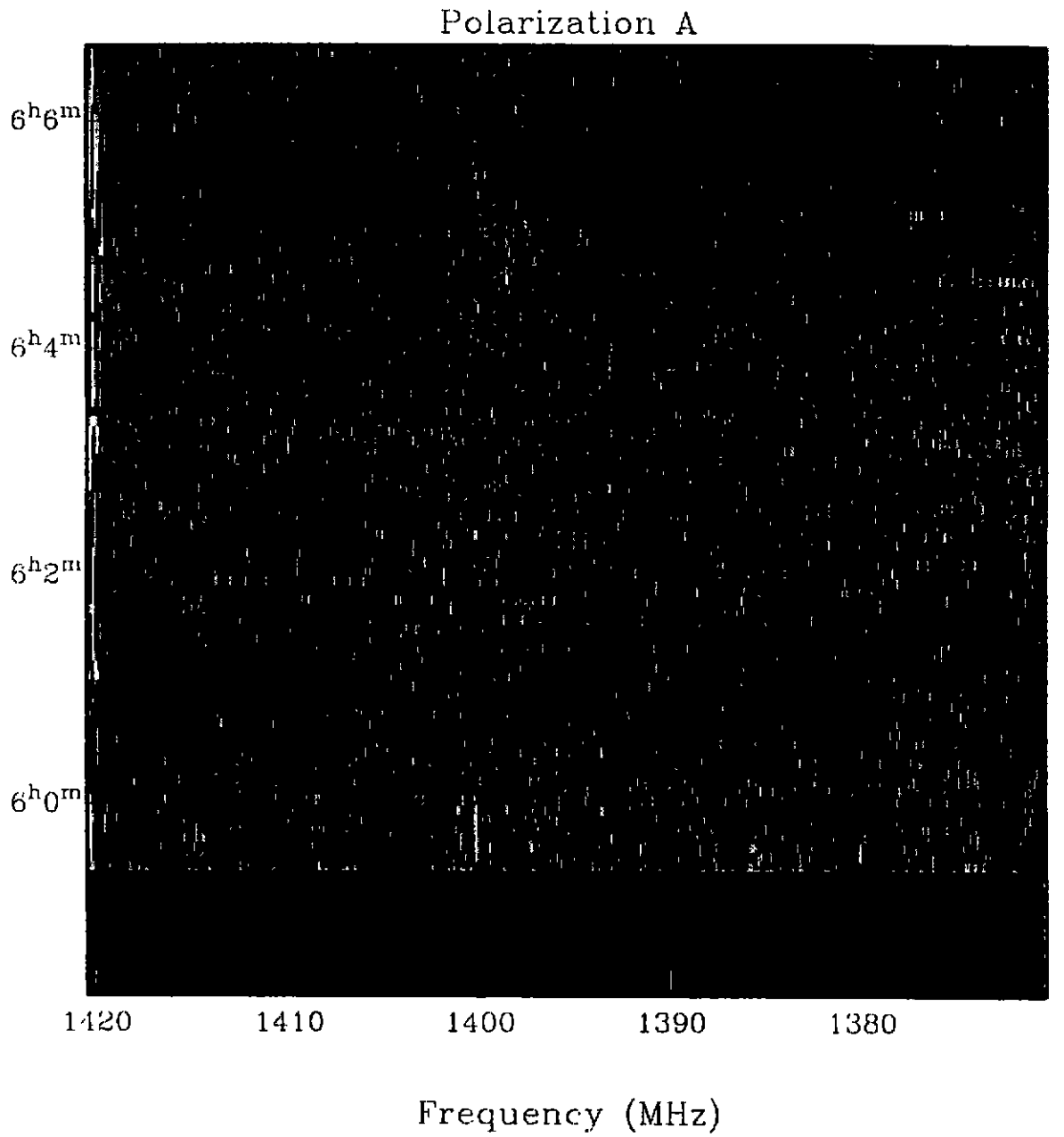

V (A)

#199

Scan Number 1

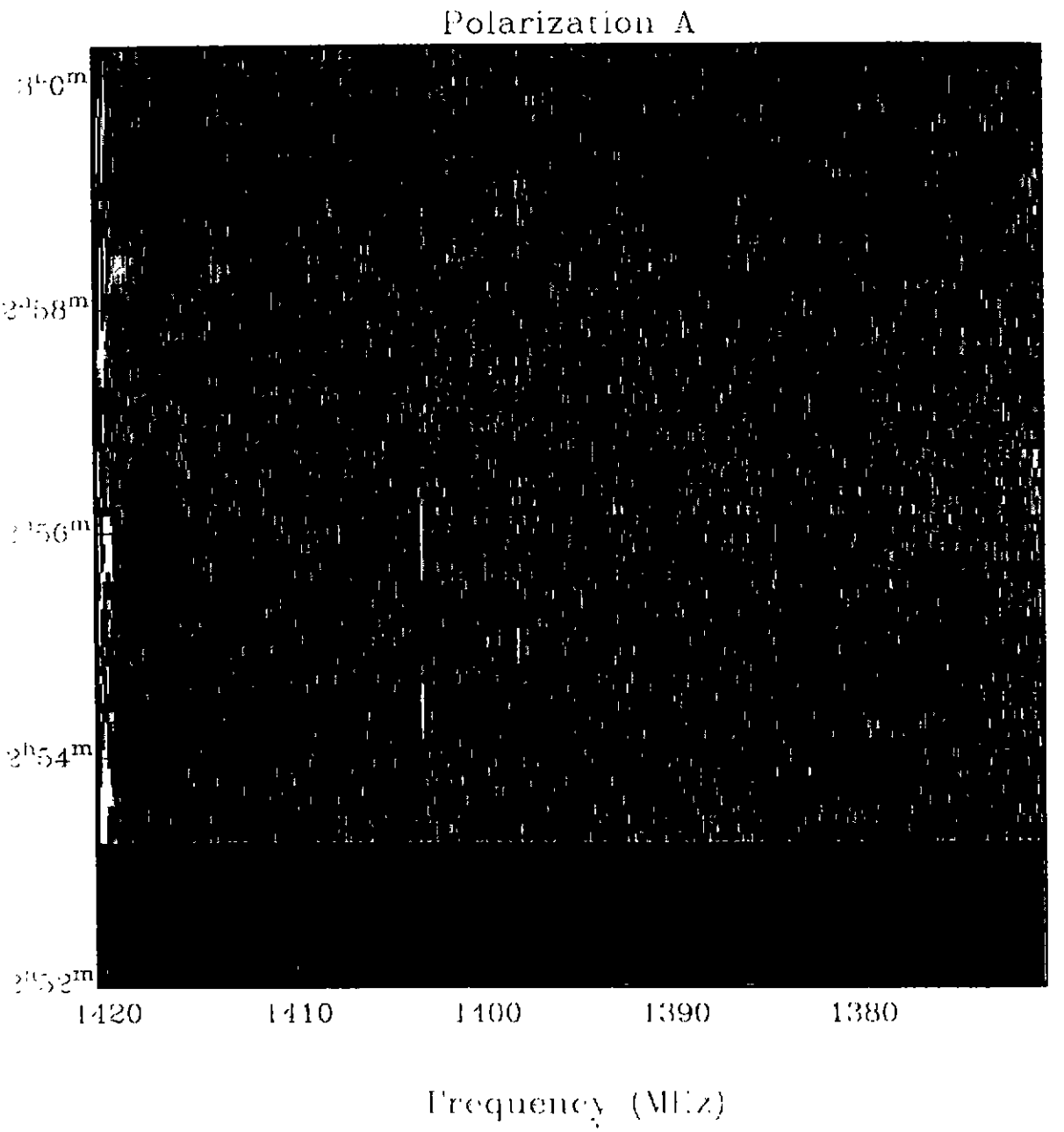

V(B)

PGPLOT Window 1

980613_0511 #46 start

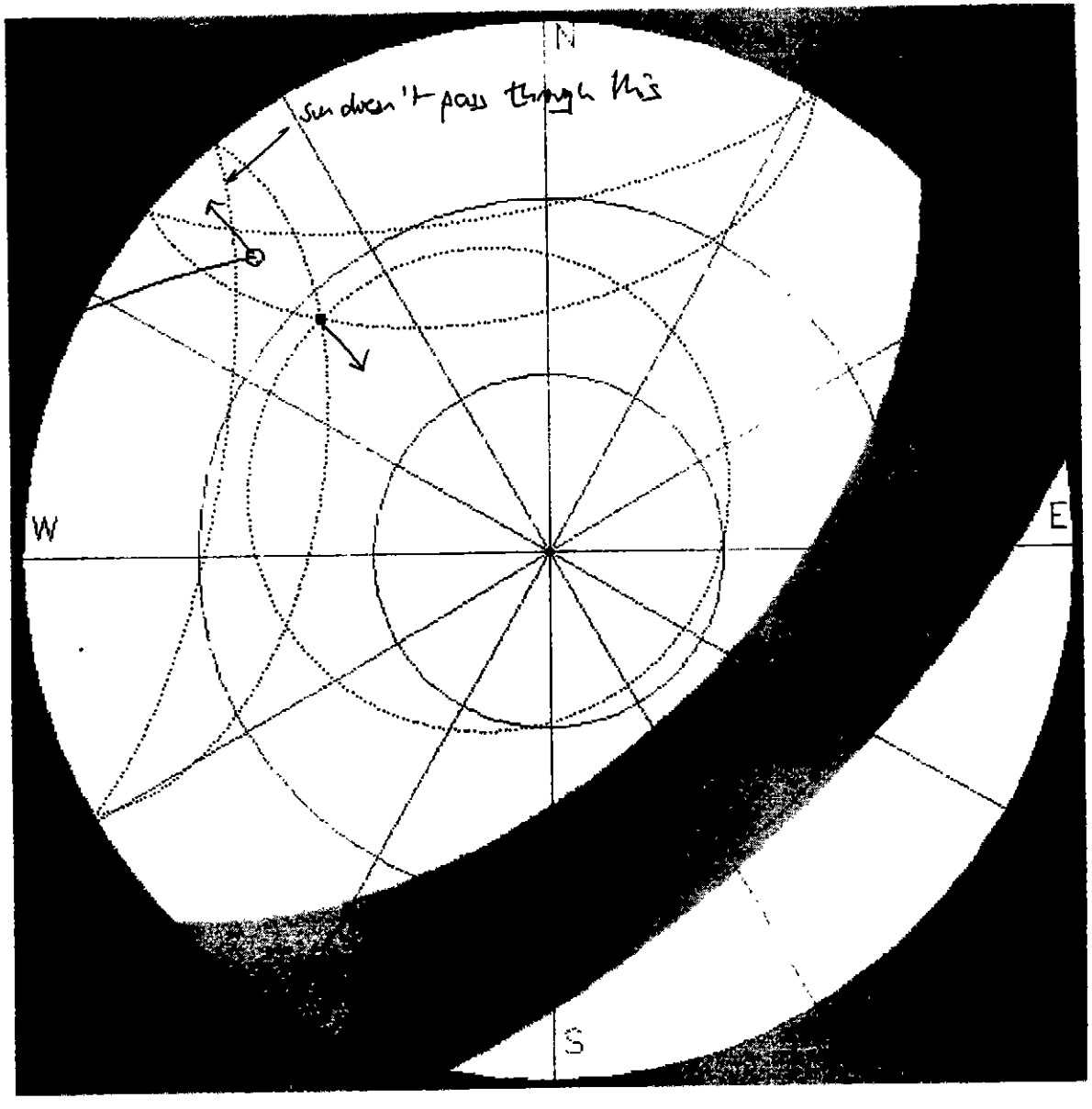

Compiled from lobo_slave_6.

Local date: 13 Jun 98
Local time: 15:11:17

Az of dish: 316.0 deg.
Ze of dish: 55.7 deg.

Tracks starting within the next 2.0 hrs are plotted.

0.16 days since last satellite data update.

Clock rate: 10

Forecast map resolution:
40 by 30

o Sun
▪ GPS
▪ Glonass

Type help for cmd summary.

W (A)

#46

Beam Number: 1

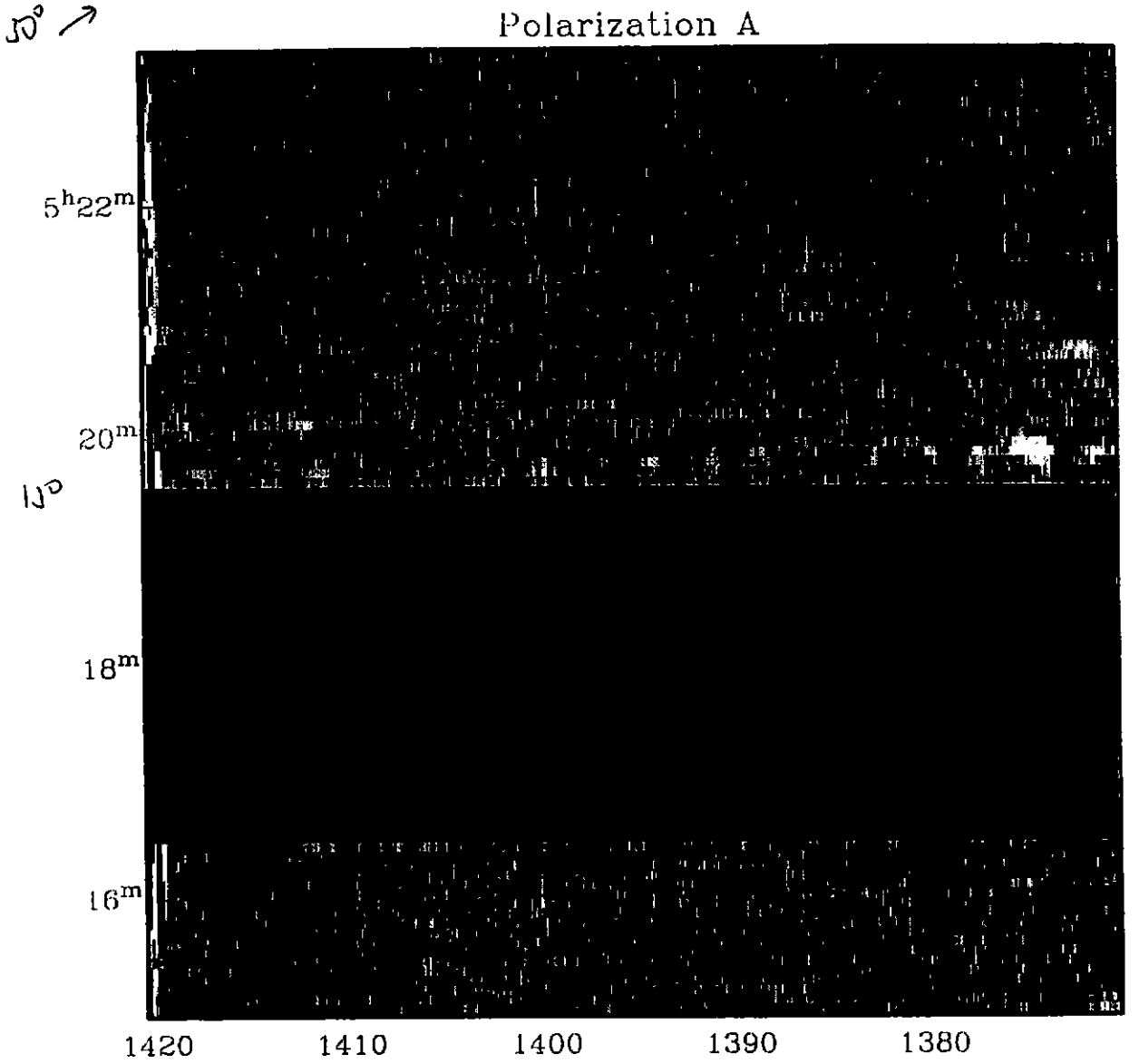

W (A)

84

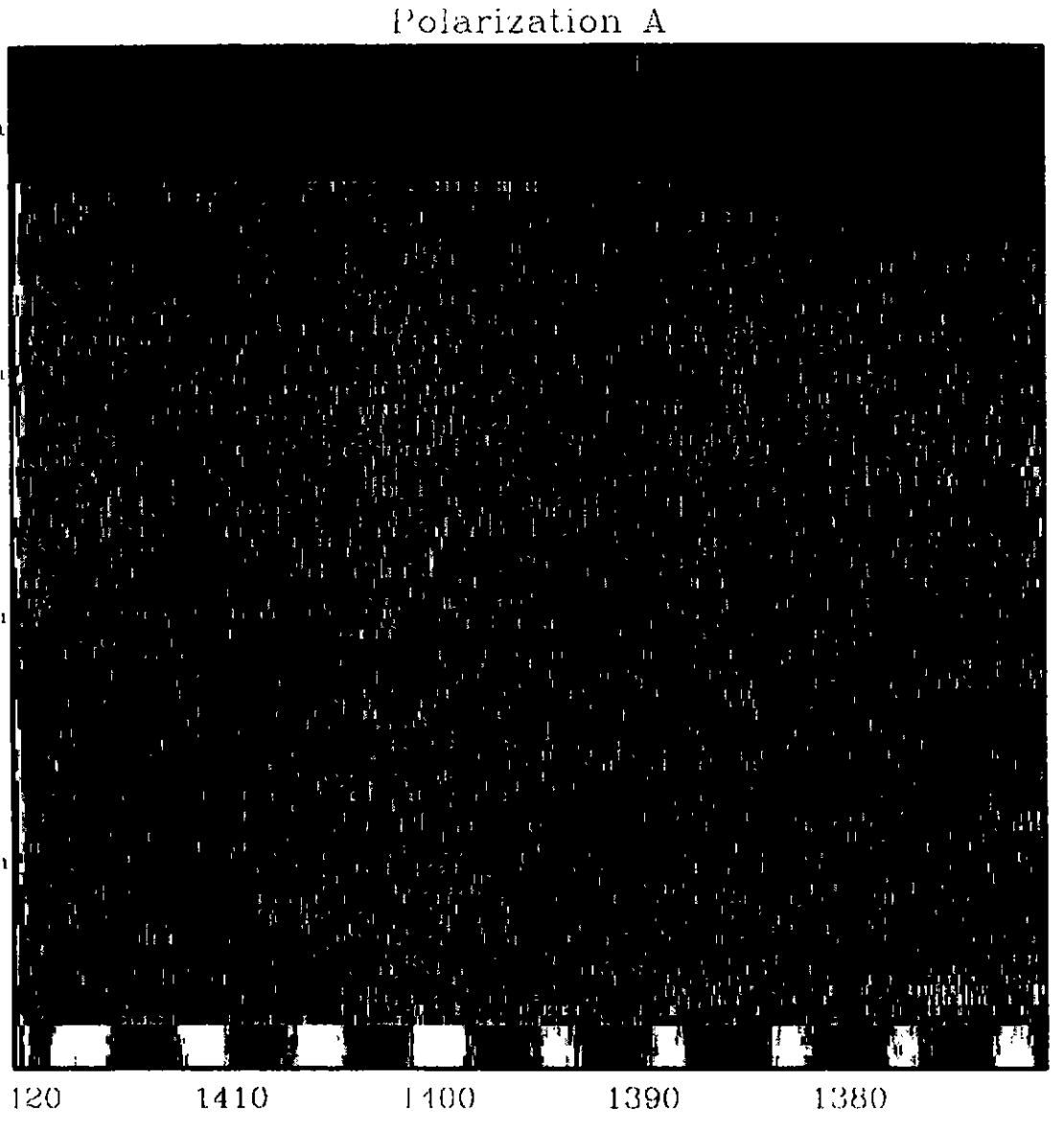

Ref from prev sa

W (B)

ATTACHMENT C

Spectral-ripple at Parkes:

Draft Paper

M.J. Kesteven, R.M. Price, L. Staveley-Smith,
B. MacA. Thomas, W.E. Wilson

Spectral Ripple at Parkes

M.J. Kesteven R.M. Price L. Staveley-Smith B.M. Thomas
W.E. Wilson

Abstract

We have investigated the baseline ripple effect at the Parkes telescope using the new 21 cm multibeam receiver. The dominant periodicity is 5.7 MHz with the on-axis ripple amplitude being 2% of the total (spillover+source) receiver noise. The ripple amplitude decreases markedly for off-axis beams. An enlarged vertex scattering cone (D = 5 m, θ = 22°) was installed but gave no substantial decrease in ripple amplitude. No reduction in ripple due to solar interference was evident. The scattering cone did however reduce anomalous polarisation by a factor of 2. We re-discuss models for ripple formation.

Keywords: telescopes – instrumentation

1 Introduction

The effect of spectral ripple on a radio telescope can be detrimental to the ability to detect broad, weak spectral features. Spectral ripple, or chromatism, manifests itself as a quasi-sinusoidal modulation of the receiver output as a function of frequency. Figure 1 shows an example of such a ripple, superimposed on the 64 MHz output of the 21 cm multibeam receiver at Parkes.

Spectral ripple is a problem at most major radio telescopes. The problem is often worst for Cassegrain and Gregorian designs which have more reflecting surfaces, and can be worst when observing strong radio continuum sources. At low frequencies, solar radiation is also a major source of spectral ripple, limiting the quality of daytime observations at many observatories. Internal reports have been written at various observatories. Only a few papers describing the problem have been widely published (Briggs 1997, Fisher 1997). At the Parkes telescope, the issue has been discussed by several previous authors (e.g. Poulton 1975, Padman 1978).

The generic mechanism for ripple formation is interference between two broadband, coherent noise sources, one of which is time-delayed with respect to the other. The frequency of the sinusoid $\Delta\nu$ is

$$\Delta\nu = \frac{1}{2\tau}, \tag{1}$$

in the case where there is a single delay, τ. The amplitude (i.e. 0.5× peak-to-peak) of the sinusoid a, relative to the power in the undelayed signal A, is given by

$$\frac{a}{A} = 2\gamma, \tag{2}$$

where γ is the *voltage* ratio of the delayed and undelayed rays (Poulton 1975). Thus, a ripple amplitude as high as 10% requires a scattered power of only 0.25%.

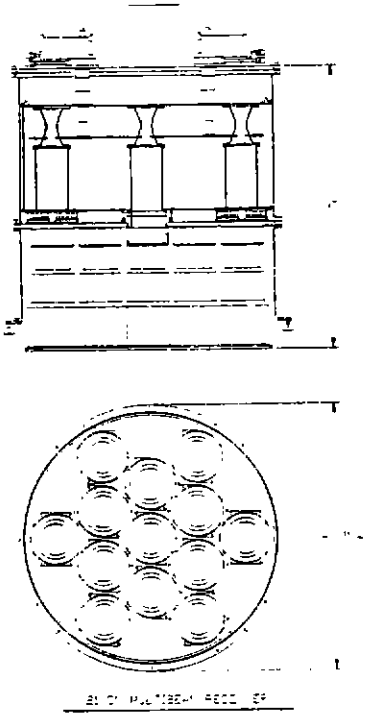

Figure 2: The 21 cm multibeam receiver.

at the vertex of the dish. This scattering cone was newly constructed out of aluminium sheet according to the dimensions shown in Figure 3. Because of the presence of the surveying mount, there was a hole in the centre of the cone.

2.1 Off-source ripple

Figure 1 is an example of so-called 'off-source' ripple. This is seen wherever the telescope is pointed, and only disappears if an absorber is placed in front of the feed. The main suspect for this ripple is spillover radiation from the ground. The magnitude of the effect for various beams was estimated by plotting the difference between a spectrum taken at two axial focus positions 50 mm apart. This $\lambda/4$ switching technique eliminates the overall bandpass shape and, by changing the phase of the 5.7 MHz sinusoid by 180°, approximately doubles the amplitude of the sinusoid.

In Table 1, the off-source ripple amplitude a/A is estimated with and without the vertex cone in position. Note that we assumed that a was a *quarter* of the peak-to-peak variation of the difference between two spectra with an axial focal position different by 50 mm.

2.2 On-source ripple

A number of on-source ripple measurements were made using the continuum source Hydra A. The detailed bandpass shape remained very similar to the off-source bandpass shape, implying that the ripple amplitude was also very similar. Quotient spectra confirmed this. To confirm this, we again used a 50 mm axial focus shift was used. This time the shift was symmetrically about the optimum focus, so that both positions had equal gain (which was < 0.1 dB down from optimum gain in any case). The inferred ripple amplitudes are given in Table 2.

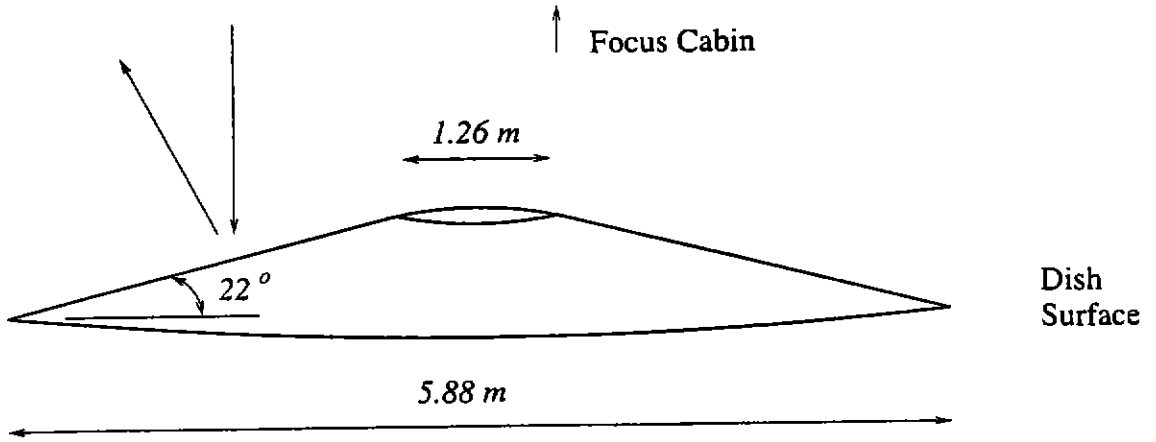

Figure 3: The above cone was placed at the vertex of the dish. The central hole was necessary because of the location of the trigonometric mount in the centre of the dish.

Beam	With Cone	Without Cone	Average T_{sys}
1	1.9%	1.7%	28 Jy (20 K)
2–7	0.8%	1.1%	30 Jy (20 K)
8–13	0.4%	0.7%	35 Jy (20 K)

Table 1: Inferred off-source ripple amplitude a as a fraction of the off-source total power A.

Oddly, the inferred $\lambda/4$ on-source ripple amplitudes are a factor of 2 below the inferred off-source ripple amplitudes. This appears to imply that a component of the on-source ripple does no change phase with axial focus as anticipated.

2.3 Rotation

The change in the amplitude of the ripple was also measured over a receiver rotation angle of 60°. A reference spectrum was taken at a rotation angle of −63.5°, and subtracted from a spectrum taken at a rotation angle of −3.5°. These observations were bothe taken near the zenith, and reveal the clearest difference between having the cone in position, and having the cone absent.

2.4 Solar Ripple

3 Theory

Mike and Bruce.

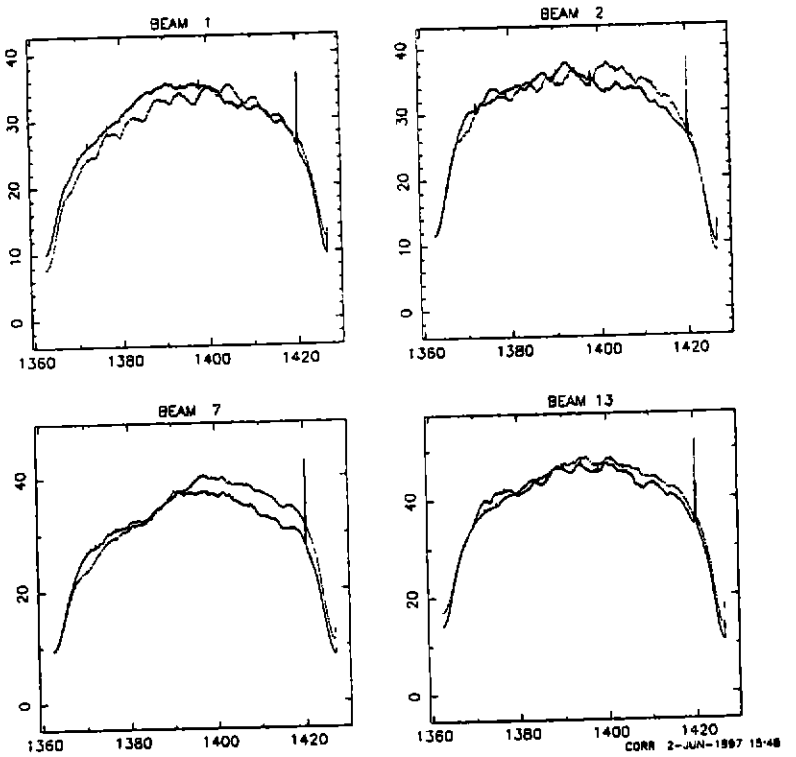

Figure 1: The total power passband for beams 1, 2, 7 and 13 from the multibeam receiver. The y-axis is in Janskys; the x-axis is the frequency in MHz. Both polarisations are plotted for each beam. The strongest 5.7 MHz ripple is evident in beam 1, polarisation B.

The purpose of the observations described in this report is to investigate factors which cause spectral ripple, and investigate ways of reducing it using the new 21 cm multibeam receiver and the upgraded focus cabin at the Parkes telescope. The multibeam receiver is a package of 13 beams arranged in a hexagonal pattern with a total diameter of 1.2 m (Figure 2). This receiver was installed for the first time in January 1997. The receiver is placed at prime focus in a cabin which was newly installed in March 1996. The cabin is significantly larger than the previous focus cabin, with an overall diameter of around 5 m. The focus cabin has a large rectangular aperture of 1.68×2.55 m, within which the receiver is placed.

2 Observations

The multibeam receiver was completed a year after the Parkes focus cabin upgrade. However, evidence from observers using the H-OH single-feed receiver is that, under most conditions, there is no noticeable deterioration of spectral ripple with the new focus cabin. An important caveat here is that, with the new cabin, extremely high isolation radio-frequency cables are required between the receiver package and the down-converters. Any radiation leaking out of equipment can much more easily escape through the enlarged focus cabin hole and back into the feed, leading to a potentially devastating ripple problem. There also appears to be no significant difference between ripple using the multibeam receiver, and using the H-OH single-feed receiver.

The observations described below were obtained with and without a scattering cone in place

Beam	With Cone	Without Cone	Average T_{sys}
1	0.8%	0.9%	68 Jy (50 K)
2–7	0.7%	0.5%	70 Jy (48 K)
8–13	–	0.3%	75 Jy (44 K)

Table 2: Inferred on-source ripple amplitude a as a fraction of the off-source total power A. Hydra A was observed at two equally out-of-focus axial positions, +25 mm and −25 mm. The predicted gain-loss at these positions is only 2%.

Beam	With Cone	Without Cone	Average T_{sys}
1	1.5%	2.7%	28 Jy (20 K)
2–7	–	2.6%	30 Jy (20 K)
8–13	0.8%	2.0%	35 Jy (20 K)

Table 3: Change in ripple amplitude Δa as a fraction of the off-source total power A for a 60° rotation of the multibeam receiver.

4 Summary

Acknowledgments

We thank John Crocker, Harry Fagg and Barry Turner for building and installing the vertex cone.

References

Briggs, F.H. 1997 PASA, 14, 37
Fisher, J.R. 1997 PASA, 14, 96
Padman, R. 1978 Radiophysics report RPP 2056
Poulton, G.T. 1975 Queen Mary College Research Report GTP/2/75

ATTACHMENT D

Another Look at Multiple Reflections on the Parkes 64m Radio Telescope: A Discussion Paper

Draft Report

B. MacA. Thomas

CSIRO - Australia Telescope National Facility

Another Look at Multiple Reflections on the Parkes 64m Radio Telescope: A Discussion Paper

1. *Introduction*

Following H-line observations using the new multi-beam receiver at Parkes by A. Wright, L. Staveley-Smith, et al during daylight hours, very strong interference was evident from the sun when fairly close to boresight. The "classic" approx. 6 MHz baseline ripple was a major characteristic of the interference. This discussion paper revisits the major mechanisms causing such interference, and proposals are made for experiments to attempt to reduce their effect.

2. *Major Mechanisms of Reflections*

For convenience, let us consider the feed as transmitting, and assume that reciprocity will apply for the receiving case. The blockage of the cabin (see Figs A and B) is approximated by a circle of diameter 6m.

Fig. 1 shows the basic "cavity-effect". Path 2, when incident on the metal cabin floor located in the focal plane will have two effects: diffraction of energy around the edge of the cabin (shown as D2), and direct reflection of energy.

In the latter case we assume an aperture of currents of diameter 6m ($D/\lambda=28.6$), neglecting the hole in the middle. (This could be more precisely modelled as an annular ring of currents, which would tend to give higher side-lobes). Fig 1(a) (from Hansen) gives an indication of the magnitude of the field near the vertex for rays 3, where range length (26.24m) is expressed in normalised form: $x\ (2D^2/\lambda)$; $x = 0.15$. Fig. 1(a) shows that there is significant energy incident in the vertex region. The pattern of the reflected energy will be dependant on the phase distribution. Note that further diffraction (D4) will take place when the return rays (4) again hit the edges of the cabin. Also, there will be a significant beating between return rays 2 and 4 at the feed.

A similar argument holds for an offset feed (shown in Fig 2 as being 1m offset).

The incident energy from the spherical wave (ray 1) can be scattered in a controlled manner by using an hyperboloidal "sub-reflector" at the vertex. The return energy, instead of forming a "cylinder" of plane waves, is scattered approximately uniformly from 0° to 70° (See Fig. 3).

Another likely area of concern is the reflection of energy from the upper region of the struts (see Fig. 4) directly into the feed. It is suggested that a "crenellated" shield (1.7x1m) be placed as shown in Fig.5 to shield the feed from this energy. It may be desirable to shape the shield in the horizontal plane in the form of a parabolic cylinder to minimise "coupling" of energy between the three shields at the strut locations. A later experiment may be to place a pointed reflector underneath the upper 3m (approx.) of each strut as shown in Fig.6.

Another area that deserves consideration is the need to "break-up" the diffracted energy at the lower edges of the focus-cabin. Although very difficult to access, a "crenellated" sheet attached to the surrounds of the focus-cabin and in the focal-plane may assist here.

3 Recommendations

It is recommended that, following consideration of the input presented here, a number of measures be implemented as part of an experimental program:

Stage 1: Addition of a 6m dia hyperboloidal reflector at the vertex (Fig.3);
Stage 2: Addition of vertical "crenellated" shields where the struts attach to the floor of the focus cabin (Fig. 5. See also Fig. A)

Other additional possibilities are:

(a) Addition of "deflector" plates at the upper sections of the struts (Fig. 6);
(b) Addition of horizontal "crenellations" around the edge of focus-cabin in the focal-plane.

Bruce MacA Thomas
6 May 1997

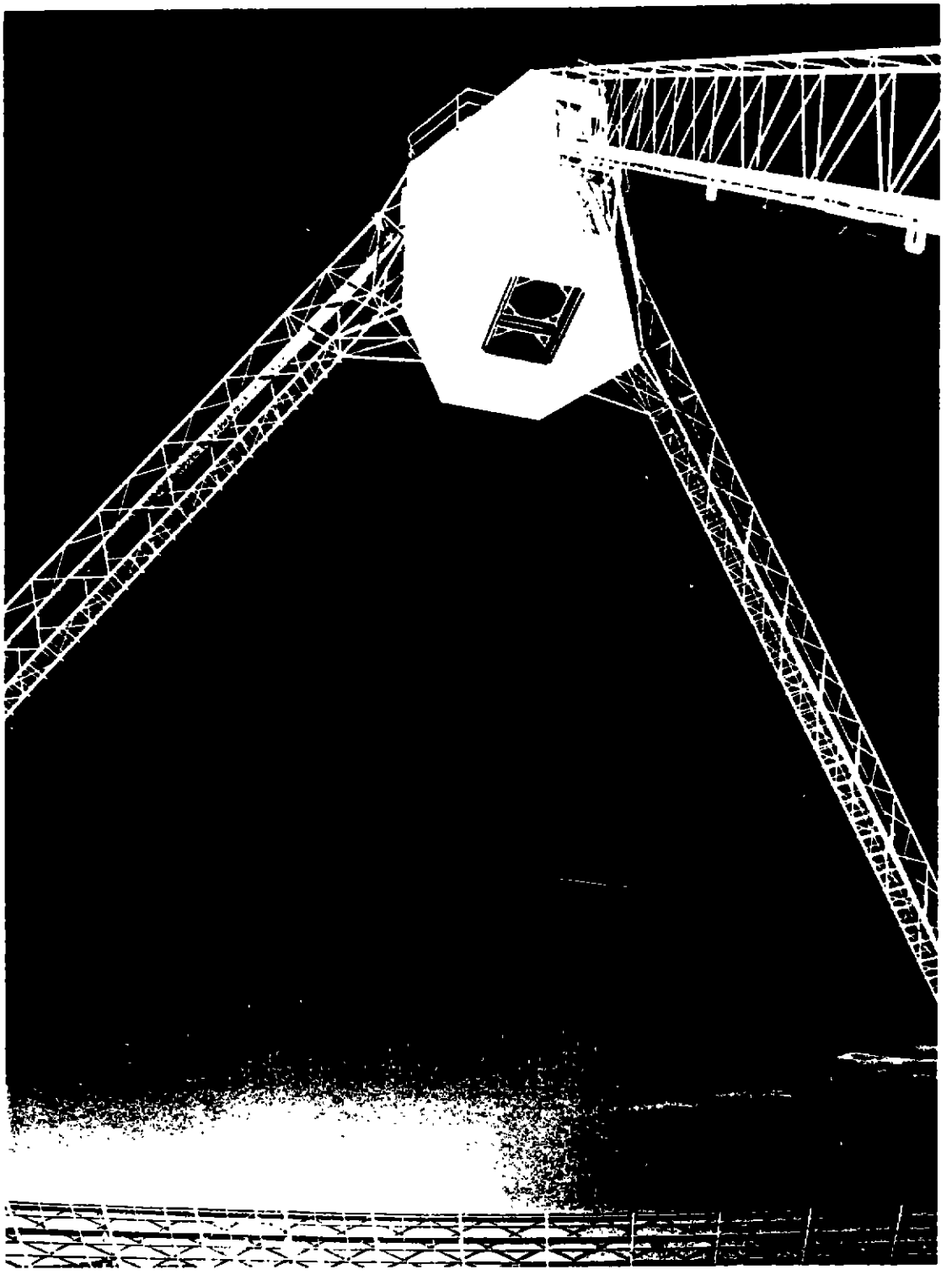

A1

FIG. A

1m.

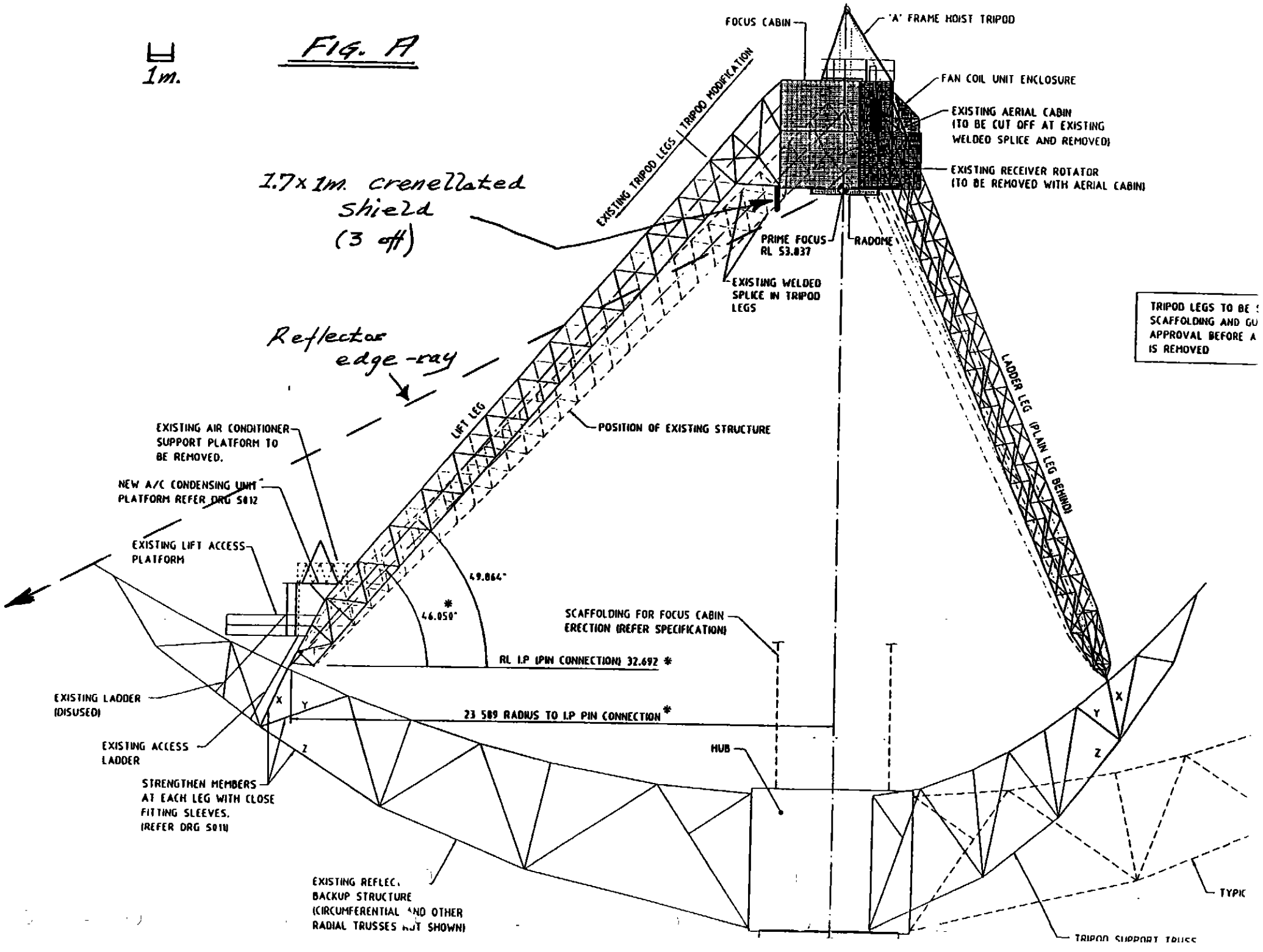
FOCUS CABIN
'A' FRAME HOIST TRIPOD
FAN COIL UNIT ENCLOSURE
EXISTING AERIAL CABIN (TO BE CUT OFF AT EXISTING WELDED SPLICE AND REMOVED)
EXISTING RECEIVER ROTATOR (TO BE REMOVED WITH AERIAL CABIN)
EXISTING TRIPOD LEGS
TRIPOD MODIFICATION
1.7x1m. crenellated shield (3 off)
PRIME FOCUS RL 53.837
RADOME
EXISTING WELDED SPLICE IN TRIPOD LEGS
TRIPOD LEGS TO BE SCAFFOLDING AND GU APPROVAL BEFORE A IS REMOVED
Reflector edge-ray
LIFT LEG
POSITION OF EXISTING STRUCTURE
LADDER LEG (PLAIN LEG BEHIND)
EXISTING AIR CONDITIONER SUPPORT PLATFORM TO BE REMOVED.
NEW A/C CONDENSING UNIT PLATFORM REFER DRG S012
EXISTING LIFT ACCESS PLATFORM
49.864°
46.050°
SCAFFOLDING FOR FOCUS CABIN ERECTION (REFER SPECIFICATION)
RL I.P (PIN CONNECTION) 32.692 *
23 589 RADIUS TO I.P PIN CONNECTION *
EXISTING LADDER (DISUSED)
EXISTING ACCESS LADDER
STRENGTHEN MEMBERS AT EACH LEG WITH CLOSE FITTING SLEEVES. (REFER DRG S011)
HUB
X
Y
Z
EXISTING REFLEC BACKUP STRUCTURE (CIRCUMFERENTIAL AND OTHER RADIAL TRUSSES NOT SHOWN)
TYPIC
TRIPOD SUPPORT TRUSS

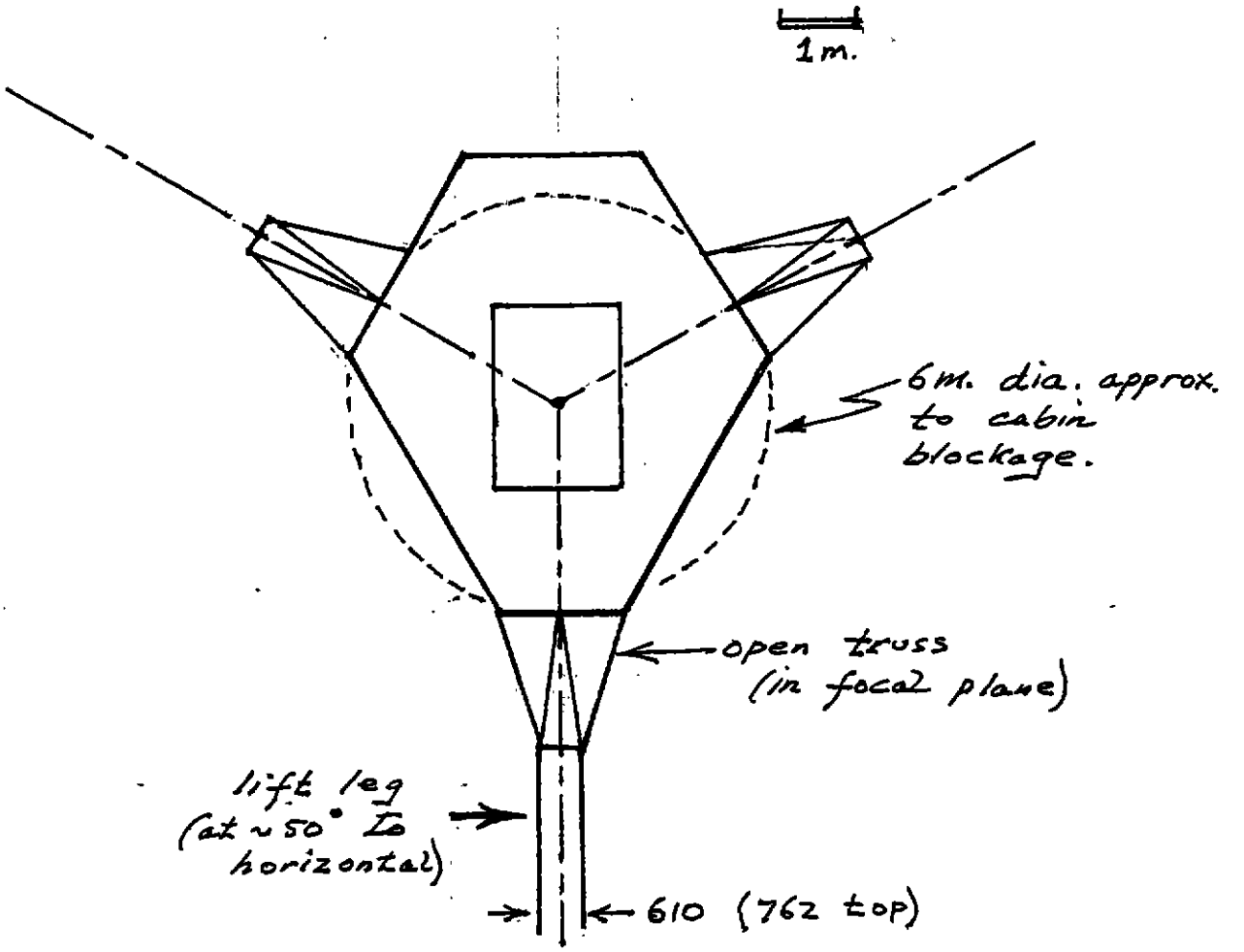

FIG. B: The cabin in the focal-plane, and the strut connections.

BMT/5.5.97

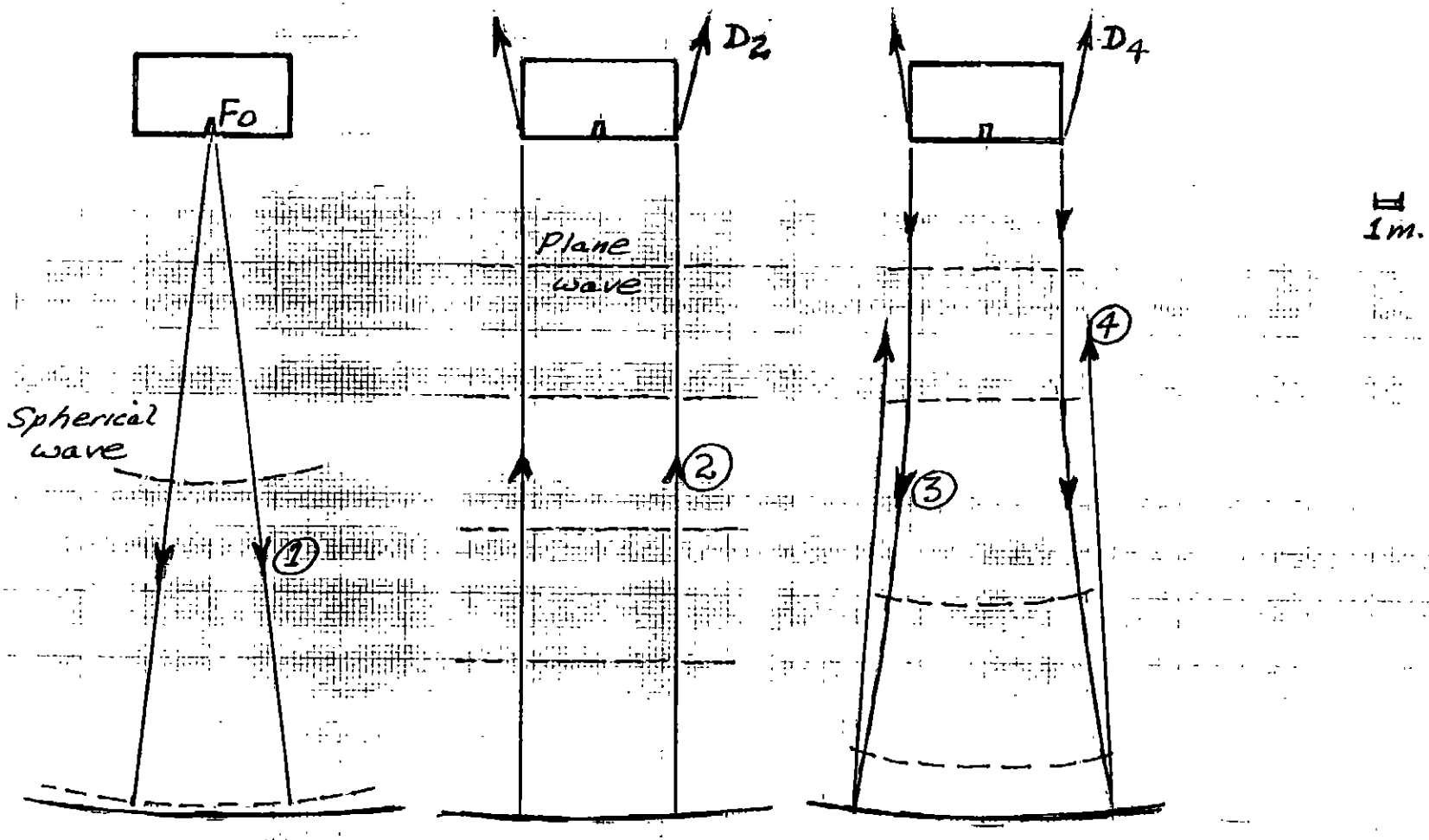

Spherical wave: path 1

Plane wave: path 2.

Focus-cabin reflection: path 3
Main-reflector reflection: path 4

FIG. 1. "Cavity-effect": on-axis feed.

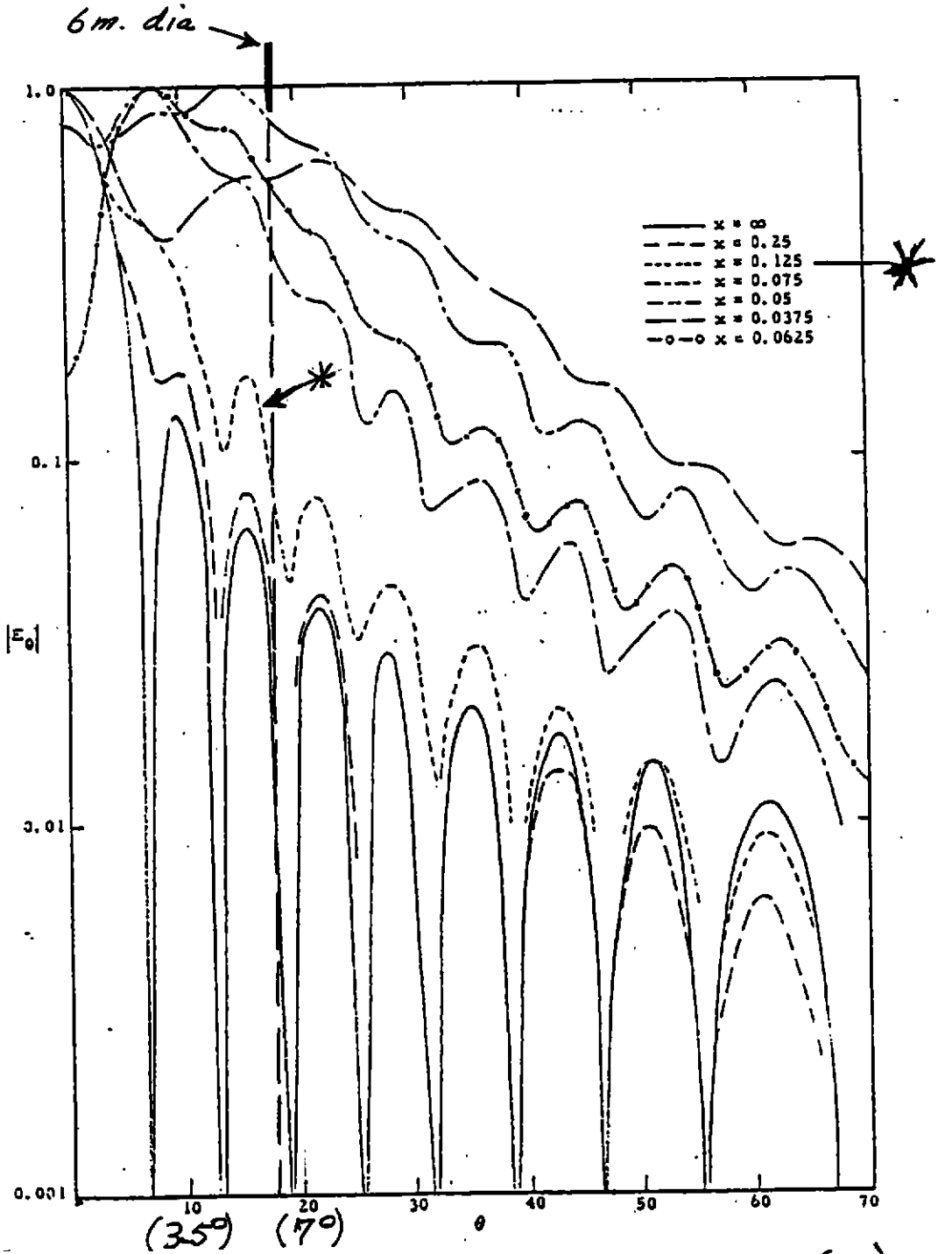

Fig. 2—Elevation patterns—uniform illumination. (10λ)

FIG. 1 (a)

Near-field patterns of an aperture, 10λ;
Range length = $\pi\left(\frac{2D^2}{\lambda}\right)$.

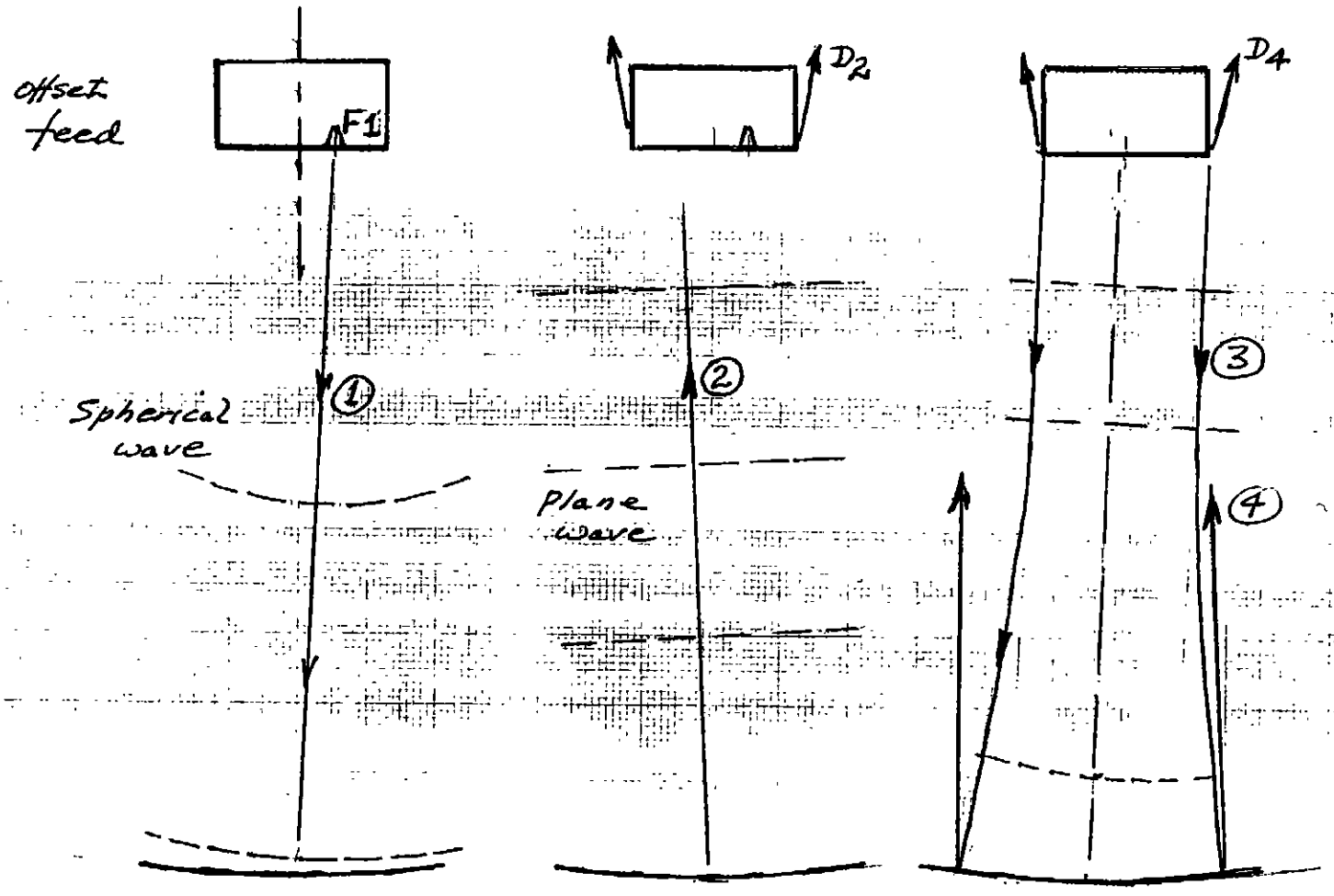

FIG. 2. "Cavity-effect": off-axis feed.

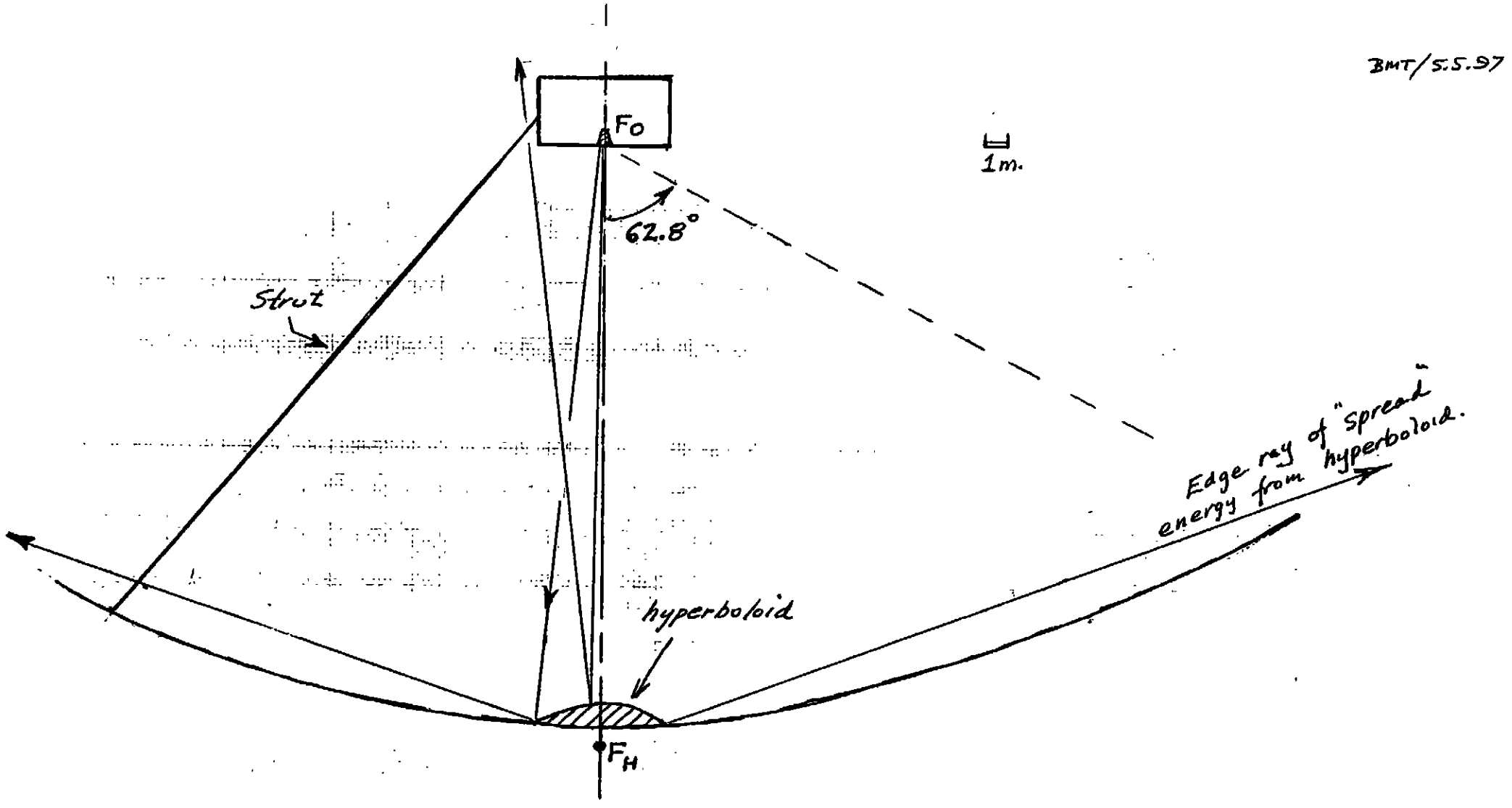

FIG. 3. Use of a hyperboloid to "spread" energy at vertex.

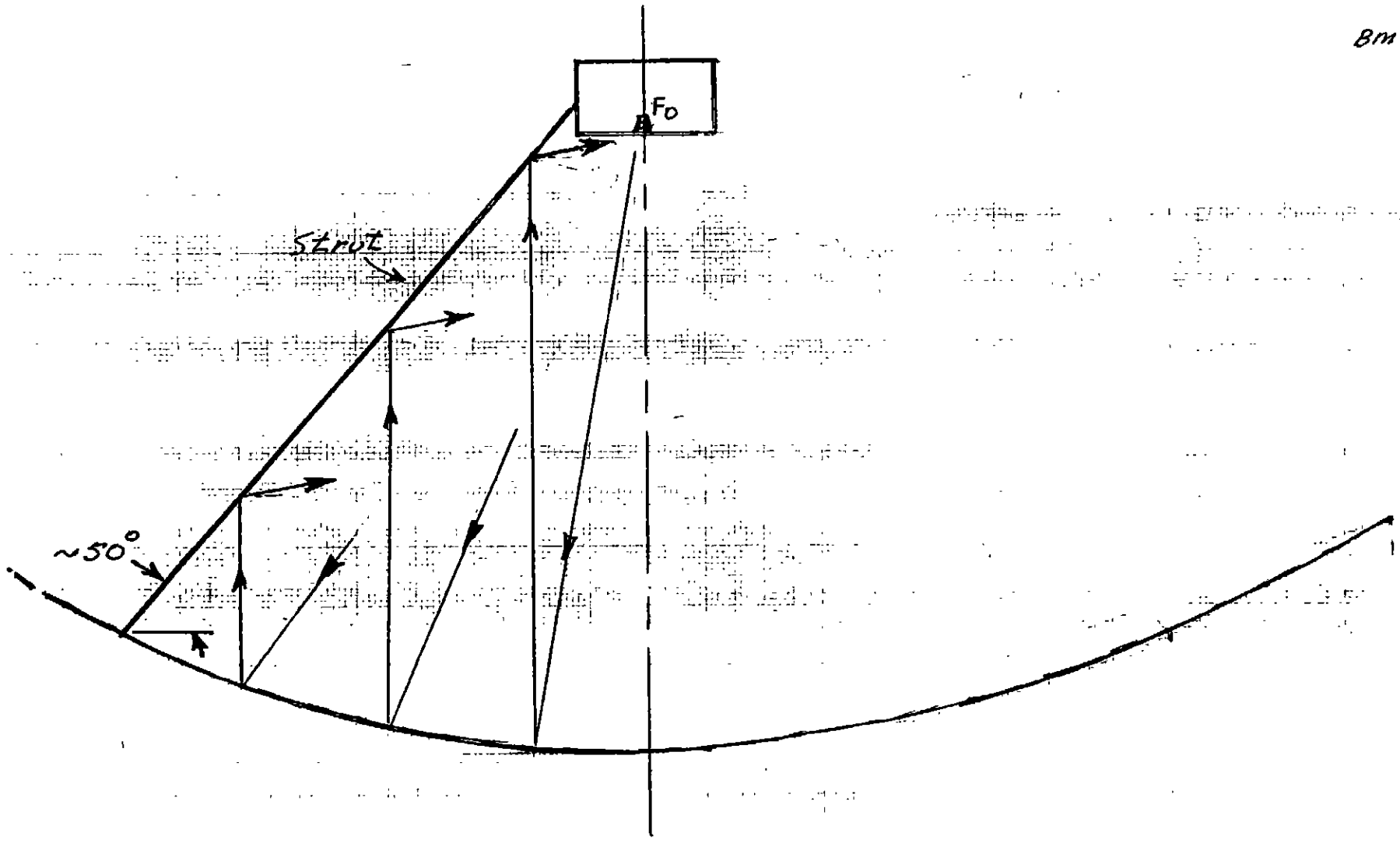

FIG. 4. Strut scatter : first path.

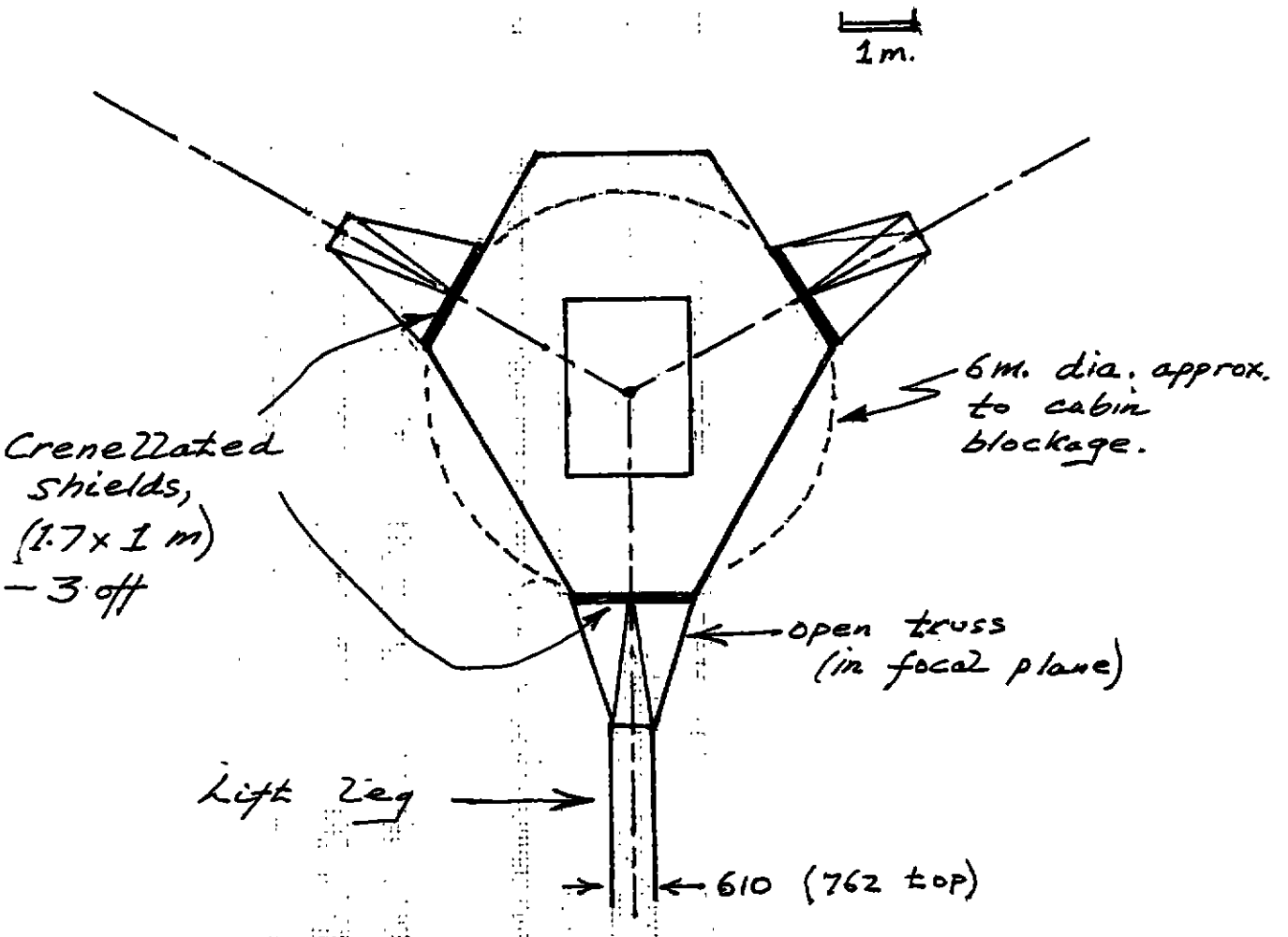

FIG. 5.
Location of crenellated shields (3 off).

BMT/6.5.97

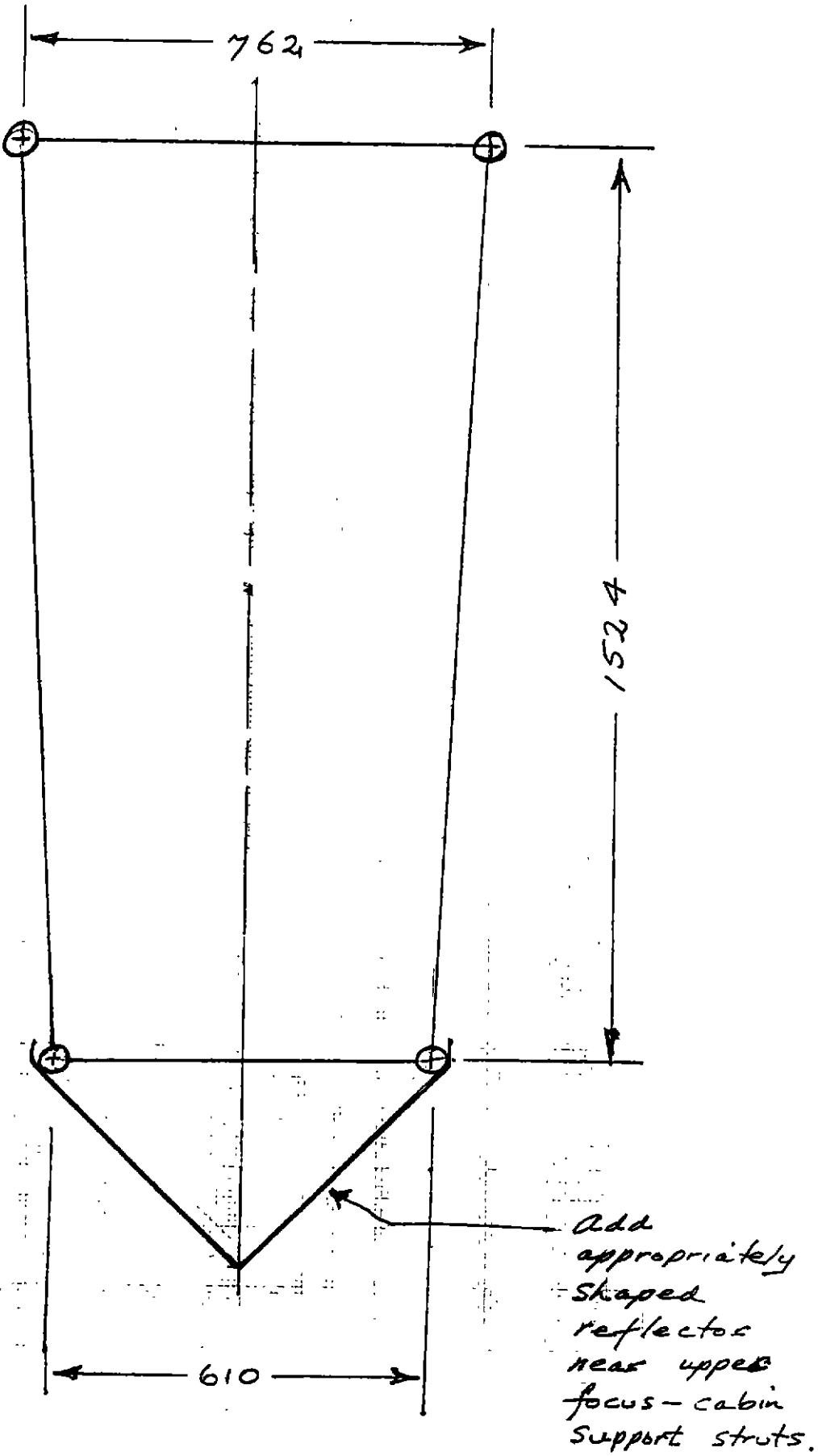

Fig. 6: Strut cross-section with reflector plate

ATTACHMENT E

The Baseline Ripple Problem: Summaries of Earlier Work

- **The Parkes spectral line baseline problem - will it be exacerbated by the upgrade** **M.J. Kesteven**

- **Some general thoughts from Padman's work (1978) at 5GHz**

The Parkes Spectral Line Baseline Problem - Will it be Exacerbated by the Upgrade?

M. Kesteven

1 Introduction

There is a well-entrenched belief at the ATNF that high sensitivity spectral observations are compromised by the notorious "5.7 MHz baseline ripple". Since the ripple is due to multi-pathing between the focus cabin and the vertex, concern was naturally raised as to whether the enlarged focus cabin of the Parkes Upgrade would result in an increase in the magnitude of the ripple.

It transpires that a large amount of work was done on this problem, both here and overseas; the published record is, however, a bit sparse, as almost all the work is only recorded in internal reports. One gains the impression that the concensus (in the 70s) was that the problem was well understood, and that with care the problem could be tamed, resulting in good quality baselines. That collective wisdom appears to be evaporating.

A general summary of the baseline problem is given in section 2; in section 3 the Parkes-specific experiments are described. A detailed discussion of the Upgrade problem is given in section 4.

2 Previous Work

2.1 The problem

High sensitivity spectral line measurements have long been troubled with baseline problems, generally in the form of a quasi-sinusoidal variation ("ripple"). The periodicity suggests multi-path interference with the secondary path length equal to twice the focal length.

A number of different mechanisms have been identified (Poulton, Morris), falling into two categories:

- Gain Chromatism. In this case the peak-to-peak ripple amplitude is proportional to the observed source intensity. This is the "ON-Source" component.
- Baseline Chromatism. This component is encountered even when the antenna is pointing at blank sky. This is the "OFF-Source" ripple.

2.2 ON-Source component

Even a well designed feed will fail to capture all the energy incident on the antenna focus; if the "uncaptured" fraction scatters off the main reflector back to the feed then interference effects will result, with a frequency interval between the constructive maxima equal to:

$$\Delta f \approx c/(2 \cdot F)$$

where F is the focal length. At Parkes this amounts to $\Delta f = 5.7$ MHz.
The ripple amplitude is surprisingly large; if the source intensity leads to an antenna temperature T_A, then the peak-to-peak ripple is:

$$\Delta T/T_A = 4\Gamma$$

where Γ is the **Voltage** reflection coefficient.

At Parkes $\Delta T/T_A \sim 1\%$ at 5 GHz (prior to remedial measures).

Γ is computed in three steps:
compute the angular distribution of the energy scattered from the feed.
compute the energy scattered back from the reflector towards the feed.
compute the response of the feed to the returned energy.

For an axisymmetric antenna these operations reduce to the integral (Poulton, 1973) :

$$\Gamma = P \int F(\theta) S(\theta) \sin(\theta) e^{-2jkr} d\theta$$

where $F(\theta)$ is the feed (voltage) pattern, and $S(\theta)$ is the angular distribution of the voltage scattered from the feed. θ is the angle between a ray and the reflector axis; r is the length of the ray from the feed to the surface at angle θ. P is a normalisation factor,

$$P = 1./\int_0^{\pi} F^2(\theta) \sin(\theta) d\theta$$

Poulton evaluated this integral for the Parkes case, over a wide range of frequencies, for three levels of reflection from the feed - reproduced here as figure 1. It shows that at 5 GHz, for example, $\Gamma \sim -31dB$, leading to a (predicted) peak-to-peak $\Delta T/T_A$ of around 0.3%.

It is worth noting here that a pointing error can rapidly increase the reflected energy, and this will increase $\Delta T/T_A$.

The ripple may also depend of the source structure, as extended structure will spill past the feed and be scattered towards the main reflector.

Note also the general frequency dependance: $\Gamma \propto \lambda$

2.3 OFF-source component

The situation with the OFF-source component is much less secure. A number of mechanisms have been identified.

- Extended structure - ground radiation, atmosphere and the general background will present a distributed radiation flux to the feed area with ripple consequences much as for extended "ON-source" structure.

- A reflection of energy from the feed-receiver junction will lead to energy transmitted from the feed which may then scatter back to the feed and interfere. In this case the initial angular distribution of the scattered energy is well defined - it is the feed's pattern.

Estimating the amplitude of the OFF-source component is difficult. Morris and Poulton both presented arguments to show that the proposed mechanisms could produce a ripple of the observed magnitude but but the estimates and the observations have large errors.

2.4 Remedies and Strategies

- Local regions of high reflectivity. Flat plates normal to direct rays from the feed are likely to make a significant contribution to the ripple. These regions can in principle be identified from the periodicity of the ripple. Fisher (1978) used a reflectometer as a sharper tool to localise such trouble spots in the Greenbank antennas. The reflections can be moderated with absorber or by tilting the plate.

  While this approach will remove serious offenders it cannot address the reflection from the entire antenna.

- Vertex Corrector Assemblies. The integral expression for Γ is a vector sum over the entire reflector surface. A detailed examination of the contribution of the various sections of the reflector to the final vector sum shows that the central area makes a large contribution; that is, we can view the reflected signal as the sum of two roughly equal components: one from the central area and one from the rest of the antenna. Given this, we can alter the

magnitude of the reflected signal by adjusting the relative phasing of the two components - by suitably raising the central region. Since the central region is blocked by the focus cabin from the incident radiation, this adjustment will not affect the reflector's main beam.

Silver (1949) and Poulton (1974) have discussed the details of this type of correction. In principle complete cancellation is possible; in practice it is hard to achieve. A simple plate will be very frequency-specific; Poulton showed that a wide-band assembly could be designed.

- Observing Strategy. Some observers (eg, Bania et al, 1993) have found that alternating the focus setting by $\pm\lambda/8$ results in a substantial improvement in the baseline. At the Greenbank 43m (at the Cassegrain focus) the uncorrected ripple is $\Delta T/T_A \sim 2\%$; the $\pm\lambda/8$ cancellation gives $\Delta T/T_A \sim 0.2\%$; further baseline processing allowed them to achieve $\Delta T/T_A \sim 0.07\%$ after long integrations.

3 Parkes

The Parkes 64m antenna exhibited all the problems described above, along with a few ideosyncracies of its own. These were investigated in detail in 1977 (Padman 1977a, b).

The ripple period is 5.7 MHz; the baseline is not sinusoidal, with the second and third harmonics present. $\Delta T/T_A \sim 0.85\%$, 1.3% and 0.35% for the three harmonics.

The relatively flat vertex produced a further twist to the problem: in effect we have a Fabry-Perot etalon between the vertex and the focus cabin ground plane. This means that quite sharp spectral features can be seen (fig. 2).

The Padman report identified three major improvements:

- Install a corrector assembly in the vertex region.
- Close the gap at radius 8.5m between the "mm" surface and the perforated panels.
- Equalise the noise level between ON and OFF observations.

Several minor improvements were also identified:

- Use 2HE feeds in preference to single mode feeds.
- Alternate observations with the focus at $\pm\lambda/8$,

Of little help:

- Placing absorber on the focus cabin ground-plane.
- Placing a cone around the feed in attempt to shield it from off-axis radiation.

In detail:

3.1 Vertex Corrector Assembly

Poulton (1974) designed a series of assemblies for the Parkes antenna, to cover a number of frequency ranges. The experience with the 3-9 GHz band assembly was disappointing: the fundamental was reduced by about 50%, but the other harmonics were unchanged. Considering that the first Fresnel zone has a radius of order 1m at 5GHz the balancing act required of the corrector assembly is enormous, so the mixed results are perhaps not surprising.

A simple cone (5 degree semi-angle) was found to be effective: the higher harmonics were essentially eliminated and the fundamental was reduced to $\Delta T/T_A \sim 0.5\%$. The ripple amplitude was independent of zenith angle.

The current corrector assembly is the cone.

3.2 Gaps at the 8.5m Radius

These gaps were left after the resurfacing campaign which provided a high precision "mm" surface in the inner 8.5m section. J.Murray showed that such a gap would make a significant contribution to the ripple - in effect we have a sizeable area of the antenna at constant phase from the feed.

The gaps have now been closed.

3.3 Noise Matching

Hard-won experience indicated that the baselines were improved if the ON and the OFF T_{sys} were made equal. It is possible that this process balanced the additional reflection at the receiver source flux density. It is not clear whether this technique is still required.

3.4 Hybrid Mode Feeds

The ripple will be reduced as the feed efficiency increases, so the switch to 2HE feeds should (and did) improve matters.

3.5 Absorber

The absorber had a modest effect on the higher harmonics, but otherwise did little to attenuate the ripple. The argument was made that the absorber could not be placed close enough to the feed - there was an appreciable gap surrounding the feed.

3.6 OFF-source ripple, anecdotes

The record is not clear: my impression is that good cancellation of the OFF-source baseline was obtained if the reference spectra were obtained from the same HA/DEC track as the ON-source spectra. Perhaps present-day observers could provide some data on this question.

I also get the impression that day-time baselines are distinctly worse than night-time. Some hard data would be appreciated. I would not be surprised if the feed legs were responsible, as they provide fertile scope for multi-paths. (I would expect this type of problem to have a periodicity somewhat greater than 5.7MHz).

J. Caswell advises that the $\pm\lambda/8$ was not entirely satisfactory; some improvement was obtained by stepping the focus in finer intervals over a larger range.

3.7 Results

When all these improvements were in place the ripple (in 1977) became much more sinusoidal, with amplitude $\Delta T/T_A \sim 0.25\%$.

4 Parkes Upgrade

The upgrade will enlarge the focus cabin from 8 to $22m^2$.

The multi-pathing requires some fraction of the direct signal to hit the feed; thus the damage is done within a few λ of the feed, and the extension from 3 to 6m (dia) is likely to be irrelevant.

The Fabry-Perot etalon problem does relate to the area of the focus cabin ground-plane, so some care is needed here. The present scatter cone extends out to a radius of 2m, so an extension may be advisable.

5 Recommendations

- The vertex scatter cone may need to be enlarged to ensure that the Fabry-Perot etalon problem does not re-appear.
- It might be useful to re-examine the OFF-source problem, since current receivers may well have significantly reduced mis-match problems, with reduced transmitted noise able to scatter back to the feed.

- The noise balancing operation should be revisited: is it a lost art, or an obsolete one?
- Attempt to reduce the scattered radiation from the tripod: the open structure is known to offer excellent scattering centres for strong off-axis sources. A smooth surface, tapered towards the vertex would have superior scattering properties.

6 References

This list is not comprehensive; nor have I been able to consult all the items; it provides some indication of what is available.

- Bania, Rood and Wilson (May 1993) - Frequency Baseline Structure in the 100m Telescope at 3.6cm Wavelength. MPIfR Technische Bericht N0. 75
- Bieging and Morris (Dec. 1976) - Further Efforts to Improve the Spectroscopic Baseline of the 100m Telescope. MPIfR Internal Report
- Beiging and Pankonin - Experimental Investigation of the Causes of Spectroscopic Baseline Ripple at 5 GHz. MPIfR, Technische Bericht, No. 16
- Brockway (1984) - NRAO Electronics Div. Technical Rep. 126.
- Caswell - Spectral Line Observations with the Parkes Radio Telescope; some notes on Spurious Instrumental Effects. RPP 1675 (?)
- Fisher (1978) - Reflection Measurements on the 140ft and 300ft Radiotelescopes. NRAO Electronics Div. Internal Rep. 184
- Gardner (1.2.72) - Notes on Instrumental Effects on Spectral Line Receivers. (file note)
- Gardner (1973) - An investigation of Instrumental Effects with Spectral Line Observations with the 100m Telescope. MPIfR Internal Report
- Lockman and Rickard (1977) - Spurious Spectral Features at the NRAO 140 ft. NRAO Electronics Div. Internal report N0. 183
- Morris (Avril 1973) - Chromatism at Millimeter Wavelengths. Rapport Technique Provisoire; GI. mm/DM/No. 125
- Morris - Chromatism in Radio Telescopes due to Blocking and Feed Scattering, Internal Report, Observatoire de Paris, 92190, Meudon
- Morris (1974) - Chromatism and Antenna design. Internal Report, G.I. mm No. 125a
- Morris and Bieging (Jan. 1976) - Progress Report on Baseline Ripple Problem. MPIfR Internal Report

- Morris (1978) - Chromatism in Radio Telescopes due to Blocking and Feed Scattering - Ast. & Astrop 67, p. 221
- Padman (Jan. 1976) - Report on Baseline Ripple - 64m Dish. CSIRO Internal Report
- Padman (1977a) - Spectrometer Baseline Ripple Observations with the Parkes 64-m Radio Telescope at 5 GHz. CSIRO RPP 2056(L),
- Padman (1977b) - Reduction of Baseline Ripple on Spectra Recorded with the Parkes 64m Radio Telescope. Proc. ASA, vol3, p.111
- Poulton (1975) - Investigation into Ripple Causing Mechanisms in a Large two-reflector Telescope. Queen Mary College, London,
- Poulton (1974) - Minimisation of Spectrometer Ripple in Prime Focus Radiotelescopes. CSIRO Research Report
- Silver (1949) (Ed.) Microwave Antenna Theory and Design. M.I.T. Series Vol 12.
- Ulich (Jan. 1978) - Telescope Standing Waves: their Causes and Cures. National Radio Science Meeting, Boulder, Colo
- Weinreb (Nov, 1967) - Effect of Feed-Paraboloid Reflections upon Line Receiver Performance on the 140ft. Telescope. NRAO Memo
- Weinreb (May 1970) - Effect of 140ft Vertex Cone on Spectral-Line Baselines. NRAO Memo
- Wilson and Hills - The Instrumental Frequency Baseline of the 100m Telescope from the Secondary Focus at 11cm. MPIfR Technische Bericht No. 11

Figures

Fig. 1 Scattered power returned to the feed. Three cases considered:
- 100% reflection at the feed.
- Main lobe (the central Airy ring) blocked.
- Main and first sidelobe blocked.

Fig. 2 The "Fabry-Perot etalon" effect.

Fig. 3 Typical baseline, before any remedial measures taken.

Fig. 4 Baselines after remedial action.

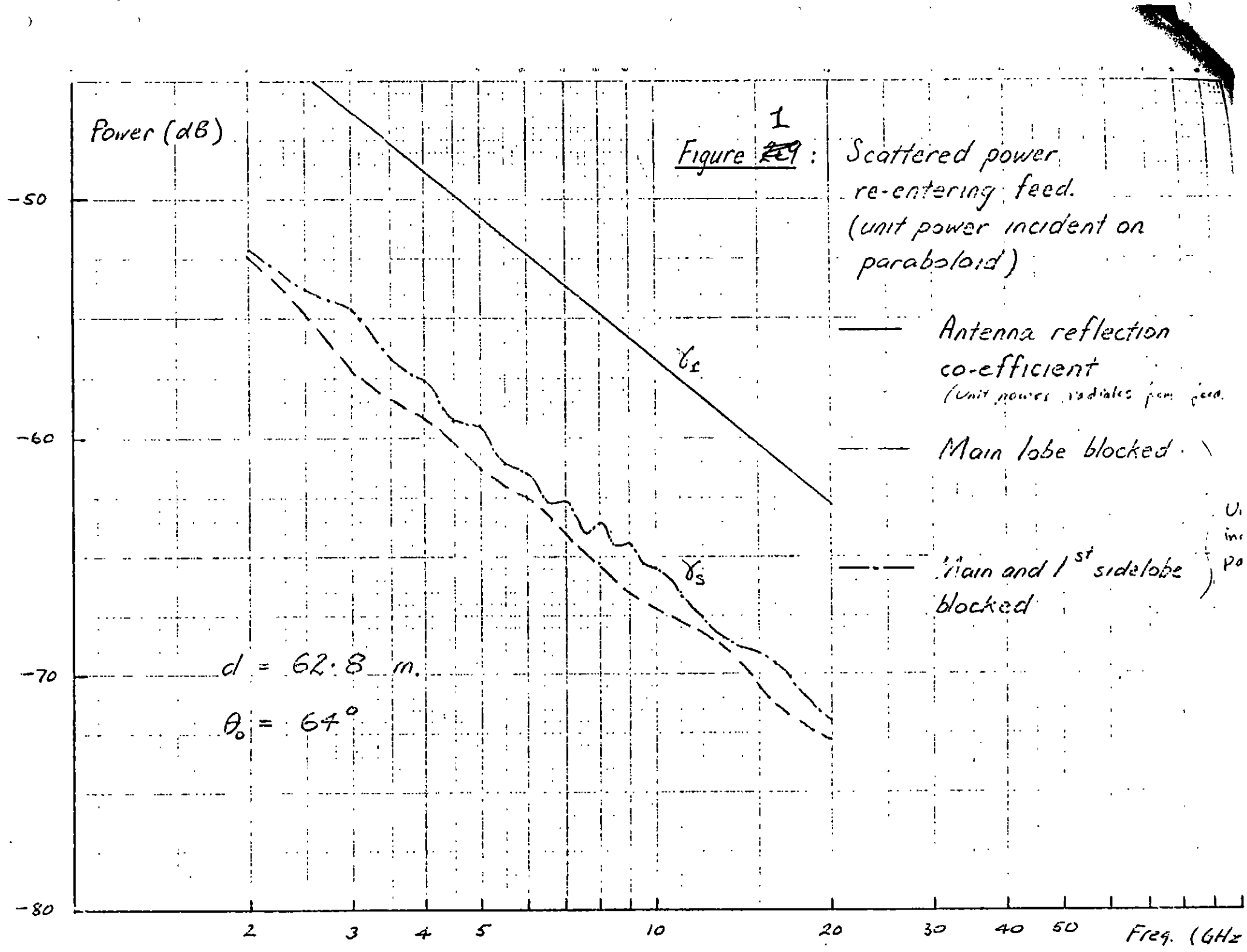
Power (dB)
-50
-60
-70
-80
2
3
4
5
10
20
30
40
50
Freq. (GHz
γ_t
γ_s
d = 62.8 m.
θ_0 = 64°
Figure 1: Scattered power re-entering feed. (unit power incident on paraboloid)
Antenna reflection co-efficient (unit powers radiates from feed
Main lobe blocked
Main and 1st sidelobe blocked

Fig. 2

4. Multiple-reflection

It is possible for some of the aperture blockage to be reflected by the parabola and then reflected again by the blockage. This would give rise to higher modulation frequencies of the order of $2\nu_o$, $3\nu_o$ ..... if the blockage occurs in the vicinity of the focal plane. An effect ot this type has been observed with the Parkes 64-m dish at wavelengths of 9 cm and longer where apparent absorption "dips" of the form shown below were obtained.

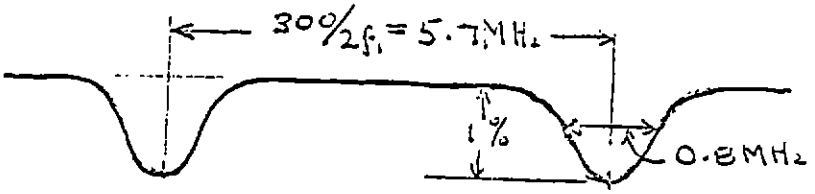

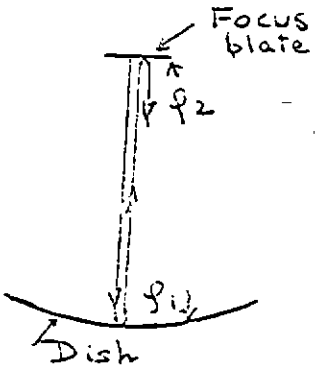

These "dips" were explained as arising from multiple reflections between the parabola vertex and the flat plate of 3 - 4 m.size in the focal plane. If ρ_1 and ρ_2 are the reflection coefficients associated with waves so trapped, then successive reflections will add as

$$\text{constant} \left\{ 1 + |\rho_1 \cdot \rho_2| e^{-i\Delta} + |\rho_1 \cdot \rho_2|^2 e^{-i2\Delta} + \ldots\ldots \right.$$

$$= \frac{\text{constant}}{1 - |\rho_1 \rho_2| e^{-i\Delta}} \text{ , in which } \Delta \text{ is the phase difference associated with the round-path.}$$

From the ratio of the half-widths of the "dips" to the spacing it was ascertained that $|\rho_1 \cdot \rho_2| \approx 0.8$. Such a high value is not impossible with a flat focal plane about a Fresnel zone in size.

By covering the focal plate with absorbing material the "dips" were removed. However, quasi-sinusoidal effects remained. At 6 cm the "dips" were not present, presumably because the focal plate was no longer a good reflector.

It is obvious that the radiation from multiple-reflections is associated with

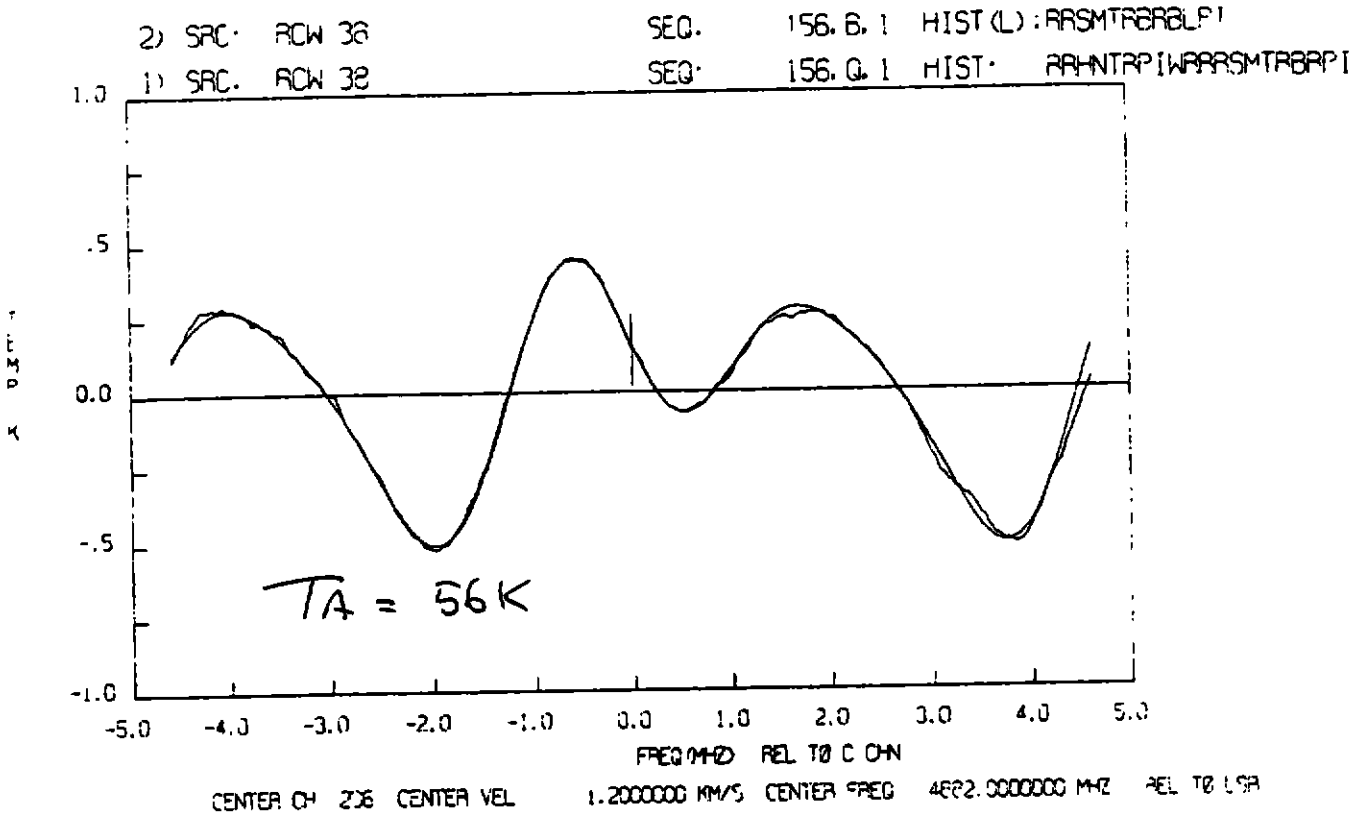

Harmonic	P-P amplitude (K)
1	0.472
2	0.578
3	0.188
4	0.002

Fig. ~~15~~ 3 - Typical spectrum from Figure 15 and tabulation of calculated least-squares Fourier baseline components up to the fourth harmonic; Z.A. = 14°.5.

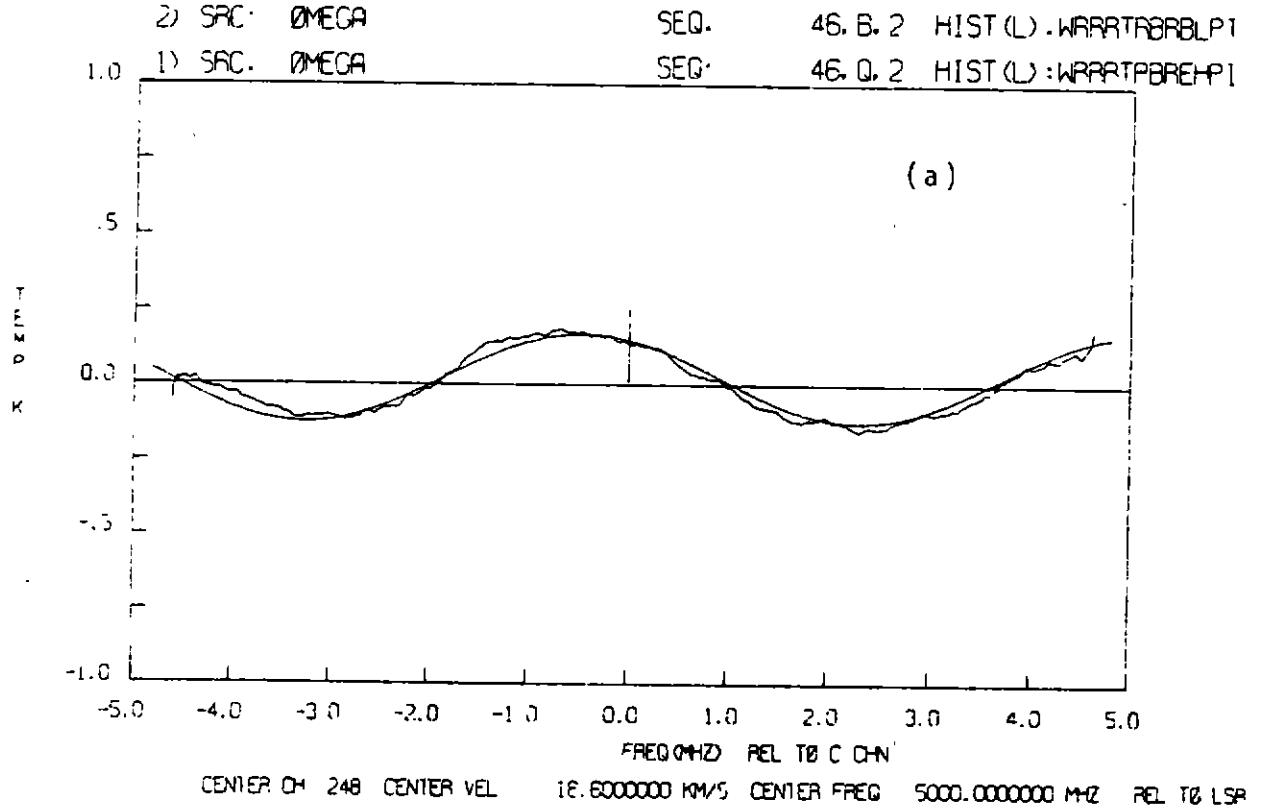

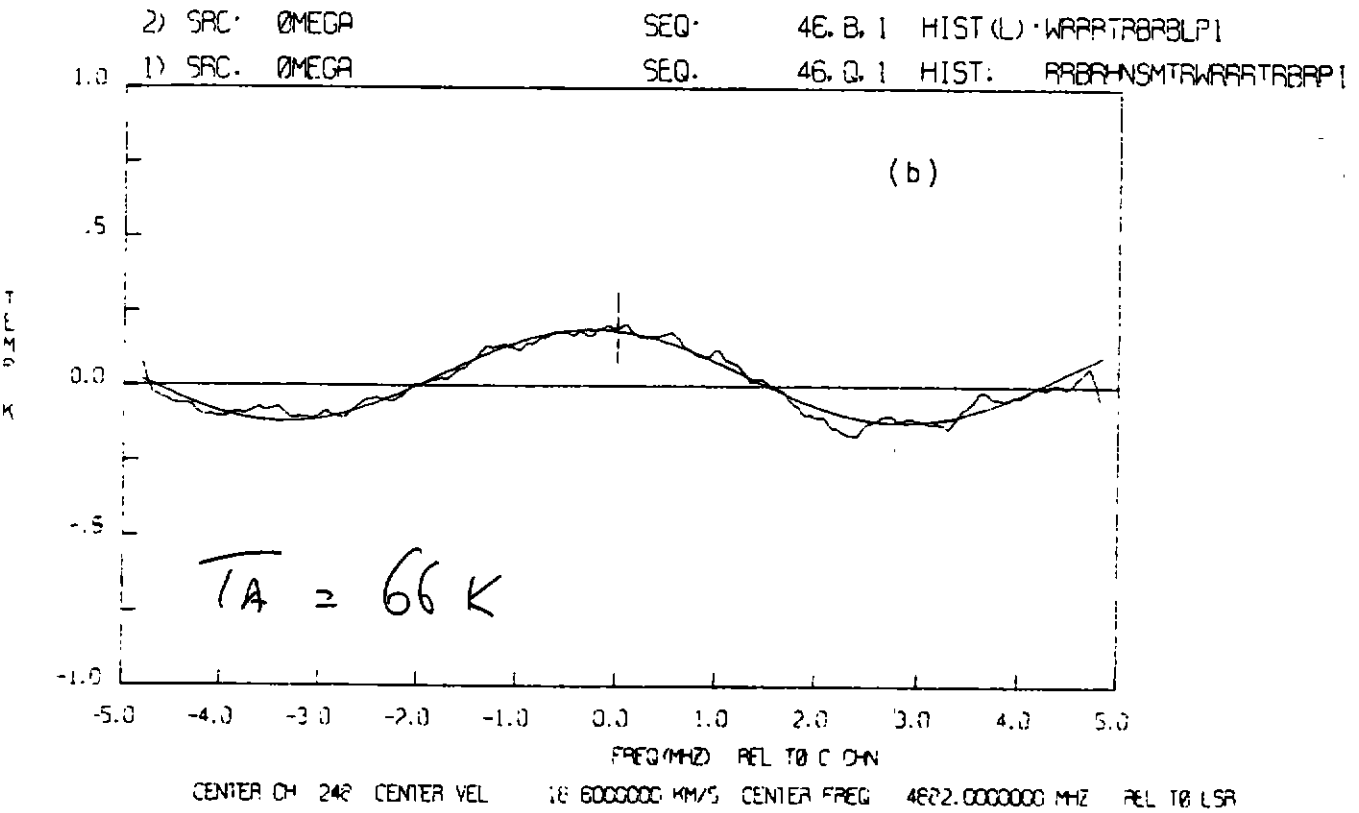

Fig. 23 - Spectra obtained using scattering cone and Mk I IIIE feed; source M17 (Omega nebula), Z.A. = 45°; no focal plane absorber. (a) f_0 = 5000 MHz; (b) f_0 = 4882 MHz.

4

Some General Thoughts from Padman's Work (1978) at 5GHz

- Reproducibility is poor
- "The effect of lift position, flexible cables.....
  introduce spurious reflections."
- Second harmonic > fundamental
- 2HE < 1HE (factor 2)
- Absorber in focal-plane has negligible effect
- Scattering cone at vertex:
  - fundamental reduced by ~ 1.7
  - Second and third harmonic $\longrightarrow$ 0
- General increase as elevation angle decreases
- Reflector gaps have significant effect
- Emphasises need to have good match of receiver to feed.